OPPORTUNISTIC HYBRID NETWORK CODING (OHNC) METHOD AND QOS METRICS MODELING FOR SMART GRID WIRELESS NEIGHBORHOOD AREA NETWORKS

Mr. Ngoc Thien Le

A Dissertation Submitted in Partial Fulfillment of the Requirements

for the Degree of Doctor of Philosophy Program in Electrical Engineering

Department of Electrical Engineering

Faculty of Engineering

Chulalongkorn University

Academic Year 2015

วิธีการเข้ารหัสโครงข่ายแบบไฮบริดเชิงโอกาส (โอเอชเอ็นซี) และการจำลองเมทริกซ์คิวโอเอส สำหรับโครงข่ายพื้นที่ระดับท้องถิ่นไร้สายสมาร์ทกริด

นายเล งอก เทียน

วิทยานิพนธ์นี้เป็นส่วนหนึ่งของการศึกษาตามหลักสูตรปริญญาวิศวกรรมศาสตรดุษฎีบัณฑิต
สาขาวิชาวิศวกรรมไฟฟ้า ภาควิชาวิศวกรรมไฟฟ้า
คณะวิศวกรรมศาสตร์ จุฬาลงกรณ์มหาวิทยาลัย
ปีการศึกษา 2558

Thesis Title	OPPORTUNISTIC HYBRID NETWORK CODING (OHNC) METHOD AND QOS METRICS MODELING FOR SMART GRID WIRELESS NEIGHBORHOOD AREA NETWORKS
By	Mr. Ngoc Thien Le
Field of Study	Electrical Engineering
Thesis Advisor	Associate Professor Watit Benjapolakul, Ph.D.

Accepted by the Faculty of Engineering, Chulalongkorn University in Partial Fulfillment of the Requirements for the Doctoral Degree

. . . . . Dean of the Faculty of Engineering
(Associate Professor Supot Teachavorasinskun, Ph.D.)

THESIS COMMITTEE

. . . . . Chairman
(Associate Professor Lunchakorn Wuttisittikulkij, Ph.D.)

. . . . . Thesis Advisor
(Associate Professor Watit Benjapolakul, Ph.D.)

. . . . . Examiner
(Assistant Professor Widhyakorn Asdornwised, Ph.D.)

. . . . . Examiner
(Associate Professor Chaodit Aswakul, Ph.D.)

. . . . . External Examiner
(Chakphed Madtharad, Ph.D.)

เล งอก เทียน: วิธีการเข้ารหัสโครงข่ายแบบไฮบริดเชิงโอกาส (โอเอชเอ็นซี) และการจำลองเมทริกซ์คิวโอเอส สำหรับโครงข่ายพื้นที่ระดับท้องถิ่นไร้สายสมาร์ทกริด. (OPPORTUNISTIC HYBRID NETWORK CODING (OHNC) METHOD AND QOS METRICS MODELING FOR SMART GRID WIRELESS NEIGHBORHOOD AREA NETWORKS) อ.ที่ปรึกษาวิทยานิพนธ์หลัก: รศ. ดร.วาทิต เบญจพลกุล, 108 หน้า.

การออกแบบระเบียบแบบแผนการเก็บรวบรวมข้อมูลที่เป็นประโยชน์ ในโครงข่ายพื้นที่ระดับท้องถิ่นสมาร์ทกริดซึ่งเป็นส่วนที่วิกฤตที่สุด ในการสื่อสารภายในสมาร์ทกริดได้รับความสนใจอย่างกว้างขวางจากผู้ทำวิจัยจำนวนมาก ในระยะเวลา 2-3 ปีที่ผ่านมา อย่างไรก็ตาม มีการศึกษาเกี่ยวกับวิธีเก็บรวบรวมข้อมูลเพื่อตอบสนองความต้องการบริการสามาร์ทกริดที่เข้มงวดเป็นจำนวนน้อยมาก

วิทยานิพนธ์ฉบับนี้เสนอแบบจำลองคุณภาพบริการเชิงนวัตกรรม สำหรับโครงข่ายไร้สายในโครงข่ายพื้นที่ระดับท้องถิ่นบนพื้นฐานของการสำรวจลักษณะเด่น โดยธรรมชาติของการประยุกต์ใช้งานสมาร์ทกริด ความต้องการด้านความเชื่อถือได้ และการประวิงเวลาได้รับคัดเลือก ให้เป็นประเด็นที่มีความสำคัญที่สุด ในบรรดาลักษณะเด่นต่างๆ เหล่านั้น แบบจำลองเส้นโค้งรูปตัวเอส (S) ได้รับการเสนอให้ใช้เป็นเครื่องมือ ในการประเมินสมรรถนะของแบบแผนการสื่อสารต่างๆ ที่เป็นตัวเลือก ในโครงข่ายพื้นที่ระดับท้องถิ่นสมาร์ทกริด เมื่อเปรียบเทียบกับแบบจำลองคุณภาพบริการอื่นๆ ที่มีอยู่ในปัจจุบันแบบจำลองที่เสนอนี้ง่ายต่อการใช้และช่วยลดเวลาและต้นทุน เราเสนอวิธีการเข้ารหัสโครงข่ายแบบไฮบริดเชิงโอกาส (โอเอชเอ็นซี) สำหรับการเก็บรวบรวมข้อมูล ในโครงข่ายพื้นที่ระดับท้องถิ่นไร้สายสมาร์ทกริด การเข้ารหัสโครงข่ายได้รับการพิสูจน์มาแล้วว่าเชื่อถือได้ และมีประโยชน์ในเรื่องการประวิงเวลา โดยเฉพาะอย่างยิ่งในสิ่งแวดล้อมของการสื่อสารแบบไร้สาย ผลการจำลองแสดงให้เห็นว่า วิธีการเข้ารหัสโครงข่ายที่เสนอสามารถตอบสนอง ความต้องการการคุณภาพบริการของการประยุกต์ใช้งานสมาร์ทกริดทั้งในปัจจุบันและในอนาคต

ภาควิชา วิศวกรรมไฟฟ้า ลายมือชื่อนิสิต .....

สาขาวิชา วิศวกรรมไฟฟ้า ลายมือชื่อ อ.ที่ปรึกษาวิทยานิพนธ์หลัก .....

ปีการศึกษา 2558 .....

5671450321: MAJOR ELECTRICAL ENGINEERING

KEYWORDS: SMART GRID / QUALITY OF SERVICE (QOS) / S-SHAPED CURVE / NETWORK CODING / SMART GRID WIRELESS NAN / ADVANCED METERING INFRASTRUCTURE (AMI) / PHASOR MEASUREMENT UNIT (PMU)

NGOC THIEN LE : OPPORTUNISTIC HYBRID NETWORK CODING (OHNC) METHOD AND QOS METRICS MODELING FOR SMART GRID WIRELESS NEIGHBORHOOD AREA NETWORKS. ADVISOR : Associate Professor Watit Benjapolakul, Ph.D., 108 pp.

Designing a useful data collection scheme in Smart Grid Neighborhood Area Network (Smart Grid NAN), which is the most critical part in Smart Grid communication, has drawn wide attention of researchers in recent years. However, there are few studies in data gathering method to fulfill the strict requirements of Smart Grid services. In this dissertation, we first propose an innovative Quality of Service (QoS) model for wireless network in Neighborhood Area Network based on exploring the nature features of Smart Grid applications. We have chosen reliability and latency requirements as the most important criteria and implemented the S-shaped curve model for performance evaluations of any candidate communication schemes. Comparing with other existing QoS models, our model is easy to use and help to reduce the time and cost. We then suggest Opportunistic Hybrid Network Coding (OHNC) method for data gathering in wireless Smart Grid NAN context. Network Coding has been proved reliable and latency-beneficial, especially in wireless environment. Based on simulation, the OHNC shows that Network Coding method can fulfill the QoS requirements of current and upcoming Smart Grid applications.

Department : ..... Electrical Engineering ..... Student's Signature .....

Field of Study : .... Electrical Engineering .... Advisor's Signature .....

Academic Year ..... 2015 .....

Acknowledgements

I am most grateful to my advisor, Associate Professor Dr. Watit Benjapolakul, for his guidance, encouragement, patience, and advice for my academic life in Chulalongkorn University. I feel so pound to have the opportunity to do research under his supervision.

I would like to express my appreciation to all professors at Department of Electrical Engineering, Chulalongkorn University for their help to establish my academic carrier. My appreciation also goes to my colleagues in Telecommunication System Research Lab, for their warmly atmosphere, the useful discussions and their encouragement.

I would like to thank the PhD support grant from Scholarship Program 2013 for ASEAN Countries, funded by Chulalongkorn University, Thailand.

I also would like to thank my family and especially to my wife, Bich Mai Nguyen. I am so lucky to meet her in my life. Thank you for her unconditional love and understanding. My final thank goes to my beautiful daughter, Bao Tram Le Ngoc, and her bright smiles, to whom I owe the renewal of my strength and perseverance to accomplish this work.

Contents

Page

Abstract (Thai) . . . iv

Abstract (English) . . . v

Acknowledgements . . . vi

Contents . . . vii

List of Tables . . . x

List of Figures . . . xi

List of Acronyms . . . xiv

Chapter

1 Introduction . . . **1**

1.1 Motivation . . . 1

1.2 Dissertation Structure . . . 2

1.3 Thesis Contributions . . . 3

1.4 List of Publications . . . 4

2 Background and Related Theories . . . **6**

2.1 Smart Grid NAN Overview . . . 6

2.1.1 Advanced Metering Infrastructure . . . 6

2.1.2 Distribution Automation and Wide Area Measurement System . . . 9

2.1.3 Data requirement in Smart Grid . . . 10

2.2 Smart Grid standardization activities . . . 14

2.2.1 Open Smart Grid (OpenSG) . . . 14

2.2.2 NIST Smart Grid Framework . . . 14

2.2.3 IEEE Vision for Smart Grid Communications . . . 15

2.3 Network Coding . . . 16

2.3.1 Overview . . . 16

2.3.2 Random Linear Network Coding (RLNC) example . . . 17

2.4 OMNeT++ Network Simulator Framework . . . 18

3 Quality of Service Modeling For Smart Grid Wireless NAN Applications . . . **21**

3.1 Introduction . . . 21

3.2 Related Works . . . 22

3.2.1 QoS based on electrical service requirements . . . 22

3.2.2 Quality of Service (QoS) for routing in Smart Grid network . . . 22

Chapter Page

3.3 Proposed QoS metrics for Smart Grid Wireless Neighborhood Area Network (SG WNAN) . . . 23
3.3.1 Latency of Smart Grid messages . . . 23
3.3.2 Packet Delivery Ratio (PDR) . . . 25
3.3.3 System Reliability . . . 26
3.3.4 Critical Latency Response, $\triangle_c$ . . . 27
3.4 System reliability and Delay relation . . . 28
3.4.1 Relation between P_G, P_S, P_R and τ . . . 28
3.4.2 S-shaped curve model . . . 31
3.5 Simulation and Results . . . 36
3.5.1 Simulation setup . . . 36
3.5.2 Performance results . . . 37
3.5.3 Learnt Lessons from Simulation . . . 38
3.6 Conclusion . . . 41

4 Evaluations Of Wireless Phasor Measurement Unit (PMU) System Reliability for Soft Delay Smart Grid Applications . . . 43
4.1 Introduction . . . 43
4.2 Phasor Measurement Techniques . . . 44
4.2.1 Introduction . . . 44
4.2.2 Phasor representation . . . 45
4.2.3 IEEE Standard C37.118.1a -2014 . . . 48
4.2.3.1 Frequency and rate of change of frequency (ROCOF) estimation . . . 49
4.2.3.2 Total vector error (TVE) Evaluation . . . 49
4.2.3.3 Frequency and ROCOF measurement evaluation . . . 50
4.2.3.4 Phasor Reporting rates . . . 51
4.3 Soft Delay Smart Grid applications . . . 52
4.3.1 State Estimation (M-Type) . . . 52
4.3.2 Transient Stability (P-Type) . . . 54
4.4 Phasor Measurement system and topology . . . 55
4.5 PMU network performance evaluations . . . 56
4.5.1 Simulation Settings . . . 57
4.5.2 The result S-shaped curve performance . . . 57

Chapter Page

4.6 Conclusion 60

5 Opportunistic Hybrid Network Coding method for Smart Grid Data Gathering . . . 63

5.1 Introduction 63

5.2 Related work 63

5.3 Proposed Opportunistic Hybrid Network Coding scheme 65

5.3.1 Assumptions 65

5.3.2 Description of Opportunistic Hybrid Network Coding (OHNC) data gathering scheme 66

5.3.3 Example of snapshot data using Non-OHNC and OHNC schemes 67

5.4 Analytical results of OHNC scheme 68

5.4.1 System Model 68

5.4.2 Markov Chain Modeling of Non-Opportunistic Hybrid Network Coding (Non-OHNC) scheme 69

5.4.3 Markov Chain Modeling of Opportunistic Hybrid Network Coding (OHNC) scheme 72

5.4.4 Analytical results 75

5.5 OHNC Simulations in Matlab 76

5.5.1 Point-to-Point scenario 77

5.5.2 Disjoint paths scenario 78

5.5.3 Butterfly scenario 80

5.6 Conclusion 82

6 Conclusion and Future Work 84

6.1 Conclusion 84

6.2 Future Work 85

Appendix 92

Appendix A PMU IEEE C37.118.1a - 2014 Standard 92

Biography 95

List of Tables

Table Page

2.1 The general concept layers of Smart Grid. 6

2.2 Requirements of Smart Grid Applications [3, 11]. 12

2.3 Traffic types for AMI application [11]. 12

3.1 Notation Summary. 24

3.2 An example Smart Grid services classification. 25

3.3 Comparison of existing QoS and our proposed QoS for Smart Grid NAN. 28

3.4 The detail constraints for Smart Grid applications. 34

3.5 AMI Periodic traffic used in simulation. 36

3.6 Simulation parameters for AMI based WiMAX IEEE 802.16 one -hop topology [40]. . . 37

3.7 Simulation parameters for AMI based ZigBee IEEE 802.15.4 multi-hop topology [41]. . 37

4.1 Required PMU reporting rates based on IEEE C37.118 Standard. Remember that low sample rate leads to long window time, and fast sample leads to the short one. 52

4.2 Summarized of application for Wide Area Mearsurement System (WAMS) based on PMUs network [48]. 55

4.3 PMU setting for concurrent applications: State Estimation and Transient Stability. 58

4.4 PMU Wireless NAN simulation settings. 58

4.5 Results summary of IEEE 802.11g for concurrent Smart Grid applications. 61

5.1 An example of Network Coding with explicit feedback using Tunable Sparse Codes for 4 nodes [18]. 65

5.2 Example of data gathering in a snapshot using Non-OHNC method in Figure 5.3a. 68

5.3 Example of data gathering in a snapshot using OHNC method in Figure 5.3b. 68

5.4 Table of Markov states in a snapshot. 69

A.1 Steady-state synchrophasor measurement requirements [IEEE C37.118.1a-2014]. 93

A.2 Steady-state frequency and ROCOF measurement requirements [From IEEE C.37.118.1a-2014]. 94

List of Figures

Figure Page

2.1 Smart Grid diagram concept [8]. 7
2.2 Smart Meter node block diagram. 8
2.3 An example of Advanced Metering Infrastructure (AMI) network topology (Adapted from [9]). 9
2.4 Phasor Measurement Unit Block Diagram. 10
2.5 Hierarchical architecture example of WAMS. 11
2.6 Hierarchical architecture example of WAMS applications based on PMUs network. . . 11
2.7 Data requirement comparison between Smart Grid and others. 13
2.8 IEEE Protocols Standards Communication Mapping [8]. 15
2.9 The concept of Intra-Source Network Coding to improve reliability [20]. 16
2.10 The concept of Inter-Source Network Coding to improve throughput [21]. 17
2.11 The process of Random Linear Network Coding over finite Galois field. 19
2.12 A typical OMNeT++ modules and network. 19
2.13 OMNeT++ network simulation workflow. 20
3.1 An example of system reliability enhancement technique with $P_G = 2$, $P_S = 4$ and $P_R \leq 2$. 29
3.2 Reliability enhancement example using Retransmission scheme. 30
3.3 Reliability enhancement example using Multi-paths scheme. 31
3.4 S-shaped curve of AMI Periodic in Table 3.4. 34
3.5 S-shaped curve of State Estimation in Table 3.4. 35
3.6 Linearized S-shaped curve of AMI and PMU applications in Fig. 3.4 and Fig. 3.5. . . . 36
3.7 The system reliability simulation result for one-hop WiMAX AMI network. 38
3.8 The system reliability simulation result for multi-hop ZigBee AMI network. 39
3.9 Linearized lines of two S-shaped curves. 40
3.11 Snapshot length example in AMI based Zigbee. 41
3.12 Snapshot length comparison of AMI network based Zigbee. 41
3.13 Maximum obtained system reliability with different snapshot rates of AMI based Zigbee. 42
4.1 Abstract model for Smart Grid application on PMUs network (Adapted from [8]). . . . 44
4.2 First PMU installed at the Power Systems Research Laboratory at Virginia Tech [8]. . 45
4.3 Example of voltage wave representation. The phasor depends upon the choice of vertical axis $t = 0$. The length of phasor vector is equal to root mean square (RMS) of sinusoid. 46

Figure Page

4.4 Example of Fast Fourier Transform technique [45]. 47

4.5 Example of traditional phasor calculation. Reference waveforms on the top move with calculation [45]. The value of phasor information is calculated from reference waveforms. 48

4.6 Example of phasor wave representation. The phasor depends upon the choice of vertical axis $t = 0$. It is impossible to calculate phasor at instant t_1. The estimation algorithm needs enough sample to process. This is called window time calculation, or window time length. 49

4.7 Example of latency from windowing calculation [45]. The timetag of phasor information is located at center of window time. 50

4.8 Example effect of timetag and window length to the accuracy of step change in phasor. Short window length helps to identify the instant timetag correctly, but requires sufficient sample data in a short latency to run estimation. 51

4.9 Example of latency from windowing and step change [45]. 51

4.10 Example of frequency calculation from phasor information [45]. 53

4.11 Example of power calculation from phasor information [45]. 54

4.12 Example of state estimation application based on PMUs network. The synchronous phasor information from A, B, and C PMU locations help to monitoring the power grid state in real time. 54

4.13 Transient stability application [45]. 55

4.14 Example of PMUs architectures [45]. The star architecture (on the left) is more common used by utilities. 56

4.15 IEEE 37 node test distribution feeder used in simulation. 57

4.16 The S-shaped curve result of PMUs network based IEEE 802.11g approach with reporting rate 30 $(samples/second)$, snapshot length 4 ms. 59

4.17 The S-shaped curve results of PMUs network based on IEEE 802.11g with Snapshot length 2 ms and 4 ms. 59

4.18 The linearized lines of PMU network based on IEEE 802.11g with Snapshot length 2 ms and 4 ms from Figure 4.17. 60

4.19 The S-shaped curve simulation results of PMUs network based on IEEE 802.11g with different Snapshot lengths. 61

4.20 The S-shaped curve simulation results of PMUs network based on IEEE 802.11g with 50 $(samples/second)$. 62

4.21 The comparison between monitoring used Supervisory Control and Data Acquision (SCADA) and PMUs systems. 62

Figure Page

4.22 The comparison between monitoring used SCADA and PMUs systems. If we image the power grid picture provided SCADA as X-ray scan (left), then the picture from PMUs as MRI scan (right). 62
5.1 Small example of network coding protocol using Tunable Sparse Codes for 4 nodes (Adapted from the reference [18]). 64
5.2 Network Coding for Monitoring Grid Network Coding for Monitoring Grid (NCMG) method (Adapted from the reference [19]). 66
5.3 Example of two data gathering schemes in one snapshot. 67
5.4 Markov model diagram of Non-OHNC scheme. Q describes the number of received packets in collector node. 69
5.5 Markov model diagram of OHNC scheme. 72
5.6 Expected data collection time slots in one snapshot with $\beta = \gamma$. 76
5.7 Expected data collection time slots in one snapshot with different γ. 77
5.8 OHNC simulation in wireless point-to-point scenario. 78
5.9 Packet loss rate at destination node in simulation using OHNC method with varying the number of redundant packets. Network Coding calculation is in Galois field (2^8). 79
5.10 Packet loss rate comparison with different finite Galois fields. $GF(2^1)$ corresponds to XORing Netwok Coding in NCMG method [19]. The packet loss probability setting in simulation is 0.05. 79
5.11 Comparison packet loss rate at sink using different finite Galois field in point-to-point scenario. The $GF(2)$ corresponds to NCMG method [19], and $GF(256)$ corresponds to Random Linear Network Coding used in our OHNC method. 80
5.12 OHNC simulation in wireless disjoint paths scenario. 80
5.13 OHNC simulation results in wireless disjoint paths scenario. 81
5.14 OHNC simulation in wireless butterfly scenario. 81
5.15 Comparison Packet Loss Rate performance between NCMG method [19] and Random Linear Network Coding in OHNC method in butterfly scenario. 82
5.16 Packet loss rate at node 5 and node 6 in simulation using OHNC method with varying the number of redundant packets in butterfly scenario. Network Coding calculation is in Galois field (2^8). 82
5.17 Effect of Network Coding method in many network topologies. In all case, the link loss probability is 0.05, and Galois field is $GF(2^8)$. 83

List of Acronyms

WAN	Wide Area Network
NAN	Neighborhood Area Network
HAN	Home Area Network
QoS	Quality of Service
SG WNAN	Smart Grid Wireless Neighborhood Area Network
Smart Grid NAN	Smart Grid Neighborhood Area Network
AMI	Advanced Metering Infrastructure
PMU	Phasor Measurement Unit
WSN	Wireless Sensor Network
OHNC	Opportunistic Hybrid Network Coding
DR	Demand Response
SE	State Estimation
DA	Distribution Automation
WAMS	Wide Area Mearsurement System
IED	Intelligent Electronics Device
SCADA	Supervisory Control and Data Acquision
LTE	Long-Term Evolution
WiMAX	Worldwide interoperability for microwave access
GPRS	General Packet Radio Service
PLC	Power Line Communication
PDC	Phasor Data Concentrator
DCU	Data Concentrator Unit
Intra-Source NC	Intra-Source Network Coding
Inter-Source NC	Inter-Source Network Coding
RLNC	Random Linear Network Coding

HD	Hard Delay Requirement
SD	Soft Delay Requirement
NCMG	Network Coding for Monitoring Grid

CHAPTER I

INTRODUCTION

1.1 Motivation

Smart Grid is an unavoidable trend for the current electric system in the 21st century in order to enhance the stability, reliability and efficiency. In Smart Grid, the data communication network is the nervous system, in which the Smart Grid Neighborhood Area Network (Smart Grid Neighborhood Area Network (Smart Grid NAN)) plays an vital role as it enables most of monitoring and controlling applications over the electric distribution network. In addition, the Smart Grid NAN plays as a bridge to real time exchange the information between the utility and customers for many Smart Grid services.

Based on the data requirements in the Smart Grid context [1–6], the Neighborhood Area Network data infrastructure should be able to handle the stringent reliability requirement to fulfill many high solution time services in Smart Grid. In general, reliability is defined as the probability that a system performs its expected functions successfully for a given period of time under particular environment conditions. For example, in Wide Area Situation Awareness application, in order to prevent the outage, a protection message must be sent to protector devices or relays within a subcycle response, that is less than 16.67 ms or 20 ms (for 60 Hz and 50 Hz electric system, respectively).

In addition, any data communications in Smart Grid NAN should be able to fulfill the multi-service priorities requirement in Smart Grid services. That means a data source in Smart Grid is not only using for a particular application, but also can support for other higher priority requirement application in some abnormal events. For instance in Advanced Metering Infrastructure application, electric consumption of customers is used for the billing service with the cycle of 15 minutes requirement. However, those consumption messages must also be successfully sent to the control center in real-time requirement in order to prevent the unbalance between supply side and demand side on the distribution grid in Demand Response (DR) service.

Designing Smart Grid NAN communication architecture has attracted a great interest from researchers. Most of the proposed data communications focus on using wireless network, termed as Smart Grid Wireless Neighborhood Area Netowrk (SG WNAN), such as Zigbee or Worldwide interoperability for microwave access (WiMAX) because they are more flexible and lower invest-

ment cost than wireline approaches. Unfortunately, existing SG WNAN solutions still have not solved two significance challengers mentioned above and need more researching contributions.

The objective of our work is to broaden current knowledge of Smart Grid data requirement and communication approach for SG WNAN by proposing a novel Smart Grid NAN data communication by Network Coding technique combining with an Opportunistic routing algorithm to fulfill the Smart Grid QoS requirements. In detail, our research findings answer two following aims: (i) to develop a usefulness and effective QoS model for SG WNAN planning and designing, and (ii) to propose an data gathering scheme using Network Coding technique for SG WNAN.

1.2 Dissertation Structure

My thesis is organized as follow:

Chapter 2 provides the background and theories related to this study. It had been divided into for sections. The first two sections discuss about the Smart Grid communication background. The third section overviews the theory behind Network Coding technique and its existing applications. The last section introduces Network Simulator OMNeT++, which is be used to simulate our proposed ideas in the thesis.

In Chapter 3 we have first proposed new QoS model for Smart Grid applications in Neighborhood Area Network (NAN). In detail, we introduce the QoS metrics: Packet Delivery Ratio, System Reliability and Critical Latency Response and describe their handiness in both communication and electric power domains. Then, we show our S-shaped curve model based on statistic theory, as a simple tool using for planning and designing wireless network approach for Smart Grid NAN. Finally, we have presented the simulation results on common wireless approach based on ZigBee and WiMAX technologies for the network of Smart Meters to prove the correctness of our proposed model.

Chapter 4 discusses the challenges in wireless network for PMU and how we choose suitable solution based on our S-shaped model. The first section introduces the overview of PMUs and many applications based on PMUs. The second section focuses on the most important application State Estimation (SE) for electric grid and the impact of packet loss and delay to the output of estimation algorithm. The PMUs wireless network based on IEEE 802.11 standard for the reference distribution power grid IEEE 37 Test Nodes Feeder is simulated and drawn the S-shaped curve to investigate their best effort delay and network reliability. The last section we discuss the learnt lessons from simulation results.

Chapter 5 we exploit the Network Coding idea for real-time data gathering task in Smart Grid communication. The first section introduces Galois field and its calculation. Then second section represents Max flow - min cut theorem, the theory behind Network Coding, guaranteeing that network can obtain maximum information flow based on applying Network Coding approach. In third section, we propose OHNC method and use Absorbing Markov Chain model to analyze and compare based on our QoS model. We implement the encoding and decoding process of OHNC using Matlab programing the fourth section. The last section we discuss the OHNC peformance results.

Finally, chapter 6 summaries our research findings and suggests relevant research topics for future plan.

1.3 Thesis Contributions

With the aforementioned objective, the contributions of our research are threefold:

1. **Defined a useful QoS metrics to evaluate any candidate wireless communication schemes in SG WNAN;**

   Planning and designing wireless communications systems for Smart Grid NAN requires fully understanding of the interdisciplinary fields of electric power and telecommunication systems. This research is still quite a challenging work because the nature characteristics of the Smart Grid packet requirements have not been explored thoroughly yet. While the QoS requirement are dependent on the power system aspect, ensuring the QoS is the task of the data communication aspect. This makes the legacy QoS metrics for multimedia applications such as voice, data, video is not a suitable assessment tool in Smart Grid applications.

   This research work has designed a new reliability metric for SG WNAN with simultaneous consideration of two important factors: packet delivery ratio and delay of messages. We refer the delay to latency because the efficiency of services in Smart Grid relies highly on the time that message arrives. Based on the Smart Grid data requirements in [3, 7], our new Smart Grid QoS definition is easy to be used to compare and evaluate the network reliability performance of SG WNAN.

2. **Proposed the S-shaped curve between network reliability and delay of message relation as a useful tool for designing communication network in SG WNAN;**

   According to the review of the communication research works for smart grid networks, many efforts are still in the process of building the data network functionality in order to match electric smart grid applications, i.e. power flow monitoring and controlling or demand

respond. Unfortunately, all authors have the common agreement that existing telecommunication networks cannot meet operational requirements for future Smart Grid [1,5,6].

A powerful approach for designing Smart Grid data network is using simulation tools. However, this approach requires co-simulation technique between electric power and communication simultaneously. This raises a critical issue because of the different modeling approaches. While power simulators use the continuous model of time, communication simulators use the discrete time models. In this thesis, we have proposed the S-shaped curve between network reliability and delay of message relation as a simple Smart Grid network design tool. Based on the S-shaped curve plot, we evaluate the performance of any candidate data network solutions for Smart Grid services. In addition, we also predict performance with network size, number of nodes, data concentrators, or relay nodes in SG WNAN so that it satisfies the data requirements. Although we limit our study in Neighborhood Area Network domain, the S-shaped curve can also be used in Smart Grid Wide Area Network or Smart Grid Home Area Network.

3. **Proposed an innovative data communication scheme for SG WNAN which also satisfies both reliability and multi-service priority based on Opportunistic Hybrid Network Coding method.**

   There are still no practical network communication solutions possible for the future Smart Grid, especially for SG WNAN, the bridged communication between customers and utilities. Our contribution in this thesis is to build an innovative SG WNAN. Our proposed OHNC method is based on the retransmission principle scheme to increase the reliability of communications networks, however, the retransmission process of packets occurs at the Encoding nodes in order to reduce latency. Both source and Encoding nodes can apply Network Coding encoding and decoding to packets before forwarding them to destination. Compared to Routing methods, Network Coding technique has been proved that it improves the reliability of network while saves the packets transmission time.

1.4 List of Publications

The research findings in this thesis have been published in the following papers:

- **Journal paper**: Ngoc Thien Le and Watit Benjapolakul, *QoS Metrics Modeling and Analysis for Neighborhood Area Network in Smart Grid Applications*, IEEJ Transactions on Electrical and Electronic Engineering, accept after minor revision, May 13, 2016.
- **Conference paper**: Ngoc Thien Le and Watit Benjapolakul, *Opportunistic Hybrid Network*

Coding Data Gathering Scheme for Non-concurrent Applications in Smart Grid Neighborhood Area Network, ECTI-CON 2016, Chiang Mai, Thailand, accepted for presentation.

- **Journal paper**: Ngoc Thien Le and Watit Benjapolakul, *Network Coding Approach in Smart Grid Communication: A Review and Potential Applications*, in preparation.

CHAPTER II

BACKGROUND AND RELATED THEORIES

In this chapter we describe necessary background and theories which are essential to the discussion on forthcoming chapters.

2.1 Smart Grid NAN Overview

Figure 2.1 illustrates the well-known picture of Smart Grid vision from [8]. The typical Smart Grid communication network infrastructure is designed in a 3 layers hierarchical network, which are Home Area Network (HAN), Neighborhood Area Network (NAN), and Wide Area Network (WAN) [4]. In the WAN layer, the optical network or WiMAX could be considered. In the HAN and NAN domains, a flexible network topology is required to coordinate self-managed nodes with dynamic behaviors. Smart Grid NAN plays important role, as a bridge, of Smart Grid data communication between the HAN and WAN. As shown in Table 2.1, this data network supports connections between the demand side and supply side to transfer the electricity data from customers to suppliers in order to run many Smart Grid applications. In addition, NAN, sometimes called Field Area Network (FAN), also connects many electric devices in the transmission and distribution lines for functions related to monitoring, controlling and protecting the power network. In our view, Smart Grid NAN is the most important network in Smart Grid communication and it needs more research effort to build up a mature communication. In next sub section, we briefly describe two important networks in Smart Grid NAN, the network of smart meters and network of on-line electric devices, and the data requirements for Smart Grid NAN.

Table 2.1: The general concept layers of Smart Grid.

Applications layer	- Distribution Generation - Distribution automation - Flexible Transmission System - Demand Response,...	- Demand Response - Wide area situational awareness - Advance Metering Infrastructure - Electric vehicles,...	- Home Energy Management System - Building Energy Management System - Smart Meters,...
Communication layer	Wide Area Network (WAN) - Fiber network - WiMAX - 3G, LTE,...	Neighbor Area Network (NAN) - Power Line Communication - Fiber network - Zigbee - WiMAX - 3G, LTE,...	Home Area Network (HAN) - Power Line Communication - Zigbee - WiFi,...
Power system layer	**Generation & Transmission side**	**Distribution side**	**Demand side**

2.1.1 Advanced Metering Infrastructure

There is no standard document defining AMI specification, and so it is still open room for development and implementation AMI networks. In general, AMI is the network of smart meters

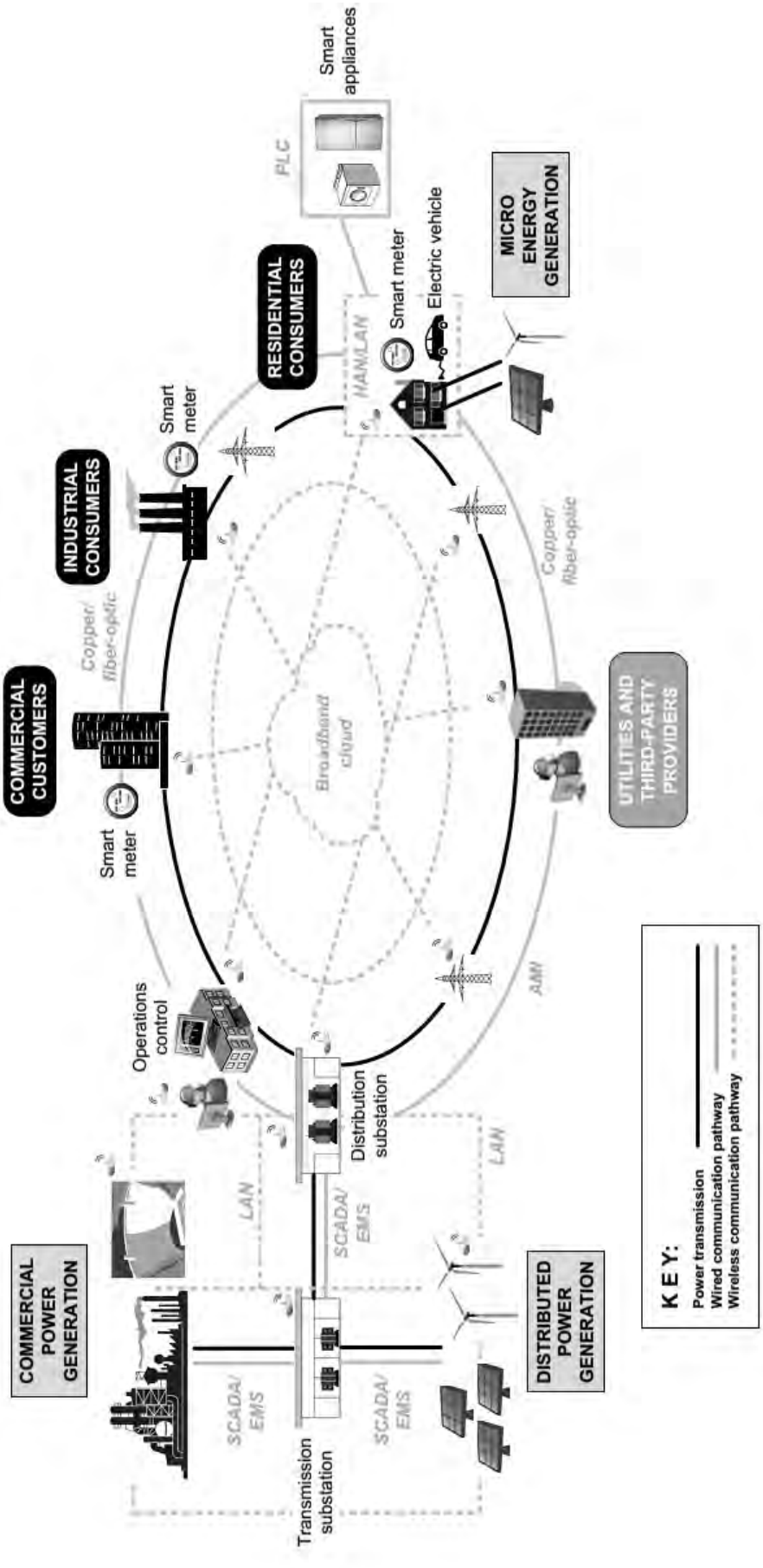

Figure 2.1: Smart Grid diagram concept [8].

at consumer's premises to exchange information between consumers and control center. A smart meter usually has block diagram as in Figure 2.2 and runs the following functions:

- Real time data of electricity use and electric energy generated locally;
- Offering the possibility to read the meter readings both locally and remotely;
- Offering the interconnection between premise-based networks and online grid devices

The purposes of AMI are energy consumption monitoring and improving energy efficiency on distribution grids. Smart meters encourage consumers to change behavior by turning down their electric appliances during peak demand period. These effects are fostered either by exposing consumers to their general consumption patterns or by financial incentives. Energy efficiency can be improved as consumer regulates power consumption based on their demands. In addition, the utility can run the DR services to balance the generation and demand power in the electric grid based on the data from AMI. The demand-side management tries to reduce or shift consumption and hence decrease the peak demand. That is because of the existing grid is designed based on the peak demand rather than the average one. The traditional communication AMI system is usually

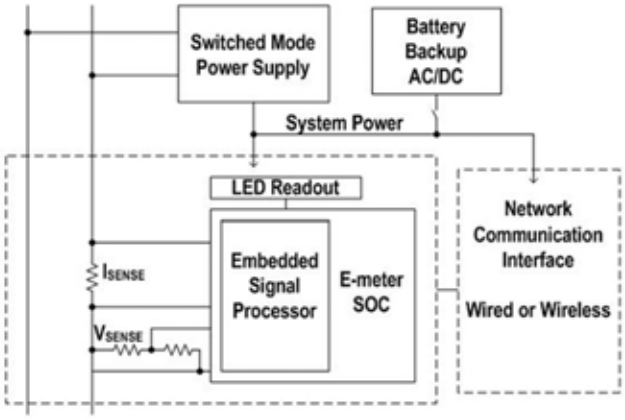

Figure 2.2: Smart Meter node block diagram.

based on communication mechanism over communication interfaces with limited performance both in throughput and reliability, e.g., General Packet Radio Service (GPRS) and Power Line Communication (PLC). Due to the mentioned technical limits, existing AMI implementation concepts provide only basic smart metering functionalities and metering data collection usually not more often than once per day. The next generation of AMI should be real-time data transfer and hence potential wireless approaches can be Zigbee, Long-Term Evolution (LTE) or WiMAX networks.

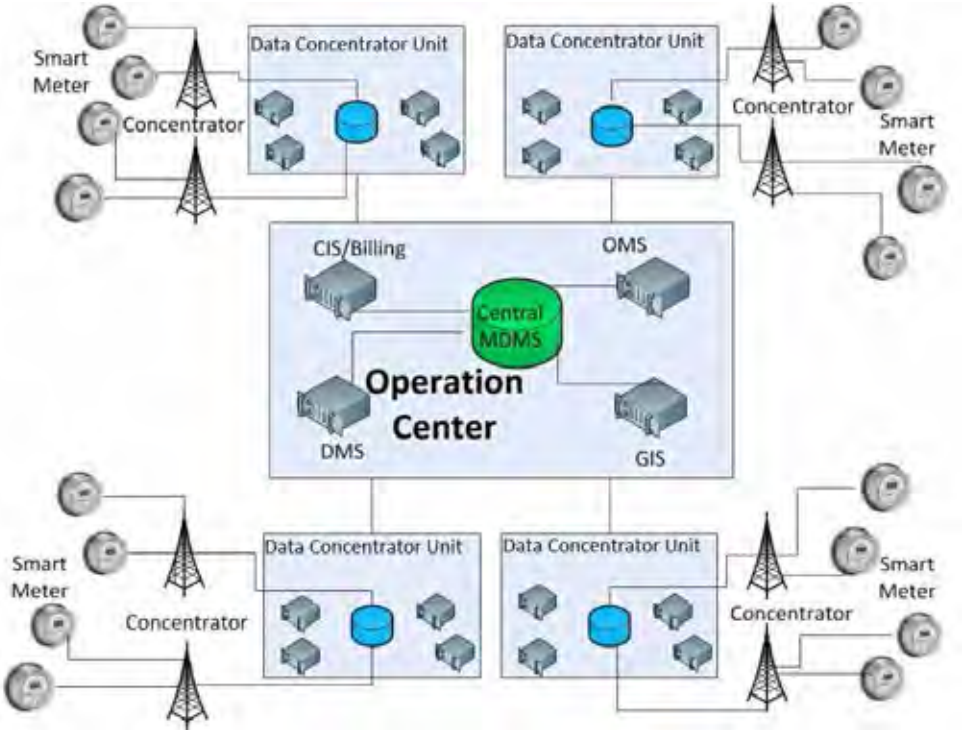

Figure 2.3: An example of AMI network topology (Adapted from [9]).

2.1.2 Distribution Automation and Wide Area Measurement System

The practical definition of Distribution Automation (DA) is the gathering, collecting the measurement data from feeder's devices such as reclosers, switches, capacitor banks, distribution transformers, Intelligent Electronics Device (IED) and the control of those from a DA master control. In legacy power grid, the DA network can be called as the SCADA system.

Unfortunately, when the emerging smart grid deploys a vast number of sensors and actuators on the transmission and distribution grids to both collect usage data and to deliver command and control information, the current SCADA system is incapable of supervising such a demanding scenario. In addition, future smart grids will be both intelligent and adaptive to the changes in the scenario and so will require instantaneous acquisition and transmission of data from different entities in the power system. This means near real-time secure communications is a vital design requirement to convey command and control information between different entities in the smart grid.

The key aspect of WAMS is to provide real-time (in order of milliseconds) monitoring and control of the electrical power grid to prevent any possible blackouts. PMU device has incorporated into a protective relay or other electric devices. In the example diagram of PMU in Figure 2.4, the voltage or current measurements plus phasor information are taken with time

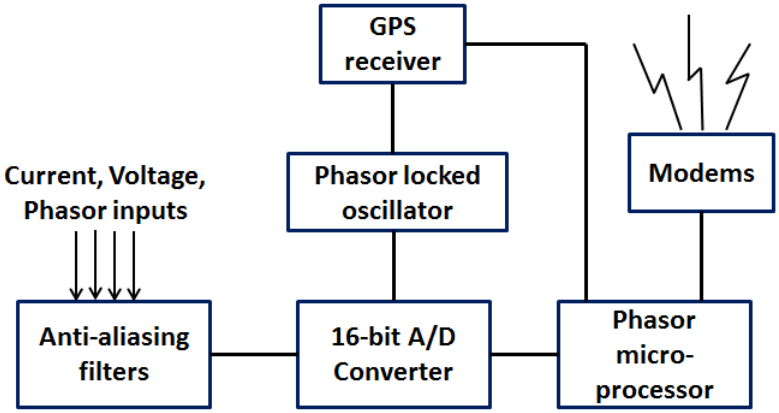

Figure 2.4: Phasor Measurement Unit Block Diagram.

stamps from Global Position System (GPS)-based clocks with microsecond time accuracy. The reporting rate usually four times of electric frequency (50 or 60 Hz). The WAMS will be used to connect PMUs with wide area and dynamic coverage. The major advantage of WAMS over conventional SCADA that provide only local monitoring and control is the larger coverage. The WAMS can transfer sampled phasor data. This data is used to support various functions of the smart grid including state estimation, instability prediction, real-time monitoring, dynamic disturbance recording and data logging, analysis of power system dynamics, and analysis of damping-oscillation. In a typical WAMS architecture, multiple PMUs are connected with a Phasor Data Concentrator (PDC) through regional network. This is referred to as the PMUs-PDC working group. A control center for WAMS collects and aggregates phasor data from multiple PMUs-PDCs working groups through a WAN (e.g., synchronous optical network-synchronous digital hierarchy) as in Figure 2.5. Because PMU performs continuous data sampling in real time (e.g., 16-bit resolution with maximum 60 samples per second per PMU), congestion and delay are two critical issues in the WAMS. Unlike SCADA, WAMS can monitor the power system state continuously and synchronously. PMU supports high sampling data rate, making WAMS application suitable for the dynamic event management and failure recovery.

2.1.3 Data requirement in Smart Grid

In most Smart Grid applications, the data requirement is that it must be reliable and available everywhere at any time [2, 3, 10]. In order to ensure reliable transfer of time critical information as requirements in Table 2.2, all communication nodes must be contactable regardless of the situation and distances involved. The system must also be capable of automatically managing redundancy and be adaptive to changes in the network topology and surrounding environment. In addition, the Smart Grid data traffic from the data center servers to the remote nodes is much less

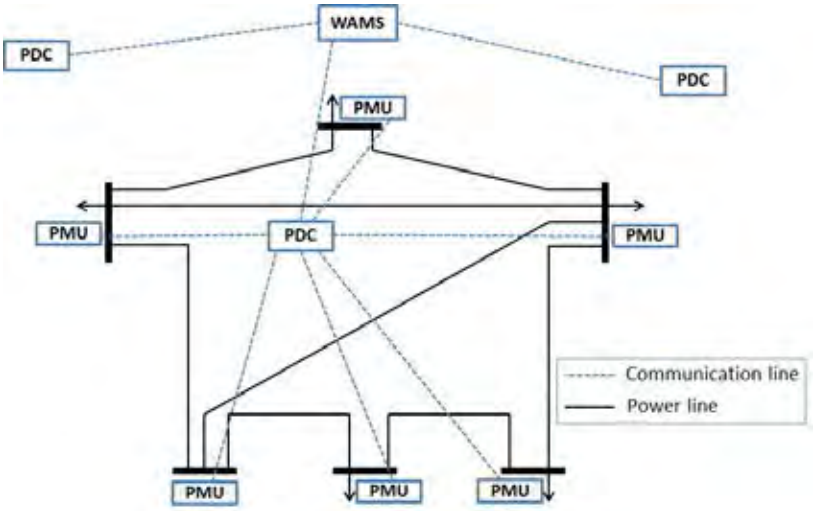

Figure 2.5: Hierarchical architecture example of WAMS.

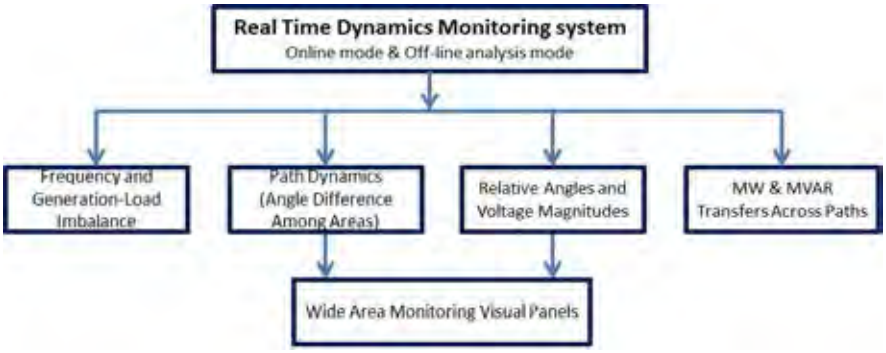

Figure 2.6: Hierarchical architecture example of WAMS applications based on PMUs network.

than the traffic generated from these endpoints. In contrast, the downlink traffic for multimedia network is significantly higher than the uplink traffic. The network designer must take this requirement into account when design the NAN data communication for Smart Grid applications. A remark in the latency requirements of critical applications also in Table 2.2 is that the time is estimated between the source and destination only in a single hop network [11]. Hence, all other delay demands have to be satisfied when using multi-hops network for Smart Grid applications.

As mentioned in Section 1.1, a special characteristic of Smart Grid is the usable data for many services; that means beside the periodic measurement data, there are additional requirement for data during the ”critical” or ”abnormal” events. In Smart Grid context, we define these mission critical applications as in the Definition 2.1. Examples of mission critical events are a power outage in parts or all of the electric distribution services area with PMUs, or an actively Demand Respond for smart meters in the service area due to critical imbalance between demand and energy supply in that area. Table 2.3 summaries the traffic types of AMI for many Smart Grid

applications. The future Smart Grid tends to implement more critical services to make the electric system more intelligent and stable.

Definition 2.1. ***Mission Critical Application***

Mission Critical application is the Smart Grid service with higher priority and more stringer reliability and end to end requirements than the normal Smart Grid services within the same data communication network.

Table 2.2: Requirements of Smart Grid Applications [3, 11].

Application	Reliability	Latency	Bandwidth
Overhead Transmission Line Monitoring	99.0-99.99%	15-200 ms	9.6-56 kbps
AMI	99.0-99.99%	250-1,000 ms	10-100 kbps per node, 500 kbps for backhaul
Wide-Area Situational Awareness Systems (WASA) based on PMU	99.0-99.99%	15-1000 ms	600-1500 kbps
Distribution Automation (DA)	99.0-99.99%	20-200 ms	9.6-56 kbps
Distribution Management	99.0-99.99%	100 ms - 2 sec	9.6-100 kbps
Meter Data Management	99.0%	2,000 ms	56 kbps

Table 2.3: Traffic types for AMI application [11].

AMI traffics	Latency requirement	Application
AMI-Periodic	1,000 ms	Power consumption, Electric billing
AMI-Priority	300 ms	Registration, Recover after outage, Upgrade software
AMI-Critical	250 ms	AMI for Demand Response

From the power system view, the latency requirement in Table 2.2 and Table 2.3 is usually calculated from the cycle of electrical wave. In electric system with frequency $f = 50\ Hz$, the time of one cycle is $T = 1/f = 20\ ms$. In order to keep the stable stage of electric system, any monitoring, controlling and protecting message have to reach the destination within latency requirements as listed in Table 2.2. In general, we have the latency calculation as in Eq. (2.1)

$$Latency = (\tau) * \frac{1}{f} \tag{2.1}$$

where τ is delay factor (in cycles) which is dependent on particular Smart Grid applications. The smaller the τ is, the more real-time scale Smart Grid network can get.

Figure 2.7 illustrates the comparison on both delay and reliability requirement between Smart Grid and other type of data. Smart Grid is the special case where it is very sensitive on required delay and strict on required reliability. We recall that the Figure 2.7 only mention

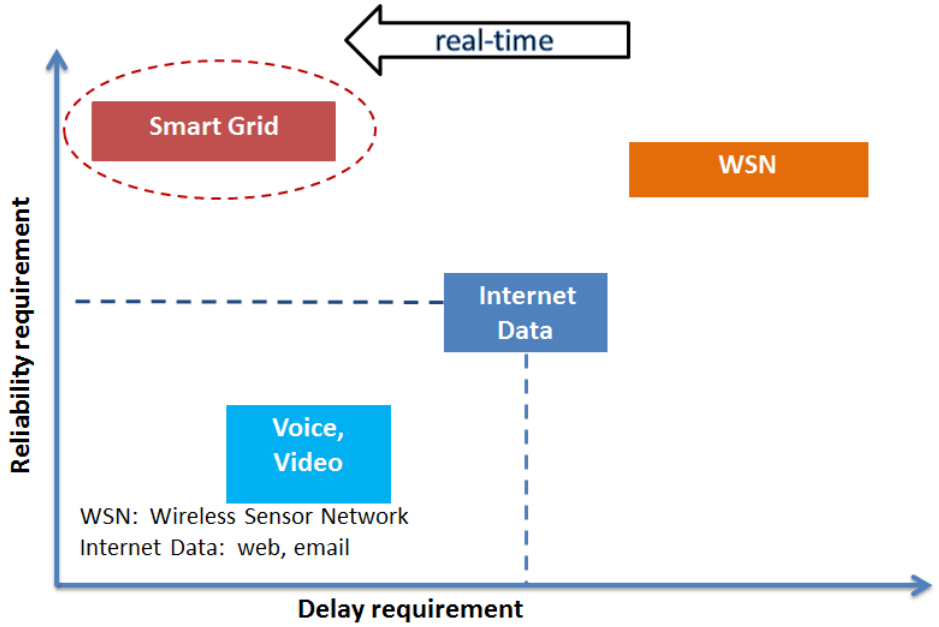

Figure 2.7: Data requirement comparison between Smart Grid and others.

the reliability requirement in telecommunication domain. Communication network reliability is usually measured in terms of *2-terminal*, *k-terminal* or *all-terminal* reliability [12]. The first case, *2-terminal*, is most common, where a source and a sink are able to communicate with each other with a certain probability. The *k-terminal* case is when a set of k nodes in network can communicate. Finally, the *all-terminal* refers to the case when all nodes can communicate with all other nodes.

On the other hand, the reliability in electric power is usually measured in terms of availability of power to the user based on IEEE 1366-2012 Standard [13]. In general, power utilities report outages and quality of energy metrics such as System Average Interruption Duration Index (SAIDI), System Average Interruption Frequency Index (SAIFI) and Customer Average Interruption Duration Index (CAIDI) as belows [13]

- **System Average Interruption Duration Index (SAIDI)**: Ratio of sum of all customeer interruption durations over total number of customer served. This index is measured per year;
- **System Average Interruption Frequency Index (SAIFI)**: Ratio of total number of customer interruptions over total number of customers served. It is usually measured per year by electric power utilities;
- **Customer Average Interruption Duration Index (CAIDI)**:Ratio of sum of all customer interruption durations over total number of customer interruptions. In other words, CAIDI

equals SAIDI divide by SAIFI.

In the Smart Grid context, there are a correlation between reliability term in electric and communication domain, however this relation is still unclear and needs significant research efforts.

2.2 Smart Grid standardization activities

There are significant efforts to make standardization in Smart Grid action plans.

2.2.1 Open Smart Grid (OpenSG)

This standardization document, Smart Grid Networks System Requirements Specification [14], was created by the SG-Network task force. This is a group formed within the Utility Communication Associations international user group (UCAiug) under the Open Smart Grid (OpenSG) technical committee in 2008. They focused on the management requirements for AMI systems. They have released the formation of the SGIPs Priority Action Plan 1 (Internet Protocol for Smart Grid) and Priority Action Plan 2 (Wireless Communications for Smart Grid [15]) and grown a need for a set of non-functional requirements for Smart Grid. The AMI-Net task force re-chartered and changed the task force name to SG-Network to meet these needs.

This work has been shown to identify, articulate and non-functional requirements for communication network within the Smart Grid. While the major use cases for Smart Grid and AMI are well known, the industry was still lacked a set of documentation that specified from business operations point of view critical aspects of these use cases such as: How Often, Reliability, Latency, etc. The goal of this document is to provide an operational perspective for how utilities and other Smart Grid entities could use communication technologies in the Smart Grid context to solve business issues.

2.2.2 NIST Smart Grid Framework

The National Institute of Standards and Technology has released this document, NIST framework and roadmap for smart grid interoperability standards, Release 3.0 [1], updated their progress made from 2012, and reviewed the achievements and direction of Smart Grid. In the Release 3.0, Smart Grid is considered from the perspective of cyber-physical systems that combines computer-based communication, controlling, and command with physical equipments to improved reliability, resiliency, performance and the awareness user and supplier. Main achievements in smart grid architecture, security, and testing and certification are also covered in Release

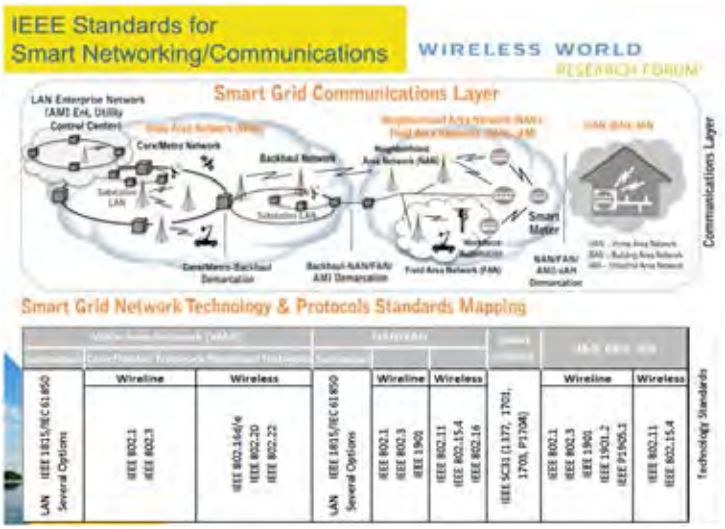

Figure 2.8: IEEE Protocols Standards Communication Mapping [8].

3.0. Additional standards from the Priority Action Plans (PAPs) fill the shortcomings identified in Release 2.0 and have been added to the list of identified Smart Grid standards.

However, Smart Grid will evolve as new requirements and technologies emerge. Engaging the diverse communities of smart grid stakeholders, the public-private partnership establishes a robust ongoing mechanism to develop requirements to guide the standardization efforts now spanning more than 25 standards-development organizations and standards-setting organizations.

2.2.3 IEEE Vision for Smart Grid Communications

This IEEE Vision For Smart Grid Communications: 2030 and Beyond [8] is a full vision document by IEEE Standards Association. Authors have agreed that Information and Communication Technology is a key enabling technology for the Smart Grid. They believe that the power grid will utilize advances in communications because information exchange requirements will scale up for the Smart Grid. Therefore, one of their main target is to develop Smart Grid Protocols Standards as shown partly in Figure 2.8. Smart Grid communication will help to improve demand forecasting, enable self-healing from power blackout events, facilitate active participation by consumers in demand-response schemes, and provide resilience against both physical and cyber attacks. Smart Grid communication will also improve quality of power, allow easy integration of renewable energy sources such as wind farms, solar farms into the electric grid, foster innovation to enable upcoming services, products and markets, assist in optimization of assets, and improve operating efficiency.

2.3 Network Coding

2.3.1 Overview

Network Coding, initially proposed by Ahlswede et al. [16] in 2000, is an innovation technique to significantly increase the reliability and the throughput of the channels, especially in noisy channels. The basic idea behind Network Coding is to consider data in the network not as immutable bits and hence change the function of relay routers from store and forward scheme to compute and forward [17]. As mentioned in Definition 2.2, the relay now mixes the packets in its queue using linear equation before forwarding new mixed packet. Since its publication, Network Coding has attracted a great interest in researchers to a wide data application ranges such as distributed storage, file transfer and peer to peer networking.

In Smart Grid communication applications, recent scholars [18] and [19] also utilize Network Coding technique to improve the network's reliability and throughput. We give more details about these existing methods in the related works section.

Definition 2.2. ***Network Coding***

Network Coding is a method to increase the amount of information flow in a network by permitting relay nodes to compute the algebraic operations on the incoming data before forwarding it [16, 17].

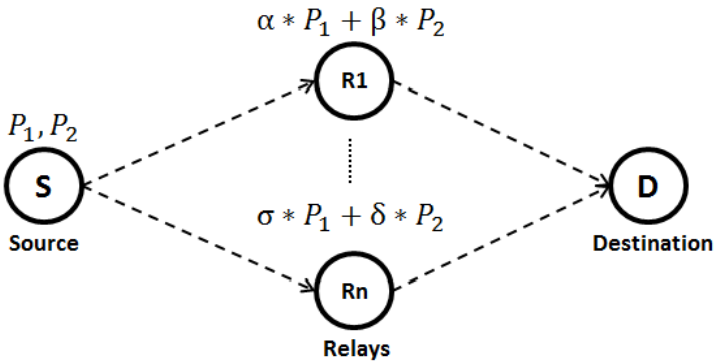

Figure 2.9: The concept of Intra-Source Network Coding to improve reliability [20].

Based on the source of mixed packets, Network Coding can be separated by Intra-Source Network Coding (Intra-Source NC) and Inter-Source Network Coding (Inter-Source NC). In Intra-Source NC, code packets come from same source as in Figure 2.9 [20]. The relay nodes can encode the packets using linear equations. The decode process occurs at the destination. Intra-Source NC is suitable for lossy links in a dynamic topology network. Figure 2.10 describes

the operation of Inter-Source NC. The source of coded packets comes from more than two sources (e.g. Alice and Bod) [21]. The router hearing two sources will perform encode packets whenever they come to its queue. The main benefit of this Network Coding scheme is reducing the transmission slot (time), hence improves the throughputs.
For both Network Coding techniques, the sink only solves the linear equations to recover original

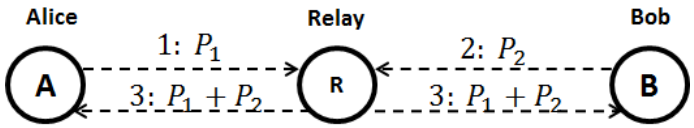

Figure 2.10: The concept of Inter-Source Network Coding to improve throughput [21].

packets if these equations are linear-independent. However, if we perform Network Coding in binary case (with 0 and 1 coefficients), the probability of independent equations will be low. To address this problem, Professor Medard et al. have proposed RLNC [22] which all encoding and decoding calculations are represented in finite Galois field. We give an example of RLNC with only two packets in Figure 2.11. The decoding process at destination node uses Gaussian elimination algorithm. In RLNC, the coefficients α_i, β_i are chosen randomly from finite Galois field. The throughput of RLNC is higher than in binary case. In general, when we increase the Galois field, the RLNC comes closer to maximum flow for each source.

Despite the success of Network Coding applications in multimedia streaming and data storage and distribution, most of the current Network Coding approach faces with two issues in order to apply to a practical implementation [17]. Because of using the linear combination of packets, the coefficients must be included in every coded packet and integrated into the header. It makes higher header per data ratio and lead to reduction of the throughput. The second challenge with Network Coding is the complexity of decoding algorithm. Because every node in the network should perform decode and recode functions. It affects to the end-to-end delay of the message. In Smart Grid NAN context, we also need to solve those challenges to get a trade-off solution.

2.3.2 RLNC example

In this subsection we give an example of encoding and decoding process using Random Linear Network Coding as in Figure 2.11. For simplicity, we use the Galois field $GF(2^3)$, which includes 8 elements $\{0, 1, ..., 7\}$. Recall that all packets and coefficients are represented in Galois field. (We have used the ***gf*** function in Matlab to calculation).

- **At source node** We assume that $p_1 = 3, p_2 = 5$. Source s generates two sets of random

coefficients $(\alpha_1, \beta_1) = (2, 5)$, $(\alpha_2, \beta_2) = (0, 6)$. The encoding process is as following (Figure 2.11a)

$$\text{First encoded packet: } \alpha_1.p_1 + \beta_1.p_2 = 2.3 + 5.5 = 6 + 7 = 1 \tag{2.2}$$

$$\text{Second encoded packet: } \alpha_2.p_1 + \beta_2.p_2 = 0.3 + 6.5 = 0 + 3 = 3 \tag{2.3}$$

Source then sends these two encoded packets into network.

- **At relay node** We assume that relay R overhears first encoded packet. Then it re-encodes this encoded packets as following (Figure 2.11b)

$$\begin{aligned} \text{Re-encode an encoded packet: } & \alpha'(\alpha_1.p_1) + \beta'(\beta_1.p_2) = \\ & = (\alpha'.\alpha_1).p_1 + (\beta'.\beta_1).p_2 = \\ & = \alpha_3.p_1 + \beta_3.p_2 = \\ & = 1.3 + 4.5 = 3 + 2 = 1 \end{aligned} \tag{2.4}$$

- **At destination node** We assume that node D receives three encoded packets $\{1, 3, 1\}$ together with the coefficient vectors in their headers $\{(\alpha_1, \beta_1), (\alpha_2, \beta_2), (\alpha_3, \beta_3)\}$. To recover packets p_1 and p_2, node D applies Gaussian elimination for two over three linear independent equations as below (Figure 2.11c)

$$\begin{bmatrix} 1 \\ 3 \\ 1 \end{bmatrix} = \begin{bmatrix} \alpha_1 & \beta_1 \\ \alpha_2 & \beta_2 \\ \alpha_3 & \beta_3 \end{bmatrix} \cdot \begin{bmatrix} p_1 \\ p_2 \end{bmatrix} \tag{2.5}$$

$$\begin{bmatrix} \alpha_1 & \beta_1 \\ \alpha_2 & \beta_2 \\ \alpha_3 & \beta_3 \end{bmatrix}^{-1} \cdot \begin{bmatrix} 1 \\ 3 \\ 1 \end{bmatrix} = \begin{bmatrix} p_1 \\ p_2 \end{bmatrix} \tag{2.6}$$

In order to improve reliability, source node s can send more than two encoded packets. We call these extra encoded packets as redundant packets.

2.4 OMNeT++ Network Simulator Framework

OMNeT++ (Objective Modular Network Testbest in C++) [23] is the open source Network Discrete Event Simulator. The version we have used in this thesis is OMNeT++ 4.6. The interested scholars is referred to *http://www.omnetpp.org* for more details.

The basic component of OMNeT++ are *modules*, which can be *single* or *compound* mod-

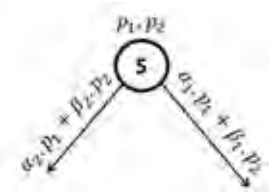

(a) Source encodes p_1, p_2 to product two encoded packets by creating two independent linear equations for two transmission paths.

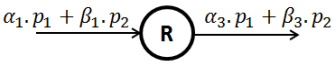

(b) Relay node catches a encoded packets and re-encodes it.

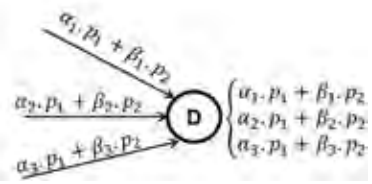

(c) Destination needs two over three independent linear equations to decode p_1, p_2 packets.

Figure 2.11: The process of Random Linear Network Coding over finite Galois field.

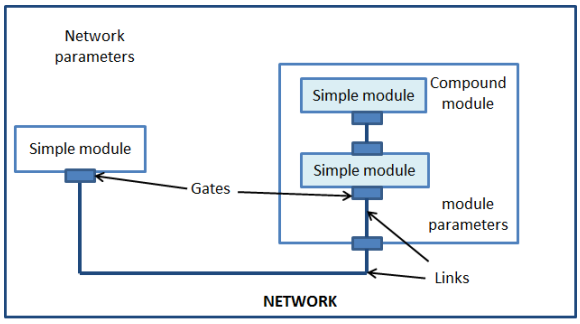

Figure 2.12: A typical OMNeT++ modules and network.

ules. The compound module includes many single modules as in Figure 2.12. Every module communicates to others through *links* and *messages*. The interface of module is *gates*, where it sends and receives messages. A network is a particular compound module, with no gates to the outside world, which sits at the top of the hierarchy. Connections are characterized by a bit rate, delay and loss rate, and cannot bypass module hierarchy: with reference to Figure 1, simple module 3 cannot connect to 2, but must instead pass through the compound module gate. Simple modules implement model behavior. Although each simple module can run as an independent coroutine, the most common approach is to provide them with event handlers, which are called by the simulation kernel when modules receive a message. Besides handlers, simple modules have an initialization function and a finalization function, often used to write results to a file at the end of the simulation. The kernel includes an event queue, whose events correspond to messages (including those a module sends to itself). OMNeT++ allows one to keep a models implementation, description and parameter values separate. The implementation (or behavior) is coded in C++.

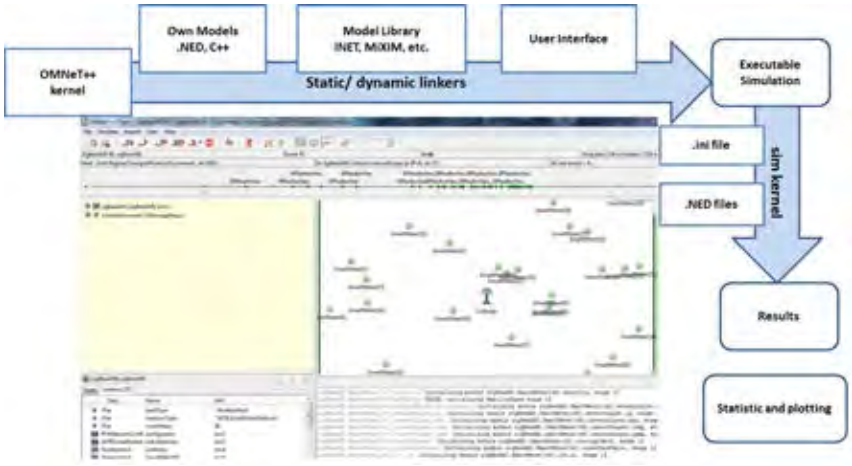

Figure 2.13: OMNeT++ network simulation workflow.

The description (i.e., gates, connections and parameter definition) is expressed in files written in Network Description (NED) language. The parameter values are written in initialization (INI) files. NED is a declarative language, which exploits inheritance and interfaces, and it is fully convertible (back and forth) into XML. NED allows one to write parametric topologies, e.g. a ring or tree of variable size. NED files can be edited both textually and graphically (through a Graphic User Interface, GUI), switching between the two views at any time. INI files contain the values of the parameters that will be used to initialize the model. For the same parameter, multiple values or intervals can be specified.

As far as coding is concerned, OMNeT++ comes with an IDE, derived from Eclipse, which facilitates debugging. In fact, modules can be inspected, textual output of single modules can be turned on/off during execution, and the flow of messages can be visualized in an animation, all of which occurs automatically. Events can be logged and displayed on a time chart, which makes it easy to pinpoint the causes or consequences of any given event.

As for workflow automation, OMNeT++ clearly separates models (i.e., C++ and NED files) from studies. Studies are generated from INI files, by automatically making the Cartesian product of all the parameter values and, possibly, generating replicas of the same instance with different seeds for the random number generators. Note that the IDE allows one to launch and manage multiple runs in parallel, exploiting multiple CPUs or cores, so as to reduce the execution time of a simulation study. Finally, data analysis is rule-based: the user only needs to specify the files and folders she wants to extract data from, and the recipe to filter and/or aggregate data. The IDE automatically updates and re-draws graphs when simulations are rerun or new data become available.

CHAPTER III

QUALITY OF SERVICE MODELING FOR SMART GRID WIRELESS NAN APPLICATIONS

3.1 Introduction

Because Smart Grid network is still in developing step, designing an efficient QoS model dedicated for SG WNAN communication architecture has attracted a great interest from researchers. Most of the current Smart Grid QoS provisioning models [7, 24–26] choose the mapping method from electrical to telecommunication view. In particular, the expected Smart Grid services requirements are based on the industry knowledge, and electrical engineering judgments. Then, they change these demands into VoIP QoS class [7] or Internet Protocol (IP) class [25]. Unfortunately, their QoSs models only list the qualitative requirements hence they are difficult to be used in Smart Grid network planning, designing and management. Furthermore, these approaches did not mention about how to handle the QoS of different Smart Grid applications in the same network.

Recent QoS studies in Smart Grid focused on the routing problem aspect to satisfy the data requirements [27–31]. The common approach in these research works is adapting the existing routing algorithm in different environment, such as Wireless Sensor Network (WSN) [30, 31] to Smart Grid by considering the Smart Grid QoS metrics in routing decision algorithms. Although Smart Grid QoS for routing methods can handle different applications in the same network, the optimization issue will appear when routing methods have taken into account many QoS constraints such as reliability, data size, and transmission rate.

In this chapter we first propose an innovative QoS metric for SG WNAN. We design QoS based on the mapping method as in [7, 24–26]. However, what we will actually do is the same as other works that have been done in existing Public Switching Telephone Network, Internet or Mobile networks, that is we should well understand the specific nature characteristics and traffics of elements in Smart Grid before designing the suitable data communication scheme. Our proposed QoS includes reliability, latency and critical latency response parameters, their definitions of which are more flexible to Smart Grid requirement than other current ones. We also present the relationship model between system reliability and latency as a graph from statistic viewpoint, named S-shaped curve. Our graph model provides a very simple tool to evaluate the

QoS parameters that a network can support with many Smart Grid applications. Hence, it helps to save time and cost in planning and designing SG WNAN.

The remains of this chapter are organized as follows. In section 3.2, we represent the related works in QoS for Smart Grid communication systems and our arguments. Our proposed QoS metrics for SG WNAN are described in section 3.3. In section 3.4, we analyze and model our proposed metrics into the QoS plot, named S-shaped curve, as a planning and designing tool for SG WNAN. We then evaluate our proposed S-shaped curve by simulation of AMI based ZigBee and WiMAX approaches using INET Framework [32] in OMNeT++ simulator [23] in section 3.5. Finally, we conclude our findings in conclusion section 3.6.

3.2 Related Works

This section reviews the QoS models and approaches for data management in Smart Grid applications. Basically, there are two research interests as follows

3.2.1 QoS based on electrical service requirements

In general, this QoS methods [7, 24–26] base on the requirements in the electrical applications domain then map them to the QoS needs in telecommunication domain. In Alcatel-Lucent QoS document [7] the authors have used the QoS in VoIP application as the reference source for different services QoS Smart Grid. In [24, 25] they have quantized the QoS Smart Grid priority into critical, high, low, very low levels then map to the existing QoS of Internet Protocol (IP). Finally, the authors in [26] have divided smart grid data into normal, abnormal, and emergency for many priority queues in router. They also have improved the QoS-MAC IEEE 802.15.4 to manage the delay, throughput and collision rate requirements in Distribution Monitoring application. Most of the reviewed QoS models here only list the qualitative requirements. As a result, it is difficult to handle and monitor these QoS metrics in any real Smart Grid networks.

3.2.2 QoS for routing in Smart Grid network

This QoS approach focuses on routing aspect of network to guarantee data transfers contracts in Smart Grid. The study in [27] and [30] have proposed QoS routing schemes for a particular Smart Grid application. Husheng Li et al. [27] have used multiple QoS-aware routing, named Optimized Multi-Constrained Routing (OMCR), for Load Price application. The QoS method [30] in wireless environment considers throughput and transmission latency requirement for Smart Meter Data Collection based on reinforcement learning technique. Another wireless QoS routing scheme in [29] has considered the interference and delay for packets in multi hop

network. All routing algorithms in these methods have to due with optimization problems, known as NP-Hard problems (Non-deterministic Polynomial-time Hard), when they want to find the solution for their routing schemes within two or more constraints factors.

Other QoS routing solutions [28, 31] have guaranteed the requirements of different Smart Grid service needs in the same communication network. The authors in [28] first have proposed Allocating QoS Resources called Multi-Gateway backup network scheme to handle concurrent Smart Grid applications. Then, they have presented QoS aware routing based on the air time cost metrics of different Smart Grid services. Actually, they have defined this metric by mapping from Smart Grid data size and transmission rate requirements in order to simplify routing decision. The study in [31] survey the single path and multi path QoS aware routings of Wireless Sensor Network in Smart Grid. In details, they have tested the routing performance under both reliability and timeliness domains in harsh environment conditions to evaluate their capability in Smart Grid.

From these efforts above, it can be obviously seen that the QoS for routing approaches do not provide any tools or models to handle and monitor the data transfer in Smart Grid network, especially in normal and abnormal conditions. In addition, these approaches face with the optimization problem in designing efficiency routing algorithms. Therefore, our model follows the data requirements in electrical domain to provide more convenient Smart Grid QoS model.

3.3 Proposed QoS metrics for SG WNAN

Given the nature characteristics of Smart Grid's message and data traffic, taking into account the requirements for electric distributed control system, we argue that existing QoS measurements are not suitable to handle data transmission in Smart Grid NAN. Therefore, we define new class of QoS metrics for Smart Grid application in NAN domain. We name these factors as Latency of message, Reliability and Critical Latency Response and give their definitions in the subsections below. For convenience, we summarize all the notations in Table 3.1.

3.3.1 Latency of Smart Grid messages

In NAN, the time when message comes to the destination node plays a vital role in Smart Grid applications. This timeliness factor not only affects the performance of data network but also has a deep impact on the stability in electric services through many applications such as real time power flow control, or phasor distribution system monitoring. However, the existing networks were not designed with the communication latency performance as the first priority and hence they may not meet the strict delay demand of Smart Grid.

Table 3.1: Notation Summary.

Notation	Description
N	The number of nodes in the wireless SG NAN
DCU	Data Concentrator Unit, or collector node
s_i	A certain node i
p_i	A certain packet from node i
P_{G_i}	Number of packets generated at source node i (excluding copied packets)
P_{R_i}	Number of packets generated at node i successfully received by collector (excluding duplicated packets)
P_G	Number of packets generated from all source nodes (excluding copied packets)
P_R	Number of packets successfully received by collector (excluding duplicated packets)
P_S	Number of packets in network going to the collector
β	Probability of a successfully received packet by collector, $[0, 1]$
HD	Hard Delay service requirement
SD	Soft Delay service requirement
τ, τ_{req}	Required delay variable, a particular required delay value
PDR	Packet Delivery Ratio, $[0, 1]$
R, R_{req}	System reliability value, a particular reliability requirement, $[0, 1]$
$\triangle_c$	Latency Response of critical service

In fact, different services in Smart Grid have particular delay requirements. Some services do not accept out-date message, while others can use old messages within several cycles. Therefore, we redefine the delay metrics in the following definitions.

Definition 3.1 (Hard Delay Requirement (HD))**.** *The message of service which has hard delay requirement becomes useless after its delay has passed even it arrived destination successfully.*

Definition 3.2 (Soft Delay Requirement (SD))**.** *The message of service which has soft delay requirement decreases its degree of usefulness with the time after the delay requirement has passed.*

In comparison with existing latency or delay metrics, our delay definition has more nature features from electrical view. Firstly, the delay requirement is inherited from the electric applications and measured in cycles of electric wave. Secondly, while we take care of the delay requirement, we also know the required bandwidth of network based on the calculation in Eq.(3.1).

$$BW_{req} = S * (8\frac{bits}{byte}) * (\frac{1}{\tau_{req}}) * N \tag{3.1}$$

where S, N, and τ_{req} are the service's data size in bytes, the number of nodes, and delay requirement, respectively. In this scene, the delay metric guarantees both time and bandwidth requirements of the communication system. This brings a simple tool to evaluate QoS of the network for Smart Grid as we present in details later.

Based on the above definitions, we can decide easily which Smart Grid services have the particular delay requirement. The Hard Delay will be applied to the applications which need the messages on time such as Mission Critical applications, while the Soft Delay will be applied to the applications which can use the out-date messages to estimate or approximate the values. We list some typical Smart Grid applications based on our delay classification in Table 3.2. Many future Smart Grid applications also can apply this criteria. Our delay definitions can be useful criteria for network designer to consider which Smart Grid services that the data communication will support.

3.3.2 Packet Delivery Ratio (PDR)

PDR can be calculated in Eq. (3.2), where P_G is the total number of packets generated by source nodes and P_R is the total number of successfully received packets at the collector (DCU). Note that we define the packet is received successfully when it arrives at the collector's queue. In fact, the arrived Smart Grid packet may be no-errors or with errors. However, because the packet size of Smart Grid application is usually smaller than other media, so Forward Error Correction (FEC) techniques can be applied to correct the errors efficiently [2].

Definition 3.3 (Packet Delivery Ratio (PDR))**.** *Packet Delivery Ratio of a Smart Grid NAN is defined as the ratio of total number of packets successfully received by collector, P_R, and the total number of packets generated by Smart Grid source nodes, P_G.*

$$PDR = \frac{\sum_{i=1}^{N} P_{R_i}}{\sum_{i=1}^{N} P_{G_i}} = \frac{P_R}{P_G} \tag{3.2}$$

In Network Coding technique, packets after generated can be mixed using linear combination to create many coded packets for transmission. When applying Equation (3.2) with Network Coding technique, we only take care the packets before and after performing encoding and decoding only.

Table 3.2: An example Smart Grid services classification.

Smart Grid networks	Hard Delay	Soft Delay
PMUs	Operator alert	State estimation
	Real time power flow control	Dynamic Line Rating
	System restoration	
AMI network	Electric Billing	Demand Response
	Upgrade software	Voltage control

3.3.3 System Reliability

Motivated by the fact that many existing QoS models in Smart Grid are adapted from only communication aspect, we propose an innovative method for calculation of Smart Grid system reliability that can cover both communication and electric domains based on HD and SD as below.

Firstly, we define the Smart Grid system reliability metric from the well-known original reliability definition in computer systems of Sahner et al. in [33]. It is defined as the probability of system that can perform its functions successfully for a given time duration. In fact, this definition is well suitable for Smart Grid NAN as their reliability and stable levels are dependent deeply on the time when message comes. Therefore, we redefine the system reliability factor as in Definition 3.4.

Definition 3.4 (System Reliability (R))**.** *The system reliability of Smart Grid NAN is the probability that the message can be successfully received by destination (PDR metric) within the delay requirement. If it is received after the delay requirement, the reliability is decreased steeply.*

Secondly, we propose two methods for calculation of Smart Grid system reliability R with HD, $\tau_{HD_{req}}$, and SD, $\tau_{SD_{req}}$ as below.

For calculation with $\tau_{HD_{req}}$, we use the Eq. (3.3)

$$R = \begin{cases} PDR & \tau \leq \tau_{HD_{req}} \\ 0 & \tau > \tau_{HD_{req}} \end{cases} \tag{3.3}$$

For calculation with $\tau_{SD_{req}}$, we use the Eq. (3.4)

$$R = \begin{cases} PDR & \tau \leq \tau_{SD_{req}} \\ \alpha_1 * PDR & \tau_{SD_{req}} < \tau \leq \gamma_1 * \tau_{SD_{req}} \\ \alpha_2 * PDR & \gamma_1 * \tau_{SD_{req}} < \tau \leq \gamma_2 * \tau_{SD_{req}} \\ 0 & \tau > \gamma_2 * \tau_{SD_{req}} \end{cases} \tag{3.4}$$

where we call α_1, α_2 close to 1 the attenuation reliability coefficients ($\alpha_1, \alpha_2 \rightarrow 1$, and $\alpha_2 < \alpha_1 < 1$), and γ_1, γ_2 the data delay sensitivity coefficients which satisfy $1 < \gamma_1 < \gamma_2$.

The system reliability in Eq. (3.3) is the same as conventional reliability definition in communication. Our new idea in Eq. (3.4) is simple and yet effective: PDR represents the QoS metric in communication view. The set of coefficients $\{\tau, (\alpha_1, \alpha_2), (\gamma_1, \gamma_2)\}$ maps the feedback of re-

liability level of data in electric domain to system reliability calculation in Eq. (3.4). τ has two meanings in electric domain and communication domain. On one hand, τ is delay requirement of Smart Grid application. On the other hand, τ is also the delay value of individual message arriving at destination. Attenuation factors α_1, α_2 are the feedback from application that uses out-of-date data reduce Smart Grid system reliability. Finally, data delay sensitivity factors γ_1, γ_2 identify the time after delay requirement has passed with make the results of Smart Grid applications cease to be operationally useful [34]. In this sense, our system reliability metric provides the level of trust for data delivered by Smart Grid NAN.

Examples of applying reliability calculation in Eq. (3.4) vary from Demand Response to State Estimation application. For instance, in a scenario where PMUs are used to send synchronized phasor data for State Estimation. This application uses estimation and prediction algorithms such as Linear State, Polar Non-linear or Least Absolute Value estimation to get the picture of voltage and phasor values of the power grid with the soft required delay of $1,000\ ms$ [34]. If phasor information arrives before $1,000\ ms$, the synchronized phasor estimation result will close to the true value and we can obtain power grid's state in real-time. However, if PMUs messages arrive at collector which have travel time longer than $1,000\ ms$, the correctness of result will reduce gradually and we only obtain a low reliable picture of power grid. By using Eq. (3.4), we have represented the reliability level of State Estimation as a feedback into system reliability calculation in communication domain to investigate the ability of Smart Grid NAN.

3.3.4 Critical Latency Response, $\triangle_c$

Latency is the most crucial requirement in Smart Grid communications, which is the most fundamental distinction between Smart Grid and other communication networks. In practice, a Smart Grid NAN has to support many applications in different moments. Therefore, it is sure that Smart Grid NAN needs some latencies to change the current running application. To measure the delay performance of data communication scheme in case of changing from normal to critical conditions, we define the Critical Latency Response metric as in Definition 3.5. This is the parameter to measure how fast the network responses with critical events.

Definition 3.5 (Critical Latency Response, $\triangle_c$)**.** *The Critical Latency Response, $\triangle_c$, is measured from the time the source sends critical messages to the time it receives successfully acknowledgment messages from collector. $\triangle_c$ can be calculated as in Eq. (3.5).*

$$\triangle_c = \triangle_{r1} + \triangle_{r2} \tag{3.5}$$

Table 3.3: Comparison of existing QoS and our proposed QoS for Smart Grid NAN.

Approach	Metrics	Objects	Remark
Legacy QoS	Reliability, Latency, and Bandwidth	Data, Voice, and Video	Adapted from data communication aspect
Our proposed QoS	Reliability, Delay, and Critical Latency	Monitoring, Controlling and Protecting electric applications	Proposed from nature requirements of Smart Grid applications

where $\triangle_c$ is the critical latency response. $\triangle_{r1}$ is the network latency, which includes transmission, processing, propagation, and queuing delays. $\triangle_{r2}$ is the network changing state latency. This delay is measured from the time when source informs the critical event to its routing paths to the time when all nodes on its paths are ready to support abnormal service. In fact, this is the essential time to active priority routes and queues, or enable some redundancy relays. In general, the critical event in Smart Grid is similar to the ambulance car running on the road situation. Based on its sound and red flash light, cars in front of it have time to serve the available route.

The value of $\triangle_{r1}$ can be identified easily by finding the latency Smart Grid services requirement in Table 2.1. In addition, it also can be classified as Hard or Soft delay as in our aforementioned definitions. However, value of $\triangle_{r2}$ has not been noticed in previous works [7, 24–26]. Hence, this paper firstly identifies the important of $\triangle_{r2}$ requirement. Actually, finding the latency value of $\triangle_{r2}$ is a challenging work because we are still unclear about how long Smart Grid NAN takes to change from normal service supporting to abnormal service supporting in real applications. In the next section, we present the proposed relation between system reliability and delay, including the latency $\triangle_c$, as the framework for any Smart Grid NAN communication solution to satisfy the service's requirements. The comparison of existing QoS methods and our proposed QoS is summarized in Table 3.3.

3.4 System reliability and Delay relation

3.4.1 Relation between P_G, P_S, P_R and τ

Given a Smart Grid communication network scheme of N nodes and one collector for gathering data has the probability of successfully receiving a packet at collector of β, $0 \leq \beta \leq 1$. We

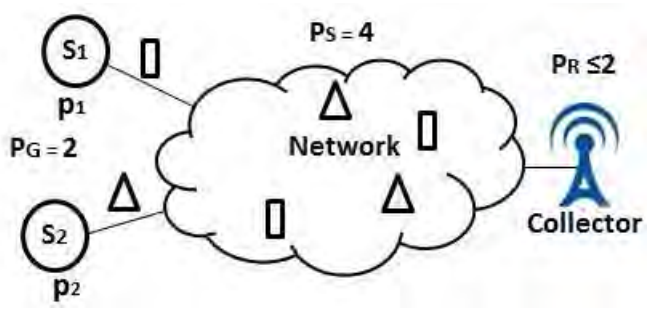

Figure 3.1: An example of system reliability enhancement technique with $P_G = 2$, $P_S = 4$ and $P_R \leq 2$.

assume that all nodes have the same rate of generating packets per second, which is dependent on the Smart Grid service demand. P_G is total number of generated packets from all source nodes. P_R is total number of packets successfully received at collector, excluding duplicated packets. P_S is total number of packets in network going to the collector. Indeed, P_S equals P_G plus the number of copied source packets by relays and the number of retransmission packets from sources. Figure 3.1 gives an example of system reliability enhancement with two generated packets p_1 and p_2 from two sources ($P_G = 2\ packets$). In order to enhance the reliability, relay nodes in network have made another copy of p_1 and another copy of p_2 during they are going to the collector ($P_S = 4\ packets$). As a result, the maximum chance for collector receiving packets from two sources successfully is two ($P_R \leq P_G$). We also assume that Smart Grid NAN has an end-to-end required delay variable τ which is determined by Smart Grid application. For simple calculation, we assume that τ belongs to HD class. Based on system reliability and statistics theories, we represent some lemmas of P_G, P_S, P_R and τ relations as below.

Lemma 3.1 (Ideal network)**.** *We have $P_R = P_S = P_G$ if and only if network has $\beta = 1$ without applying any improving system reliability techniques. We call such network an Ideal network.*

In practical networks, packets loss phenomenon always occurs due to the background noise, or interference channels. Hence, network designers have to improve the number of successfully received packets at destination by using the system reliability techniques. This leads to Lemma 3.2.

Lemma 3.2 (Practical network)**.** *If practical network has $\beta < 1$ and an improving system reliability technique is applied, we always have $P_S \geq P_G \geq P_R$.*

We describe the principles of two popular methods to enhance the system reliability in Fig. 3.2 and Fig. 3.3. The retransmission scheme in Fig. 3.2 is based on the timer in source and feedback Acknowledged (ACK) message in collector. The multi-paths scheme in Fig. 3.3 further improves system reliability by making copy of message and sending it to destination through

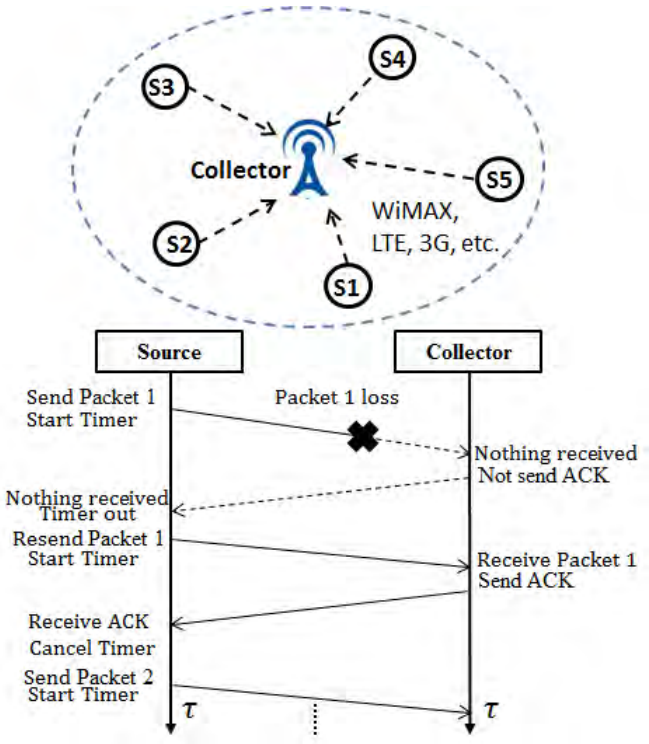

Figure 3.2: Reliability enhancement example using Retransmission scheme.

disjoint paths. In statistic aspect, both techniques have the same principle, that is making many copies of original messages in order to improve the chance that it can be delivered to destination successfully. This leads to Lemma 3.3 belows.

Lemma 3.3 (P_S and P_G, β, τ relation)**.** *The value of P_S can be expressed as function of P_G, β and τ as in Equation (3.6).*

$$P_S = f(P_G, \frac{1}{\beta}, \frac{1}{\tau}) \tag{3.6}$$

In practice, it is difficult to calculate exactly the amount of additional reliability of communication system when adding retransmission scheme or multi-disjoint paths. However, we can easily predict that P_S is proportional to P_G and is inversely proportional to β and τ in Eq. (3.6). As we can see in Fig. 3.2, if we extend the value of delay requirement τ, the number of retransmission loss packet is increased. In Fig. 3.3 collector also has more time waiting for the copied packets from relay nodes or retransmission packets from source with the longer τ. Hence, in both cases, collector will have large chance to collect loss packets again.

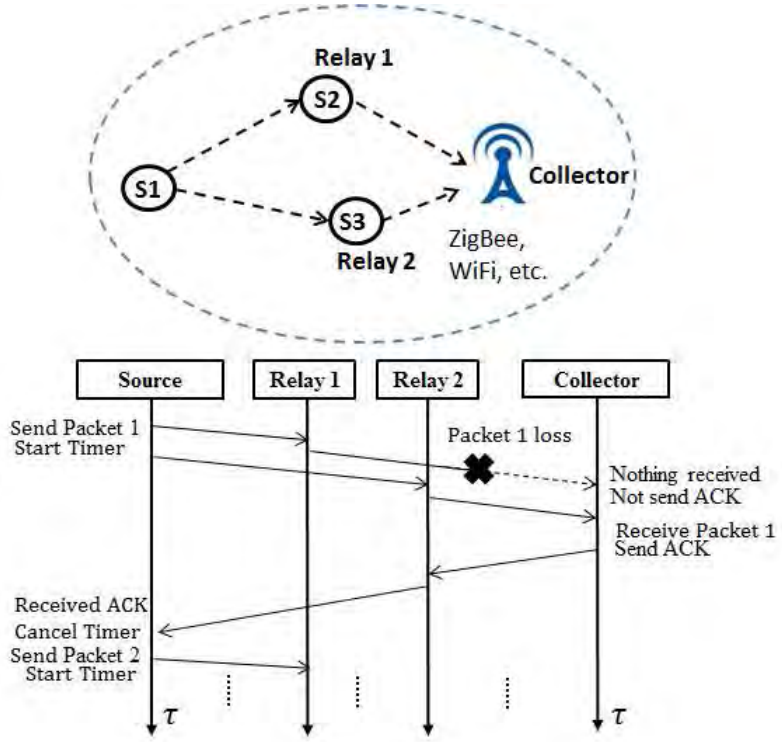

Figure 3.3: Reliability enhancement example using Multi-paths scheme.

3.4.2 S-shaped curve model

From Lemmas 3.1, 3.2, 3.3 in previous subsection, we see that it has the binomial distribution characteristic in the relation between variable P_R and β as follows:

- The number of packets in the network P_S that must be sent are fixed and dependent on the delay value τ;
- Each node sends packets independently;
- Each delivery result only has two outcomes: ”success” or ”failure”;
- The probability of ”success” β of network is the same for each outcome.

Therefore, if we define X as a random variable with Binomial distribution $B(P_R, \beta)$, the probability that X is equal to the value P_R, where $P_R = 1, 2, 3, .., P_G, ..., P_S$, is given by Eq. (3.7).

$$Prob[X = P_R] = \binom{P_S}{P_R} \beta^{P_R} (1-\beta)^{P_S - P_R} \tag{3.7}$$

where binomial coefficient $\binom{P_S}{P_R}$ is calculated by Eq. (3.8).

$$\binom{P_S}{P_R} = \frac{P_S!}{P_R!(P_S - P_R)!} \tag{3.8}$$

Cumulative distribution function (CDF) $F_X(P_R) = Prob[X \leq P_R]$ of Binomial distribution is the summation of all probabilities within a particular range $[0, P_R]$ as in Eq. (3.9).

$$\begin{aligned} F_X(P_S; P_R, \beta) &= Prob[X \leq P_R] = \\ &= \sum_{P_R=0}^{P_S} \binom{P_S}{P_R} \beta^{P_R} (1-\beta)^{P_S - P_R} \end{aligned} \tag{3.9}$$

In general, the CDF of Binomial distribution is usually expressed as the sigmoid function which has the S-shaped curve. The method commonly described this curve uses the logistic model as in Eq. (3.10), where x is a random variable, x_0 is the sigmoid midpoint, k is the steepness of the curve and L is the curve's maximum value [35, 36].

$$f_{sigmoid}(x) = \frac{L}{1 + e^{-k(x - x_0)}} \tag{3.10}$$

It is easy to recognize that variable P_S is dependent on τ, so we can convert P_S to τ without loss of generality meaning. Therefore, based on the standard form of CDF function in Eq. (3.10), we propose the curve which represents the relation between system reliability and delay in Theorem 3.1. The horizontal axis is the delay requirement τ in seconds or milliseconds and the vertical axis is system reliability value which is the ratio from zero to one of (P_R/P_G).

Theorem 3.1. *The relation between the system reliability R in Definition 3.4 and required delay factor τ in Smart Grid communication networks has the same feature as the CDF function of Binomial distribution and is represented by S-shaped curve, with a sigmoid function as in Eq. (3.11).*

$$R\big(\tau; \tau_0, \lambda\big) = \frac{L}{1 + e^{-\lambda(\tau - \tau_0)}} \tag{3.11}$$

where L is the curve's maximum value, τ is the delay variable, τ_0 is the sigmoid midpoint delay which yields $R = 0.5$ and λ is the factor which is dependent on the characteristics of improving system reliability techniques.

Proof. *We can easily prove that the relation between R and τ is a growth process [36]. In particular, when the delay value is equal to zero, it means that message goes to destination immediately. This impossibility makes zero in the reliability.*

If we want R to goes up to one, delay value τ should also rise properly in order to satisfy this grow-up. It means that the communication network uses some techniques such as multi-paths or retransmission to improve the successfully received packets ratio before delay time goes over.

At the midpoint τ_0, the reliability begins increasing exponentially to reach maximum value. In communication view, τ_0 identifies that the bandwidth of network environment is fixed to the Smart Grid bandwidth's service demand.

In practice, the acceleration time of S-shaped curve to reach the required reliability in an amount of time is an important factor to evaluate the system performance. In order to use this factor, we use Fisher-Pry technique [37] to transform S-shaped curves to linear lines. From Eq. (3.11) we have

$$(\frac{L}{R}) = 1 + e^{-\lambda(\tau-\tau_0)} \tag{3.12}$$

$$(\frac{L}{R}) - 1 = \frac{(L-R)}{R} = e^{-\lambda(\tau-\tau_0)} \tag{3.13}$$

$$\frac{R}{(L-R)} = e^{\lambda(\tau-\tau_0)} \tag{3.14}$$

Hence,

$$ln(\frac{R}{L-R}) = \lambda(\tau-\tau_0) \tag{3.15}$$

The right hand side of Eq. (3.15) is the linear version of S-shaped curve with the slope λ. Plotting Eq. (3.15) produces a straight line hence we can compare many acceleration times of S-shaped curves rapidly. However in the performance evaluations part, we limit the value of the left hand side of Eq. (3.15) around 10, when $R \approx 0.9999L$, to compare the acceleration times of S-shaped curves easily.

Based on the Theorem 3.1, we draw the example S-shaped curves for AMI and PMU applications in Fig. 3.4 and Fig. 3.5 respectively. We assume AMI-Periodic service needs hard required delay and PMU-State Estimation has soft required delay. We also assume the example parameters in Eq. (3.4) as in Table 3.4. Actually, the correct parameters are dependent on the estimation algorithm used in State Estimation [34]. We first apply four constraints below to find the approximated parameters λ and τ_0 for the curve in Fig. 3.4 by parameter fitting curve tool in Matlab. Then, we apply the Eq. (3.4) for the result curve to obtain the curve for PMU State Estimation in Fig. 3.5. The detail constraints are given in Table 3.4.

- To ensure the stability of services, we assume that $\tau_0 = (0.5) * \tau_{req}$; i.e. AMI-Periodic has $\tau_0 = (0.5) * \tau_{req} = (0.5) * 1 = 500\ ms$;
- Reliability value $R = 0$ at $\tau = 0\ (s)$;
- $R = R_{req}$ at τ_{req}; i.e. AMI-Periodic has $R_{req} = 0.99$ at $\tau_{req} = 1,000\ ms$;
- $L = 1$ for all services.

Table 3.4: The detail constraints for Smart Grid applications.

Application	**Reliability at $\tau = 0$**	**Reliability at τ_0**	$\tau_0 = = 0.5 * \tau_{req}$	**L**	**Parameter**	**Delay**
AMI- -Periodic	0	0.99	500 ms	1	-	Hard
PMU- -State Estimation	0	0.99	500 ms	1	$\alpha_1 = 0.98$ $\alpha_2 = 0.95$ $\gamma_1 = 1.25$ $\gamma_2 = 1.5$	Soft

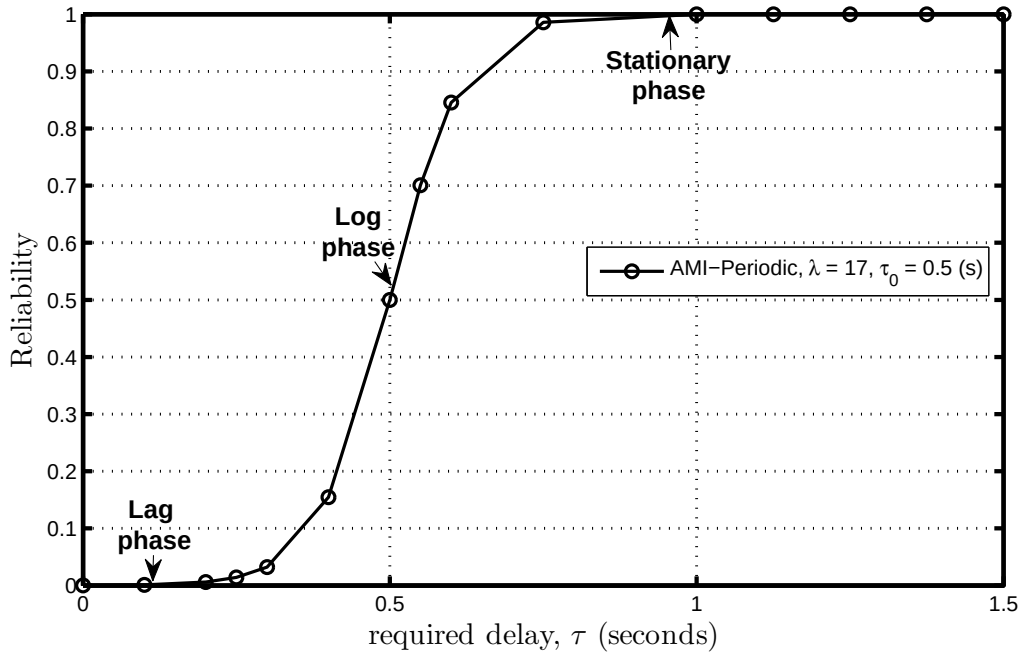

Figure 3.4: S-shaped curve of AMI Periodic in Table 3.4.

We note that these curves just represent the example curves that a particular network should satisfy to support Smart Grid applications. For different network approaches, these curves will change τ_0 and λ values. Our model is effective in Smart Grid network design because it can show fully the system behavior. We highlight the meaning of every phase as following:

- **Lag phase**: This phase has the very slow system reliability growth due to the Smart Grid channel bandwidth is less than the service bandwidth requirement.
- **Log phase**: This phase has the fastest system reliability growth because the longer required delay makes smaller service bandwidth demand. Hence, the percentage of packets delivered by collector increases exponentially.
- **Stationary phase**: Smart Grid NAN shows the highest system reliability ability that can support Smart Grid applications in this phase.

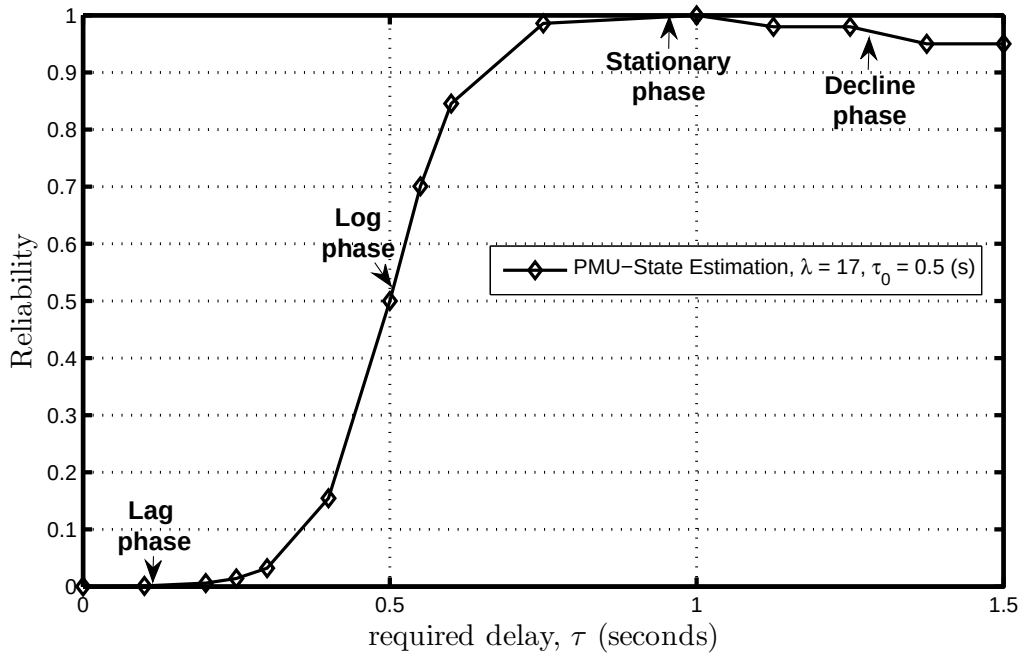

Figure 3.5: S-shaped curve of State Estimation in Table 3.4.

- **Decline phase** (in Fig. 3.5): The Smart Grid NAN system reliability decreases gradually in this phase. This reduction reflects the effect of out-of-date message to the accuracy of the output from State Estimation service having soft required delay as described in example in subsection 3.3.3.

We plot the linearized S-shaped curve of the S-shaped in both Fig. 3.4 and Fig. 3.5 as in Fig. 3.6. The acceleration time identifies the required time to increase system reliability level in the Log phase. We easily conclude that the less acceleration time, the more useful of system reliability enhancement technique.

The S-shaped curve establishes a useful mathematical base for network designers to design and evaluate the network communication approach for Smart Grid. We list two benefits of our model in Smart Grid network designing and planning as described below:

(i) Our S-shaped model is simple and robust by capturing system reliability, delay and bandwidth requirements into one plot. Therefore, Smart Grid engineer can forecast easily the QoS that can be supported in both communication and electric domains of any Smart Grid NANs solutions before deployment;

(ii) We can easily study the impact of reliability enhancement technique because our S-shaped model can fully investigate its effects by using S-shaped curve and its linearized curve.

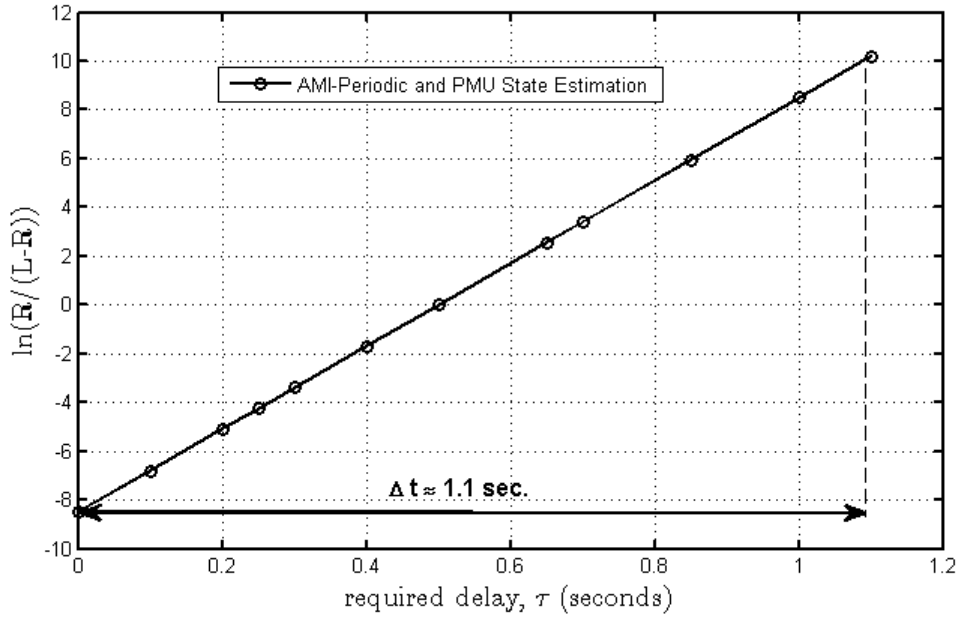

Figure 3.6: Linearized S-shaped curve of AMI and PMU applications in Fig. 3.4 and Fig. 3.5.

Table 3.5: AMI Periodic traffic used in simulation.

Traffic class	Application	Protocol	Packet Size	Packets rate	Required Hard Delay (ms)	Required Reliability	Standard
AMI Power consumption	Electric Billing	UDP	100 Bytes UDP header: 28 Bytes	1 packet per 5 minutes	1,000	99.999%	IEEE C37.118 Standard

3.5 Simulation and Results

3.5.1 Simulation setup

We consider a basic AMI scenario in which 100 nodes smart meters are uniformly distributed in a 1,000 m x 1,000 m service area. The collector node is located at the center. This scenario corresponds to a widely used AMI network for urban area, with the assumption that each house has a smart meter [2]. We choose two current wireless network approaches, WiMAX and ZigBee, to simulate the above AMI network. In the one-hop approach using WiMAX, collector is the Base Station and smart meters send their data to the collector directly. The detail parameters setting is given in Table 3.6. In the multi-hop approach using ZigBee, we configure the AMI network based on the cluster tree topology. The smart meters in AMI based ZigBee network are full function devices, which can be the source nodes or relay nodes. The detail parameters setting is given in Table 3.7. We use the default parameters related to propagation and path loss models in OMNeT++ for both simulations.

Since we aim to the future Smart Grid applications, smart meters not only send power con-

Table 3.6: Simulation parameters for AMI based WiMAX IEEE 802.16 one -hop topology [40].

Wireless NAN standard	WiMAX IEEE 802.16
Network topology	Random nodes over 1,000 m x 1,000 m
Number of Smart Meters	100
Maximum bitrate	4 Mbps
Simulation time	900 seconds
Propagation Model	Log Normal Shadowing
PHY Modulation	CSMA/CD
Carried Frequency	3.5 GHz
Bandwidth	7 MHz
Smart Meter transmission power	2 W

Table 3.7: Simulation parameters for AMI based ZigBee IEEE 802.15.4 multi-hop topology [41].

Wireless NAN standard	ZigBee IEEE 802.15.4
Network topology	Random nodes over 1,000 m x 1,000 m
Number of Smart Meters	100
Maximum bitrate	250 kbps
Simulation time	900 seconds
Propagation Model	Log Normal Shadowing
PHY Modulation	CSMA/CD
Carried Frequency	2.4 GHz
Bandwidth	2 MHz
Smart Meter transmission power	100 mW

sumption information to collector periodically but also can report that information for the Demand Response service in real time. Hence, we set the packet size for both services at 100 bytes [38]. The transmission interval for periodic service is 5 minutes and random for the other [38, 39].

We study the effect of required delay on the system reliability of two above AMI networks based on Eq. (3.3). We range the required delay of Smart Grid service from 0 to 100 milliseconds to limit the number of simulation runs. We simulate 50 times for every required delay and take the average reliability value. The resultant simulation curve after that is used to find the $L,\ \lambda$ and τ_0 values of the approximated S-shaped curve by using parameter fitting tool in Matlab.

3.5.2 Performance results

We plot the S-shaped curve simulation results of two wireless AMI networks approaches in Fig. 3.7 and Fig. 3.8, respectively. By comparing to Fig. 3.4, we can easily find that both networks satisfy the delay requirements for two AMI applications. Unfortunately, the system reliability value of both networks are lower than the requirement of $R_{req} = 0.99$ in Table 2.1. The reduction in reliability is caused by collision among source nodes when they shared only one transmission channel.

Using parameter fitting, we find out the approximated S-shaped curves in Fig. 3.7 and

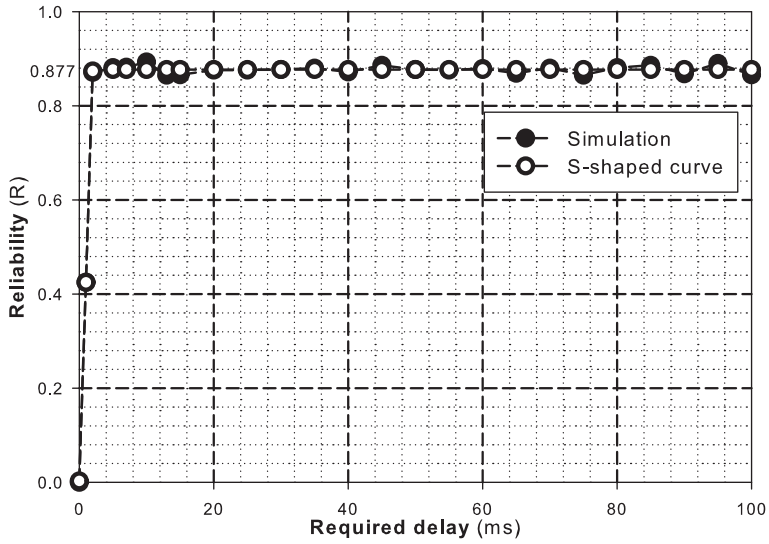

Figure 3.7: The system reliability simulation result for one-hop WiMAX AMI network.

Fig. 3.8 are as in Eq. (3.16) and Eq. (3.17), respectively, where τ is in milliseconds. We plot the linearized version of S-shaped curves after applying Fisher-Pry transform in Fig. 3.9 and apply the vertical limit around 10. This figure points out that WiMAX AMI network needs only $\Delta t_1 \approx 2.75\ ms$ to accelerate to 99.99% of L value while ZigBee AMI take over 3 times of that ($\Delta t_2 \approx 9.5\ ms$). The reason for this result comes from the larger bandwidth and higher bit rate supports of WiMAX than ZigBee.

$$R_{one-hop} = \frac{0.877}{1 + e^{-5.662(\tau - 1.01)}} \tag{3.16}$$

$$R_{multi-hop} = \frac{0.654}{1 + e^{-3.856(\tau - 6.783)}} \tag{3.17}$$

To investigate the trend of S-shaped curve parameters with the number of source nodes, we simulate the ZigBee AMI 50 nodes and 150 nodes and compare with the results of ZigBee AMI 100 nodes in Fig. 3.10a and Fig. 3.10b. The highest system reliability level is obviously belonged to 50 nodes case. However, the midpoint τ_0 and acceleration time are similar and not dependent on the number of Smart Meters. We can easily indicate $\tau_0 = 6.78$, as shown in Fig. 3.10b. These simulation results indicate that the characteristic of the S-shaped curve is dependent on network bandwidth and reliability enhancement techniques, which is fixed with our proposed theorem.

3.5.3 Learnt Lessons from Simulation

From the simulation results in previous subsection 3.5.2, we argue that the random access scheme by a shared channel using in our simulation cannot obtain required system reliability in

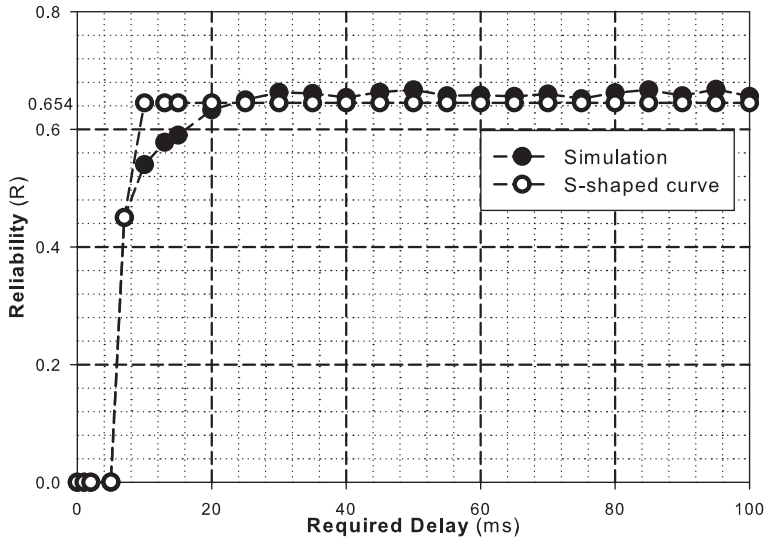

Figure 3.8: The system reliability simulation result for multi-hop ZigBee AMI network.

AMI network because of collision. However, random access scheme is refereed to scheduling access schemes because critical Smart Grid services do not need to wait for their time slot, hence reducing the transmission delay. In this subsection, we try to increase the system reliability by reducing packet collision.

Packet collision in our AMI network occurs when Smart Meters try to send data at the same time. Recall that if we want to use power consumption information for DR application, all data should go to collector as fast as possible. However, this causes the packet flooding problem on SG WNAN. To observe the effect of packet flooding, first we define *snapshot data*, as done in WSN [42] and *snapshot length* related to data gathering in Smart Grid communication as belows

Definition 3.6 (Snapshot data of Smart Grid)**.** *Snapshot data of Smart Grid is the union of all information from all source nodes (Smart Meter or PMU) at particular sampling time. The goal of Smart Grid NAN is to gather these snapshots to the collector as quick as possible.*

Definition 3.7 (Snapshot length)**.** *Snapshot length (in miliseconds or seconds) is the measured time between when first source node sends its data and last source node sends data during the same snapshot. The shorter snapshot length is, the more real-time data that Smart Grid NAN can support.*

Definition 3.8 (Snapshot rate)**.** *Snapshot rate (measured by Byte per second or KBytes per second) is the ratio between the size of data in one snapshot and the snapshot length.*

Figure 3.11 illustrates an example of AMI network based Zigbee 100 smart meters with

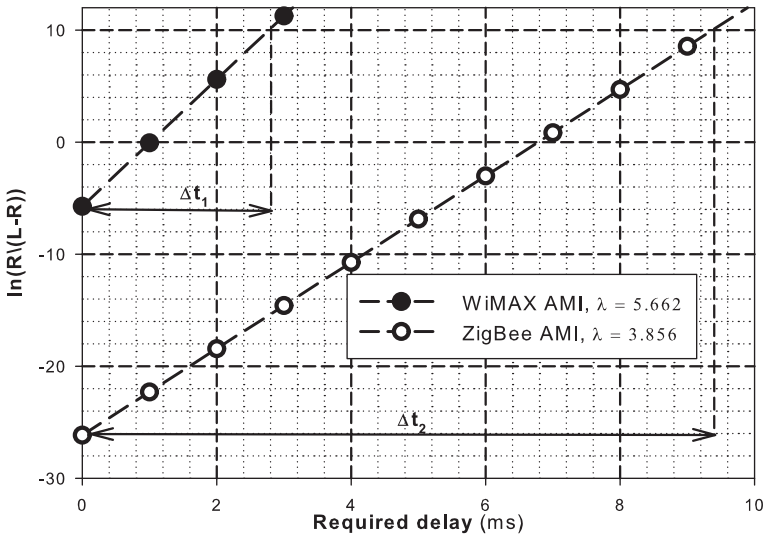

Figure 3.9: Linearized lines of two S-shaped curves.

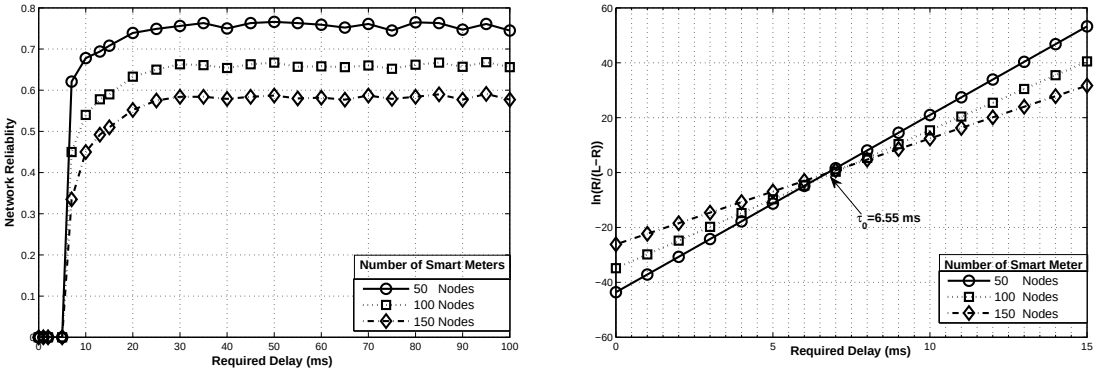

(a) Simulation curves with different number of smart meters in multi-hop ZigBee AMI network.

(b) Linearized S-shaped curves in Fig. 3.10a.

snapshot length equals to 10 seconds. The snapshot rate in this case is calculated in Eq. (3.18)

$$\begin{aligned} Snaphot\ rate &= \frac{(Packet\ Size) \times (Number\ of\ Nodes)}{Snapshot\ length} \\ &= \frac{100\ Bytes \times 100}{10\ seconds} = 1,000\ (Bytes/second) \end{aligned} \tag{3.18}$$

In the last simulation of this chapter, we investigate the S-shaped curve of SG WNAN with different snapshot lengths of AMI network 100 nodes based Zigbee and based WiMAX technology. Figure 3.12 shows the S-shaped curve of AMI based Zigbee. We can see that the longer snapshot length, the higher system reliability Zigbee can support. However, the rising trend of reliability goes to stable value about 0.86 when the snapshot length is 15 seconds (snapshot rate = 0.67 KBytes/second), as shown in Figure 3.13. The reason that system reliability cannot get 1 is that some smart meters have been isolated.

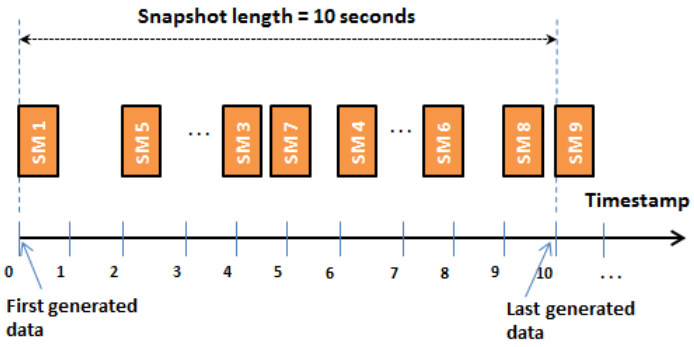

Figure 3.11: Snapshot length example in AMI based Zigbee.

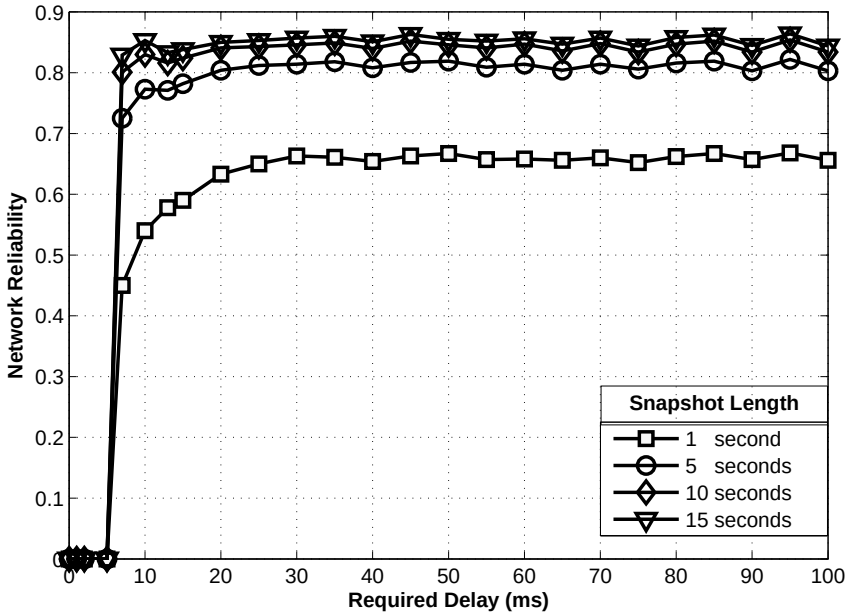

Figure 3.12: Snapshot length comparison of AMI network based Zigbee.

3.6 Conclusion

In this chapter we have proposed the first quantitative QoS method to overall system reliability evaluation of Smart Grid Wireless Neighborhood Area Network communication. Our S-shaped model provides an important tool since it bypasses the difficulty of having efficient simulation tools such as NS-2, OMNeT++, etc. for Smart Grid communication planning and designing, while improving the quality of QoS model exceeding previous ones. Our model also helps to define the type of Smart Grid applications and choose the approximation system reliability technique based on different services requirements or environment conditions.

Our finding is the first step towards a more comprehensive understanding of the nature

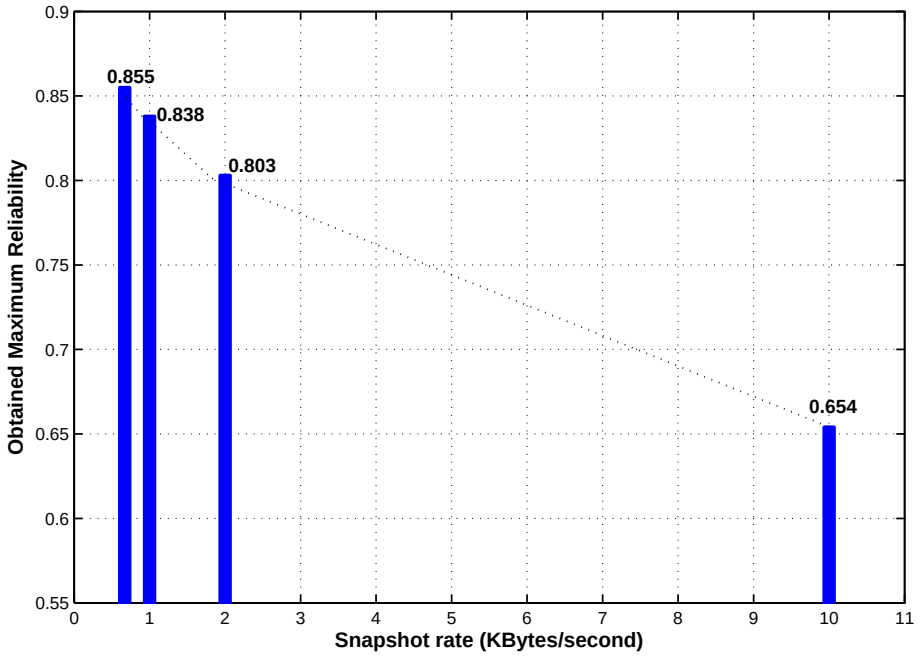

Figure 3.13: Maximum obtained system reliability with different snapshot rates of AMI based Zigbee.

characteristics of Smart Grid communication system behaviors. In particular, the mathematic model of system reliability enhancement method and delay requirement should be analyzed in more details. Despite the lack of those details, our study can give different points of view in the Quality of Service benchmark for Smart Grid and it can be a very useful tool to overcome the limitation of the existing approaches.

In many next chapters, more analysis will be added to find the suitable parameters of Smart Grid services which have Soft Delay requirement taking into account both electrical and communication domains. A series of simulations for evaluating the performance of our QoS model in network of Phasor Measurement Units (PMUs) will help to forecast the behaviors of this SG WNAN to system parameters.

CHAPTER IV

EVALUATIONS OF WIRELESS PMU SYSTEM RELIABILITY FOR SOFT DELAY SMART GRID APPLICATIONS

4.1 Introduction

The North American Synchro-Phasor Initiative (NASPI) [34] shows the recent achievements using PMU as a core technology for monitoring, control and protection electric grid. The measured information help to achieve situation awareness and serve as input for control functions. WAMS manage the information exchange among control centers and state estimators, which use statistical methods to make decisions based on the collected data. Because distributed renewable energy sources and electric cars become more widespread, the applications of WAMS become increasingly critical.

Figure 4.1 illustrates an abstract model for Smart Grid applications based on PMUs network. Above is the electric power flows on transmission or distribution grids. Below is a monitoring, control and protection system senses a set of power parameters and makes the necessary decisions to send signals to the receivers. An application on the top has high-level management of the system. In this model, we assume perfect sensing, actuation, monitoring, control and protection. The system has a perfect model of the power flow and make perfect decisions with no computational latency. The only potential imperfect component is communication environment with noise. In this chapter, we want to know the best that can physically be achieved between communication and electric power grid.

Section 4.2 provides a comprehensive introduction on the principles, designs and applications of phasor measurement unit (PMU), which is the important instrument device to collect real-time and fine data for analyzing the status of the power network. It helps to understand how the data is collected and analyzed for monitoring and controlling power networks. In section 4.3, we represent principle and algorithm of State Estimation application, the most important service of WAMS that SG WNAN must support for the transmission and distribution electric grids. Although, State Estimation requires the strictly delay, we can apply its as SD classification. In addition, we propose the principle of uncertainty in these application, which affects to the usefulness of applications.

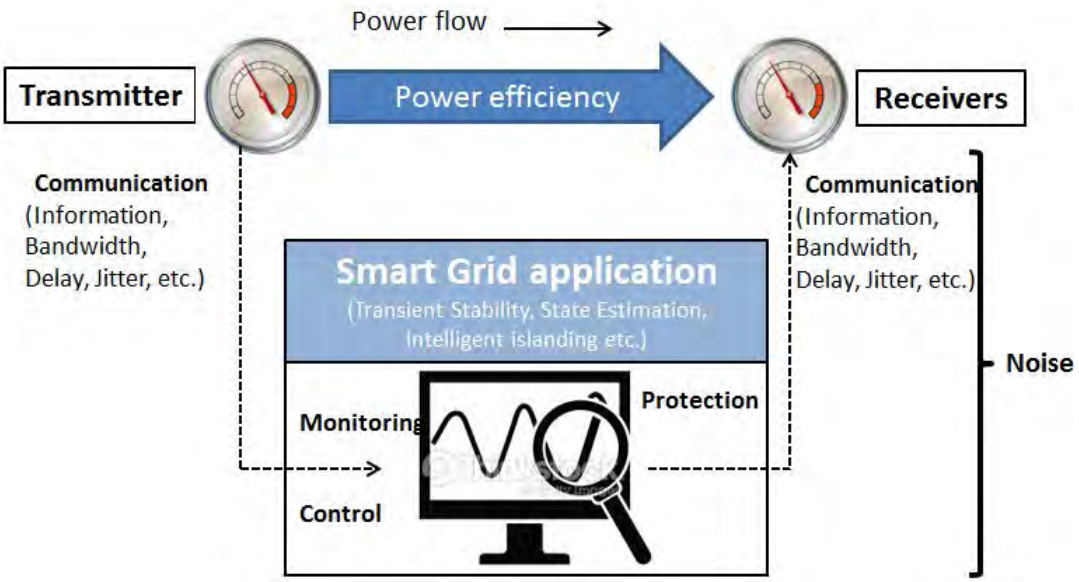

Figure 4.1: Abstract model for Smart Grid application on PMUs network (Adapted from [8]).

Based on our proposed S-shaped curve in previous chapter 3, we suggest to use this tool as a simple investigate approach in order to designing and planning suitable SG WNAN approach for PMUs network running State Estimation application provide high accurate and reliable results. We also show how reliability of State Estimation results against PMU measurement errors due to packet loss and delay.

4.2 Phasor Measurement Techniques

4.2.1 Introduction

Phase angles of voltage or current in electrical network have always attached special interest to power system engineers. It is common-known that active power flow in a power line is very nearly proportional to the sine wave of the angle difference between voltages at two terminals of the line. As many of the planning and operational considerations in a power network are directly concerned with the flow of real power, measuring angle differences across lines has been of concern for many years. The oldest application measurement of phase angle differences was reported in three papers in early 1980s [43]. These systems have used LORAN-C, GOES satellite transmissions, and the HBG radio transmissions (in Europe) to obtain synchronization of reference time at different locations in a power system. These measurement have only calculated the single-phase voltages angles and of course not taken into account the harmonics in the voltage waveform.

The first model of the modern PMUs using GPS were built at Virginia Tech in early 1980s,

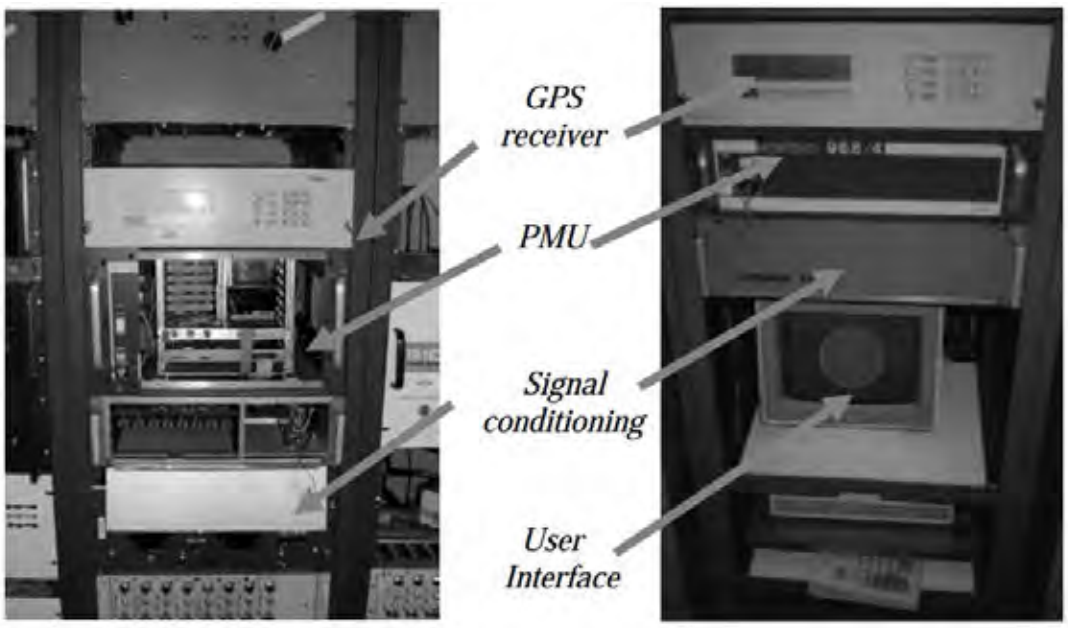

Figure 4.2: First PMU installed at the Power Systems Research Laboratory at Virginia Tech [8].

and two of these models are shown in Figure 4.2. The PMUs built at Virginia Tech were installed at a few substations of the Bonneville Power Administration, the American Electric Power Service Corporation, and the New York Power Authority. The first commercial manufacture of PMUs with Virginia Tech collaboration was started by Macrodyne in 1991 [43]. At present, a number of manufacturers offer PMUs as a commercial product, and deployment of PMUs on power systems is being carried out in earnest in many countries around the world. IEEE published a standard in 1991 governing the format of data files created and transmitted by the PMU. A revised version of the standard was issued IEEE C37.118.1a-2014 standard in 2014 [44].

4.2.2 Phasor representation

In electrical domain, a voltage or current waveform shape described mathematically is called a phasor. The phasor representation is a complex value representing and AC signal, given by Eq. (4.1)

$$x(t) = \sqrt{2}A.cos(2\pi\omega_0 + \phi) \tag{4.1}$$

ω being the frequency of the signal in radians per second, and ω being the phase angle in radians. $\sqrt{2}A$ is the peak amplitude of the signal. The root mean square (RMS) value of the input signal is A. Recall that RMS quantities are particularly useful in calculating active and reactive power in an AC circuit. Equation (4.1) can also be written as

$$x(t) = Re\{\sqrt{2}A.e^{j(2\pi\omega_0+\phi)}\} = Re[\{e^{j(2\pi\omega_0)}\}\sqrt{2}A.e^{j\phi}] \tag{4.2}$$

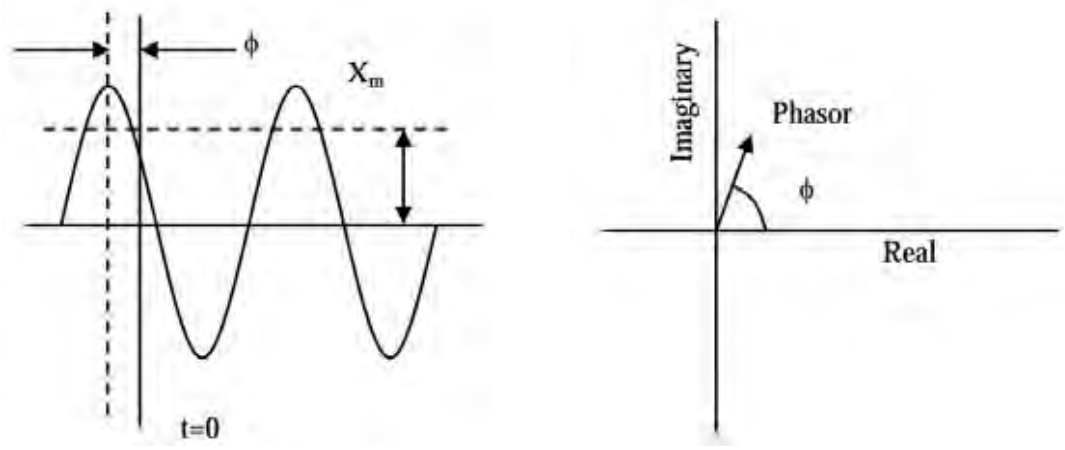

(a) A sinusoid voltage wave

(b) Sinusoid representation as a phasor

Figure 4.3: Example of voltage wave representation. The phasor depends upon the choice of vertical axis $t = 0$. The length of phasor vector is equal to root mean square (RMS) of sinusoid.

It is normally to ignore the term $e^{j(2\pi\omega_0)}$ in Eq. (4.1), with the understanding that we knew the frequency. Hence, given the AC waveform formula, the phasor value can be determined by inspection as Eq. (4.3) below

$$\mathbf{X} = A.e^{j\phi} \tag{4.3}$$

However, if there is no formula, only a waveform, how do we determine the phasor value because no inherent frequency or phase reference. It was stated earlier that the phasor representation is only possible for a pure sinusoid. In practice a waveform is often corrupted with other signals of different frequencies. It then becomes necessary to extract a single frequency component of the signal (usually the principal frequency of interest in an analysis) and then represent it by a phasor.

Extracting a single frequency component is often done with a *Fourier transform* calculation. In sampled data systems, this becomes the *Discrete Fourier Transform* (DFT) or the *Fast Fourier Transform* (FFT). The DFT of electric wave is the set of Fourier coefficients $\{k\phi\}$ of cosine waves and sine waves. The result is phasor of voltage or current in complex number as in Eq. (4.4) belows.

$$\begin{aligned} \mathbf{X} &= X_r - jX_i \\ X_r &= \frac{\sqrt{2}}{N}\sum x_k.\cos(k\phi) \\ X_i &= \frac{\sqrt{2}}{N}\sum x_k.\sin(k\phi) \end{aligned} \tag{4.4}$$

Figure 4.4 illustrates the example from Eq. (4.4), where $\{x_k\}$ are the set of samples from waveform (bottom wave) and on the top are cosine and since waves $\{k\phi\}$. The result is phasor $\mathbf{X}$ in

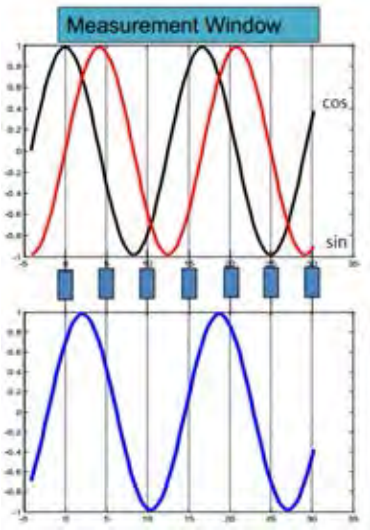

Figure 4.4: Example of Fast Fourier Transform technique [45].

complex number.

Traditional phasor calculation uses one set of Fourier coefficients. The sine and cosine reference waveforms move with calculation. The result phasor rotates clockwise at system frequency (50 Hz or 60 Hz) as in Figure 4.5. Synchrophasor calculation requires reference waveforms fixed in time and applies new Fourier coefficients at every window. We recall that the angle is constant at nominal frequency. In this method, window can or cannot overlap.

The phasor is actually the shorthand for sinusoid formula which has specify magnitude and phase, and assumed frequency based on nominal f_0. We have used to seeing constant phase and amplitude as in following Eq. (4.5) for phasor representation.

$$\mathbf{X} = X_m e^{j\phi} \tag{4.5}$$

However, in true dynamic system, all parameters in phasor presentation have change with time. The dynamic phasor is below

$$\mathbf{X}(t) = (X_m(t)/\sqrt{2})e^{j(2\pi \int gdt + \phi(t))} \tag{4.6}$$

where $X_m(t)$ is amplitude, $g(t)$ is frequency and $\phi(t)$ is phase. Given the dynamic phasor equation, we can specified the phasor value at an instant of time t_1 At time t_1,

$$\mathbf{X}(t_1) = (X_m(t_1)/\sqrt{2})e^{j(2\pi \int gdt + \phi(t_1))} \tag{4.7}$$

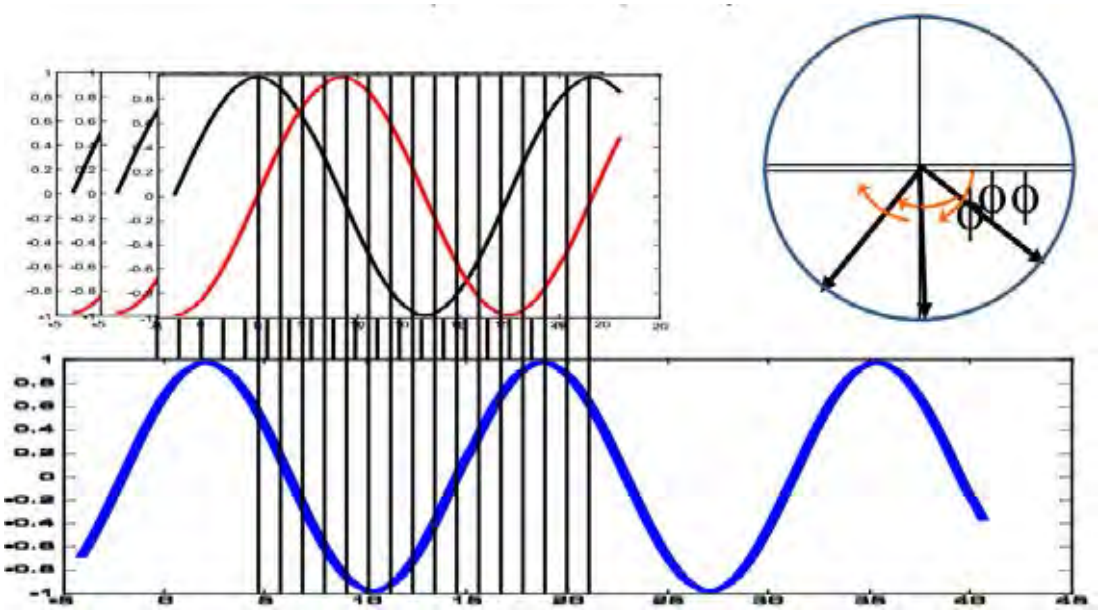

Figure 4.5: Example of traditional phasor calculation. Reference waveforms on the top move with calculation [45]. The value of phasor information is calculated from reference waveforms.

will generate the sinusoidal formula

$$x(t_1) = X_m(t_1)\cos(2\pi f_0 t_1 + (2\pi \int gdt + \phi(t_1))) \tag{4.8}$$

the term $(2\pi \int gdt + \phi(t_1))$ generates a point on the waveform at t_1 as in Figure 4.6a. On the other hand, given waveform, we cannot measure an instantaneous phasor information. Instead, we observe the waveform over interval (window time) and estimate over that interval around t_1 as in Figure 4.6b. Therefore, in phasor measurement we have to trade off between the time stamp correctness (short window time demand) and the accuracy of estimated phasor value (long window time demand). Usually, the timetag of phasor value is located at the center of window time as described in Figure 4.7.

Figure 4.8b and Figure 4.9 illustrate the relation between timetag and window time length to the variation in phasor magnitude. From this relation, we obtain that Smart Grid applications for protection purpose will require short window time while controlling or monitoring applications can accept larger window time for their measurements.

4.2.3 IEEE Standard C37.118.1a -2014

Based on the IEEE Standard C37.118.1a -2014, PMUs can be specify into two classes (P and M) of performance. The M-Type is intended for measurement applications requiring *high precision* and avoiding aliased signals. The P-Type is used for protection applications requiring

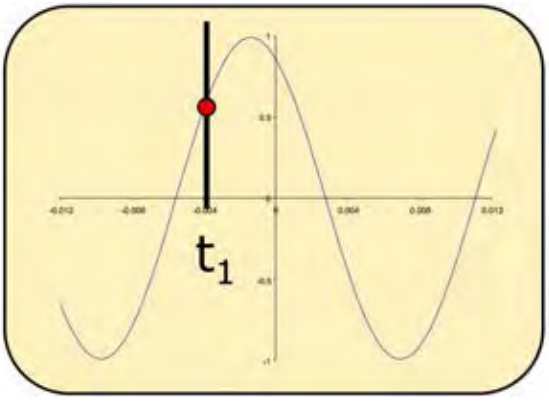

(a) A phasor value calculation at an instant time t_1

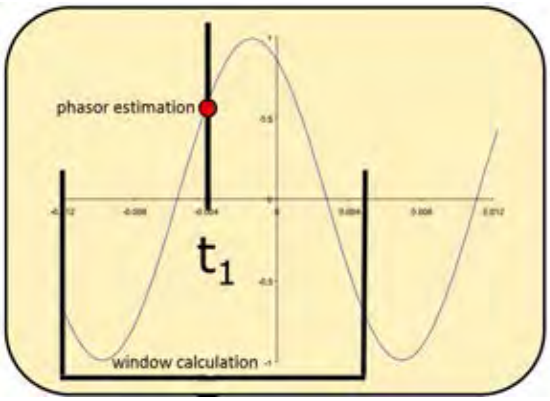

(b) Sinusoid representation as a phasor

Figure 4.6: Example of phasor wave representation. The phasor depends upon the choice of vertical axis $t = 0$. It is impossible to calculate phasor at instant t_1. The estimation algorithm needs enough sample to process. This is called window time calculation, or window time length.

fast response. Both class designations do not indicate that which class is adequate or required for a Smart Grid application. The utility or operator must choose a performance class that satisfies the requirements of each applications. All measurement requirements for M and P classes are given in details in IEEE Standard C37.118.1a -2014. In the following subsections, we only list the introduction of measurement accuracy, evaluation, and reporting times criteria for phasor calculation.

4.2.3.1 Frequency and rate of change of frequency (ROCOF) estimation

The phasor data concentrator receives phasor information from many PMUs and represents as vectors as in Figure 4.11 and Figure 4.11. Then, it calculates frequency F at a particular location in electric power grid as in Eq. (4.9) below

$$F = \Delta \left(\frac{\Phi_2 - \Phi_1}{t_2 - t_1} \right) = \frac{\Delta \phi}{\Delta\, t} \tag{4.9}$$

and the Rate of Change of Frequency ($ROCOF$)

$$ROCOF = \frac{(F_2 - F_1)}{\Delta\, t} \tag{4.10}$$

4.2.3.2 Total vector error (TVE) Evaluation

The theoretical values of a synchrophasor representation of a sinusoid and the values obtained from a PMU may include differences in both amplitude and phase. While they could be

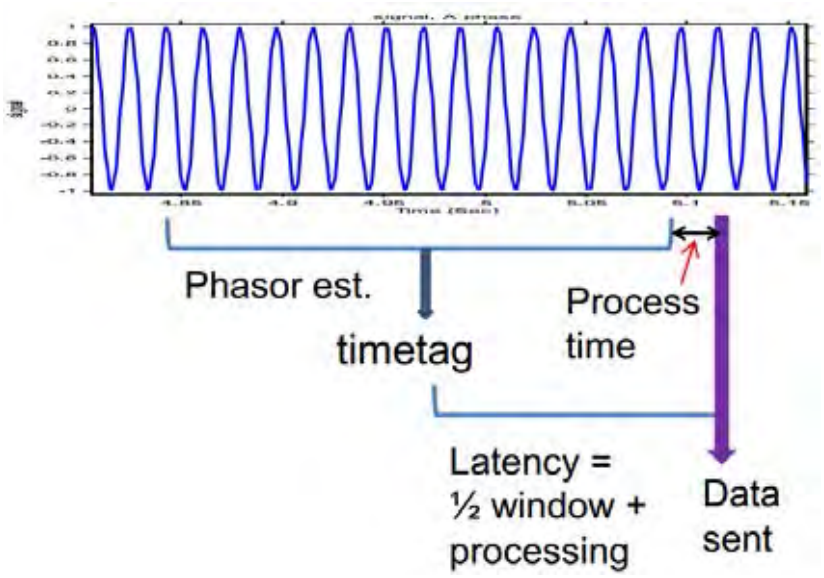

Figure 4.7: Example of latency from windowing calculation [45]. The timetag of phasor information is located at center of window time.

separately specified, the amplitude and phase differences are considered together in this standard in the quantity called total vector error (TVE) TVE is an expression of the difference between a perfect sample of a theoretical synchrophasor and the estimate given by the unit under test at the same instant of time. The value is normalized and expressed as per unit of the theoretical phasor.

$$TVE_{(n)} = \sqrt{\frac{(\hat{X}_r(n) - X_r(n))^2 + (\hat{X}_i(n) - X_i(n))^2}{(X_r(n))^2 + (X_i(n))^2}} \tag{4.11}$$

where $\hat{X}_r(n)$ and $\hat{X}_i(n)$ are the sequences of estimates given by the unit under test, and $X_r(n)$ and $X_i(n)$ are the sequences of theoretical values of the input signal at times (n) assigned by the unit to those values. The $X_r(n)$ and $X_i(n)$ values can be determined in specific testing situations in standard, such as constant phase offsets or frequency.

4.2.3.3 Frequency and ROCOF measurement evaluation

Frequency and ROCOF measurements shall be evaluated using the following definitions. With these criteria, frequency, and ROCOF errors are the absolute value of the difference between the theoretical values and the estimated values given in Hz and Hz/s respectively. See Eq. (4.12) and Eq. (4.13)

$$FE = |f_{true} - f_{measured}| = |\Delta f_{true} - \Delta f_{measured}| \tag{4.12}$$

$$RFE = |(df/dt)_{true} - (df/dt)_{measured}| \tag{4.13}$$

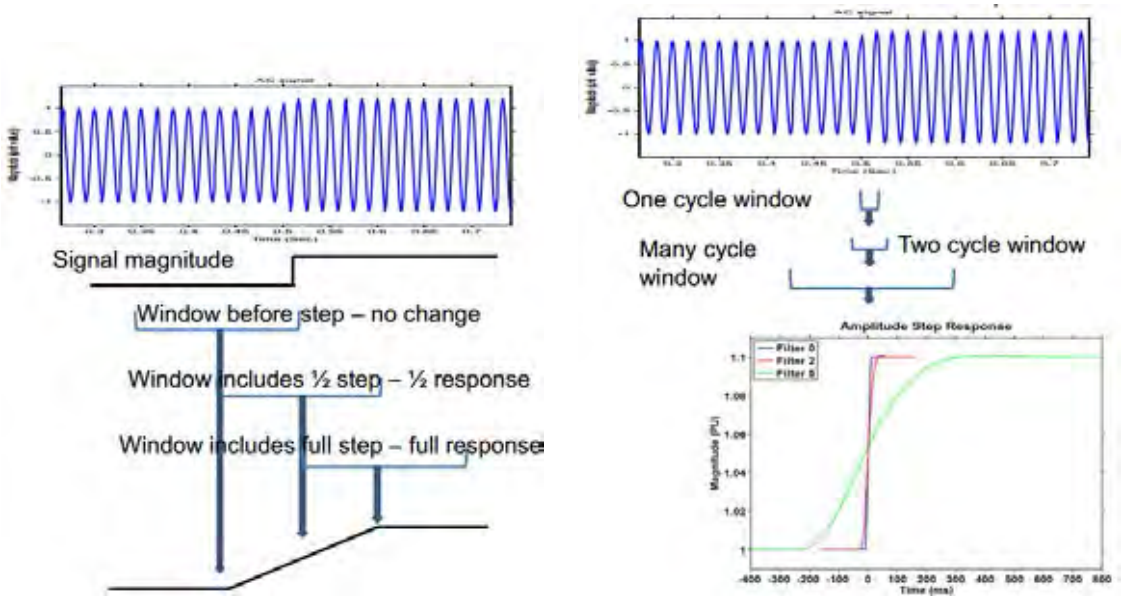

(a) Timetag and step change relation

(b) Windowing and step change relation

Figure 4.8: Example effect of timetag and window length to the accuracy of step change in phasor. Short window length helps to identify the instant timetag correctly, but requires sufficient sample data in a short latency to run estimation.

The measured and true values are for the same instant of time, which will be given by the time tag of the estimated values. Hence, we conclude that window time length impacts to the time tag.

4.2.3.4 Phasor Reporting rates

According to the C37.118.1a Standard, every PMU reports phasor information (by recording or sending to phasor data collector) at sub-multiples of the nominal electric frequency. Table 4.1 illustrates the required rates for 50 Hz and 60 Hz electric systems. The specific reporting rate to be used is dependent on the purpose of Smart Grid application (P-Type or M-Type). We recall that rates lower than 10 frames per second are not subject to dynamic requirements. This

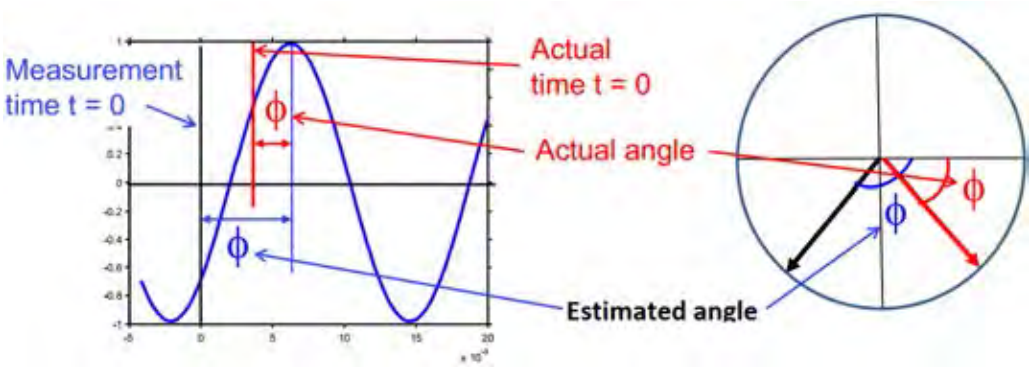

Figure 4.9: Example of latency from windowing and step change [45].

Table 4.1: Required PMU reporting rates based on IEEE C37.118 Standard. Remember that low sample rate leads to long window time, and fast sample leads to the short one.

System frequency	**50 Hz**			**60 Hz**					
Reporting rates from PMU (Fs - frames per second)	10	25	50	10	12	15	20	30	60

means that no filtering is required inside PMU, so lower 10 frames per second can be supported directly by selecting every n^{th} samples from a higher rate phasor stream.

The particular reporting rate is dependent on WAMS applications and the class of these applications. To summary, we list main different in timeliness factors of P-Type and M-Type classes as below

- **P-Type applications**
  - Needs less filtering in PMU;
  - Less latency (than M-Type) in estimation (from $30\ ms$ to $100\ ms$);
  - Applies for real-time controlling and protection requiring minimum delay.
- **M-Type applications**
  - Needs anti-alias filtering in PMU;
  - Longer latency (depends on reporting rate, such as $30\ ms$ required delay at 60 samples per second, or $100\ ms$ required delay at 30 samples per second);
  - Applies for monitoring applications requires precisely measurement.

4.3 Soft Delay Smart Grid applications

In this section, we brief introduce two important WAMS applications, State Estimation and Transient Stability. The former provides a reliable picture of power grid situation. The later supports stable state of the grid after a transient disturbance. In Smart Grid communication point of view, a success Smart Grid NAN has to fully support at least these applications.

4.3.1 State Estimation (M-Type)

The termed State Estimation (SE) has first introduced by Schweppe in 1970 to estimate the voltage magnitudes and angles at all buses in electric power grids [46, 47]. He then has proposed a Weighted Least Square (WLS) estimator using the Jacobian of the measurement matrix. Two important approximation techniques, which are presented to minimize the computational efforts

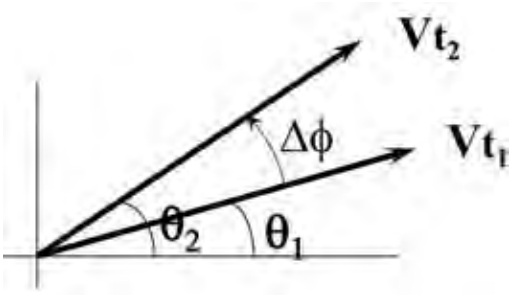

Figure 4.10: Example of frequency calculation from phasor information [45].

of the WLS SE, are fast-decoupled SE by zeroing the coupling sub matrices in the Jacobian matrix, and DC-estimator by abandoning all branch resistances and shunt elements. In order to have a reliable state estimation, the estimator should be able to identify the large measurements errors. In addition, the measurement placement should satisfy sufficient redundancy requirement to detect untrusted data. Nowadays, SE has become a key function in Smart Grid system. It provides to monitor, control and protect the electric power grid and establishes real-time network models for the grid, optimizing power flows, and bad data detection and analysis. Another example of SE is the SE-based reliability and security assessment to analyze emergency and determine necessary responses against possible outages in the power systems.

The invention of phasor measurement units (PMUs) have given hope for real-time monitoring of the power grid. Typically, a PMU reports phasor information at 30 measurements per second, thereby offering the possibility of a much more timely view of the power system dynamics than SCADA. More importantly, all PMU measurements are synchronized, as they are times tamped by the global positioning system clock. However, PMUs with their high measurement report put huge pressure on the Smart Grid communication infrastructure. This leads to the demand for resource-efficient, event-triggered SE approaches that relates to compress sensing, network coding techniques.

Recall that phasor measurement actually estimates of a certain value; hence, the terms *measurement* and *estimate* are used somewhat interchangeably in this standard. Power calculation from phasor information in Figure 4.11 and Figure 4.12 as in Eq. (4.14) and Eq. (4.15) below. The active power P and reactive power Q are also estimated values.

$$P = VI\cos(\Phi - \phi) = \mathbf{VI} = V_x I_x + V_y I_y \tag{4.14}$$

$$Q = VI\sin(\Phi - \phi) = \mathbf{V}(j\mathbf{I}) = V_y I_x - V_x I_y \tag{4.15}$$

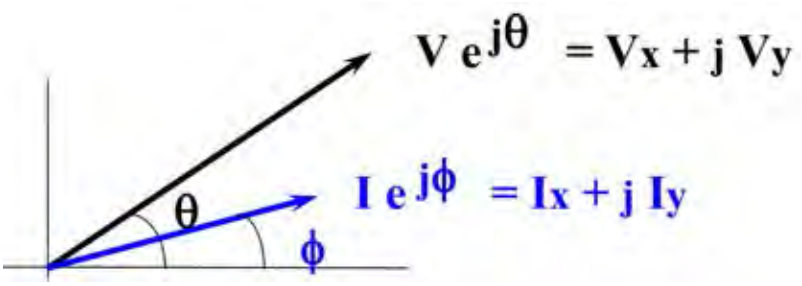

Figure 4.11: Example of power calculation from phasor information [45].

4.3.2 Transient Stability (P-Type)

When the synchronous generator is fed with a supply from one end and a constant load is applied to the other, there is some relative angular displacement between the rotor axis and the stator magnetic field, known as the load angle which is directly proportional to the loading of the machine. The machine at this instance is considered to be running under stable condition. Now if we suddenly add or remove load from the machine the rotor decelerates or accelerates accordingly with respect to the stator magnetic field. The operating condition of the machine now becomes unstable and the rotor is now said to be swinging with regard to the stator field and the equation we so obtain giving the relative motion of the load angle δ regard to the stator magnetic field is known as the swing equation for transient stability of power system. Here for the sake of understanding we consider the case where a synchronous generator is suddenly applied with an increased amount of electromagnetic load, which leads to instability by making PE less than PS as the rotor undergoes deceleration

The speed and internal angles of the generators in a power grid but for micro-grid that is not using synchronous machines. This refer to the behaviors of the system when it is subjected

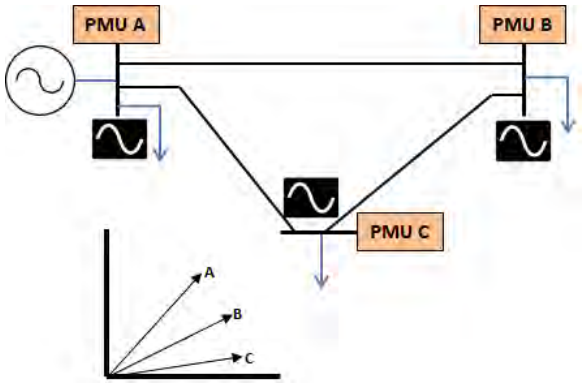

Figure 4.12: Example of state estimation application based on PMUs network. The synchronous phasor information from A, B, and C PMU locations help to monitoring the power grid state in real time.

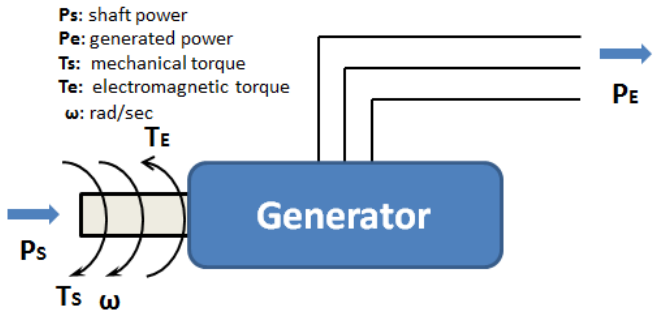

Figure 4.13: Transient stability application [45].

Table 4.2: Summarized of application for WAMS based on PMUs network [48].

Main application	Sub-applications	Source of Data	Data	Latency requirement	Number of PMUs we may need to optimally run the application	Data time window
State Estimation	Power flow, Dynamic Voltage assessment, Contingency analysis, Energy markets	All substations Operation centers	Voltage, Current, Power, Reactive power phasor	1 second	Number of buses in the system	Instant
Transient Stability	Load trip, Generation trip, Islanding	Generating substations Application servers	Generator internal angle, frequency df/dt	100 milliseconds	Number of generation buses	10-50 cycles
Small Signal Stability	Modes, Modes shape, Damping, Online update of PSS, Decreasing tie-line flows	Some key locations, Application server	V phasor	1 second	1/10 buses	Minutes
Voltage Stability	Capacitor switching, Load shedding, Islanding	Some key locations, Application server	V phasor	1-5 seconds	1/10 buses	Minutes
Postmorterm analysis	Model validation, Engineering setting for future	All PMU data historian	All measurements	NA	Number of buses in the system	Instant and Event files

to heavy transient disturbances such as loss of large loads or loss of generations. The latency is as small as possible so that the system can enable some fast control schemes to prevent the grid from becoming unstable transiently. The ability of a synchronous power system to return to stable condition and maintain its synchronism following a relatively large disturbance arising from very general situations like switching on and off of circuit elements, or clearing of faults etc. is referred to as the transient stability in power system.

In this subsection, we have just represented two important applications in WAMS, which are operated based on the PMUs network. For others applications, we only list the summary as in Table 4.2.

4.4 Phasor Measurement system and topology

It is clear from the above discussion that in order to avoid errors due to aliasing, the bandwidth of the input signal must be less than half the sampling frequency utilized in obtaining the sampled data. This requirement is known as the *Nyquist criterion*. The IEEE C37.118 standard guarantees the Nyquist requirement by required data report rate in Table 4.1. Choosing a opti-

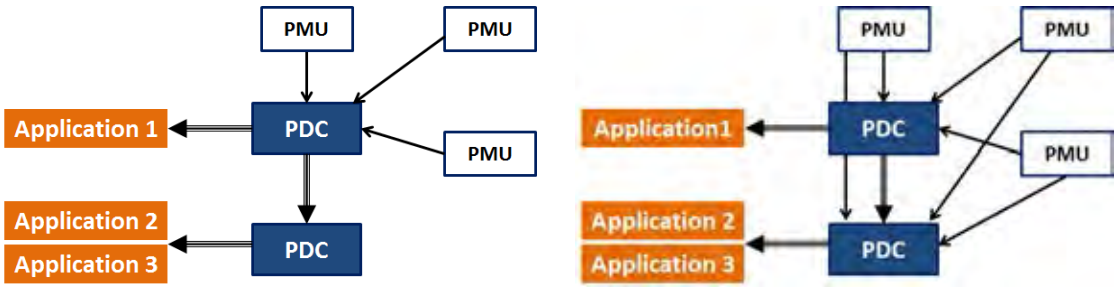

(a) Star architecture (b) Dual star architecture

Figure 4.14: Example of PMUs architectures [45]. The star architecture (on the left) is more common used by utilities.

mal deployment of PMUs is the key success for WAMS in Smart Grid. However, there are still argument in finding the suitable topology approach that represents the placement of PMU nodes in the network and the optimal packet rate and window time for application in WAMS.

From the discussions in section 4.2 section 4.3, in this thesis we firstly propose following the *Theorem of Uncertainty* in PMUs measurement.

Theorem 4.1. *In the PMUs network with a constant reporting sample rate, the more precisely timetag of phasor information, the less precisely its true value can be known and vice versa.*

Actually, the proposed theorem also implies the relation between window time length and the estimated phasor value. Our proposed Theorem 4.1 affects to the choice of PMUs network topology. Figure 4.14a and Figure 4.14b illustrate the architectures of PMUs network in order to support the coexistence of many WAMS applications. The star topology in Figure 4.14a uses the centralized approach, which many PDCs cascade to higher management levels. PMUs are connected to nearest PDC. This topology helps to easy management, but it is not suitable to many delay sensitive applications. On the other hand, the dual star in Figure 4.14b uses the decentralized architecture. PMUs sent phasor data directly to all PDCs. This topology helps to reduce delay but it costs bandwidth and manages difficultly.

4.5 PMU network performance evaluations

In this section we investigate the performance of IEEE 802.11g SG WNAN approach for PMU network based on our proposed S-shaped model in Chapter 3. The main problem is the PMU topology is dependent on the particular electric system and not having the optimal node positions. Therefore, we choose the network topology IEEE 37 nodes feeder test as in Figure 4.15 to evaluate the performance of IEEE 802.11g SG WNAN. In details, IEEE 37 nodes model represents an underground radial distribution feeder in California operating at 4.8kV under heavy unbalanced

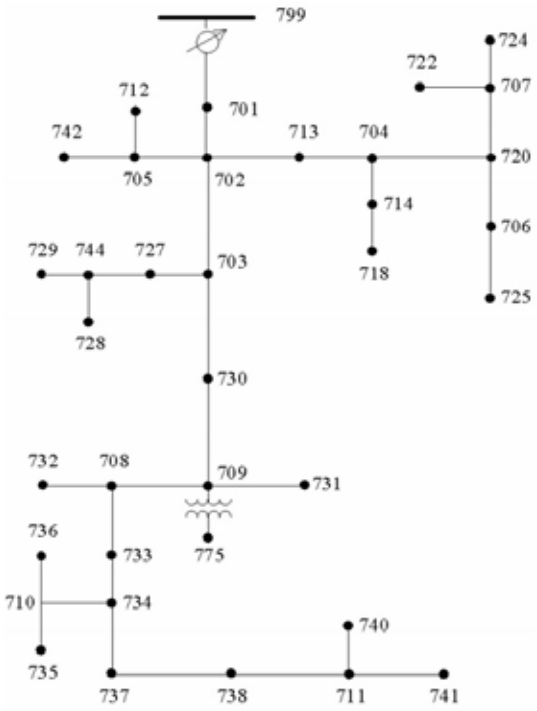

Figure 4.15: IEEE 37 node test distribution feeder used in simulation.

phase conditions. The collector node (Phasor Collector Unit) of feeder is placed at the power substation at node number 799.

4.5.1 Simulation Settings

Table 4.3 lists two co-existing applications in PMUs network for WAMS. In these service, PMU node sends phasor information to PDC periodically. These applications use the same data source for their own processes, except the required delays. Then the PDC uses this information for State Estimation, Transient Stability in order to monitoring, controlling and protecting the power grid. In this thesis, we follow IEEE C37.118 standard for service requirements in PMUs network.

The detail IEEE 802.11g SG WNAN simulation settings in OMNeT++ is shown in Table 4.4. In this study, we consider the IEEE 37 nodes Test Feeder as the network topology reference since the PMUs network is dependent on the particular distribution grid. As we intend to show the performance of wireless multi-hop approach for SG WNAN, we choose the wireless IEEE 802.11g since it can support the highest bitrate up to $54Mbps$.

4.5.2 The result S-shaped curve performance

In the first simulation, we choose the reporting rate is 30 samples per second, vary the required delay from 0 to 50 milliseconds Figure 4.16 illustrates the S-shaped curves obtained from

Table 4.3: PMU setting for concurrent applications: State Estimation and Transient Stability.

Traffic class	Application	Protocol	Packet Size	Packets per second	Required Delay (ms)	Required Reliability	Standard
PMU Phasor Information	State Estimation	UDP	40 Bytes UDP header: 28 Bytes	10, 20, 30, 50	1,000 (Soft delay)	99.999%	IEEE C37.118 Standard
PMU Phasor Information	Transient Stability	UDP	40 Bytes UDP header: 28 Bytes	10, 20, 30, 50	100 (Hard delay)	99.999%	IEEE C37.118 Standard

Table 4.4: PMU Wireless NAN simulation settings.

Wireless NAN standard	IEEE 802.11g
Network topology	IEEE 37 nodes Test Feeder
Number of PMU nodes	37
Maximum bitrate	54 Mbps
Simulation time	60 seconds
Propagation Model	Log Normal Shadowing
PHY Modulation	CSMA/CD
Carried Frequency	2.4 GHz
Bandwidth	22 MHz
PMU transmission power	1.5 W

simulation. In this setting, we have observed that when required delay is more than $25\ ms$, the supported system reliability from IEEE 802.11g reaches 1. This supported delay already satisfies both M-Type and P-Type applications.

To observe the effect of snapshot length to the system reliability level, we simulate the SG WNAN based on IEEE 802.11g with two snapshot lengths $2\ ms$ and $4\ ms$, corresponds to $(1/10)\ cycle$ and $(1/5)\ cycle$ of electric wave $50\ Hz$. The S-shaped curve results in Figure 4.17 show no different in reliability level, excepts non significant gain in delay of S-shaped curve with snapshot length $2\ ms$. The log phases of two curves nearly have the same slope factors, as we have obtained in the linearized curves in Figure 4.18.

To investigate whether this IEEE 802.11g with data rate 30 $(samples/second)$ satisfies to both application requirements in Table 4.4 or not by plotting the reference reliability line of Transient Stability as in Figure 4.17. The required delay of Transient Stability is $100\ ms$, so that this wireless network already fulfills its requirement.

In the last simulation in this chapter, we set highest sample rate up to $50\ (samples/second)$. The results in Figure 4.19 indicates that system reliability of IEEE 802.11g, with reporting rate $50\ (samples/second)$ can not support Transient Stability application because its highest reliability value is only about 0.7 when required delay $\tau = 100\ (ms)$. In order to check the capability of IEEE 802.11g reporting rate $50\ (samples/second)$ to support State Estimation, we extend the required delay parameter to $1,500\ (ms)$ to investigate the supported reliability. Figure 4.20 shows the simulation results. Fortunately, from $\tau = 600\ (ms)$ the reliability level goes up to 1,

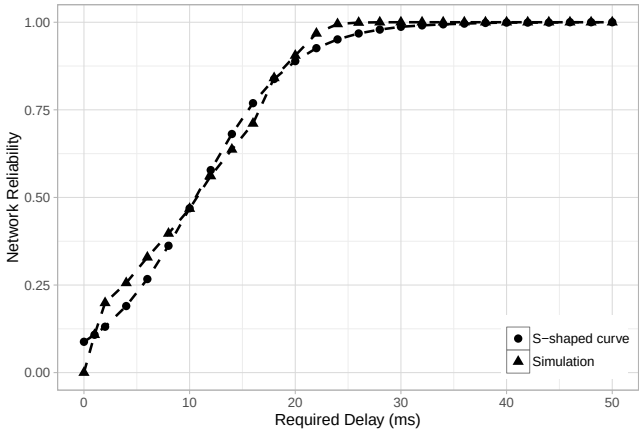

Figure 4.16: The S-shaped curve result of PMUs network based IEEE 802.11g approach with reporting rate 30 $(samples/second)$, snapshot length $4\ ms$.

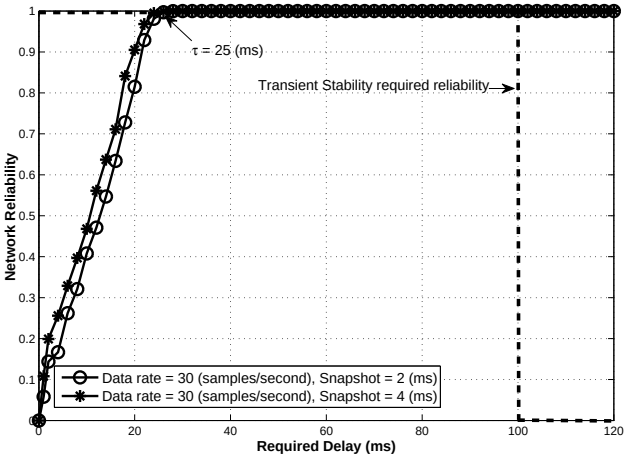

Figure 4.17: The S-shaped curve results of PMUs network based on IEEE 802.11g with Snapshot length $2\ ms$ and $4\ ms$.

that means it fulfills to support State Estimation application in Table 4.4. Recall that if we apply Soft required delay constraint as in Eq. (3.4) and Table 3.4, the system reliability curve should be decreased because the required delay has passed the soft delay requirement of State Estimation. It means that when the delay is more than $1,000\ (ms)$, the estimated values obtained from SE application has reduced the accuracy and timetag level of trust.

To summary the simulation results, we report as in Table 4.5. Our finding results also supports the argument that in order to support real time WAMS application, the PMUs network should be decentralized approach, i.e. dual star architecture as in Figure 4.14b. This approach helps to reduce the phenomenon, termed as *data tsunami*, in PMU phasor measurement.

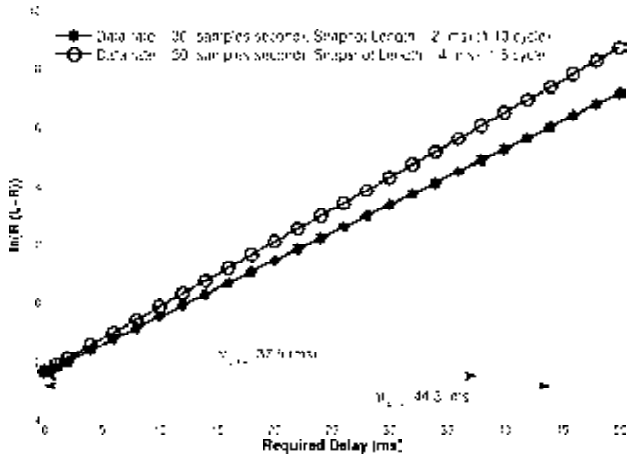

Figure 4.18: The linearized lines of PMU network based on IEEE 802.11g with Snapshot length 2 ms and 4 ms from Figure 4.17.

4.6 Conclusion

It is obvious that SCADA network is not enough to fully capture the dynamic characteristics of the power system when compared to the PMUs network, as shown in the Figure 4.21. Therefore, when a blackout happened, there is too little time for processing controller responded. Meanwhile, the SE model with individual PMU captures and track real-time power system. As shown in Figure 4.22, if we see the picture from SCADA look like X-Ray scan, then the picture provided by PMUs will be MRI scan. Therefore, the main content of this chapter is about PMUs network and its applications for WAMS well as the challenges posed to move towards a smart grid network for real-time power grid. Not taking account of other influential factors, latency still remains a major challenge should be solved for the PMUs network.

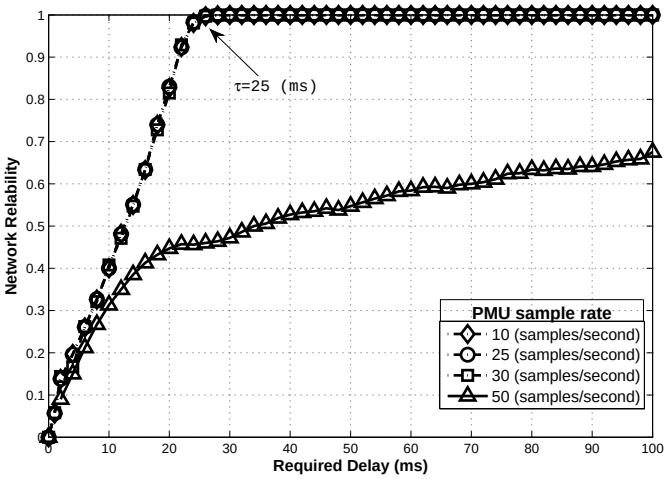

Figure 4.19: The S-shaped curve simulation results of PMUs network based on IEEE 802.11g with different Snapshot lengths.

Table 4.5: Results summary of IEEE 802.11g for concurrent Smart Grid applications.

SG WNAN	**Transient Stability**		**State Esimation**	
IEEE 802.11g approach PMU report setting	Reliability	Delay	Reliability	Delay
PMU, 10 $(samples/second)$	✓(supported)	✓	✓	✓
PMU, 25 $(samples/second)$	✓	✓	✓	✓
PMU, 30 $(samples/second)$	✓	✓	✓	✓
PMU, 50 $(samples/second)$	χ (not supported)	χ	✓	✓

In this chapter, we have proposed the method to investigate the SG WNAN performance for concurrent applications based on PMUs network by using S-shaped model. Our effort in this chapter helps to solve the problem that is how to take into account the phenomena of incomplete phasor information occurring in the measurement and design the suitable State Estimation or Transient Stability algorithms resilient to this issue.

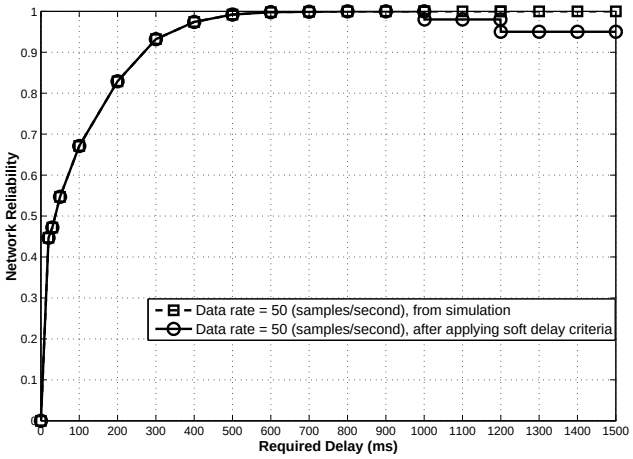

Figure 4.20: The S-shaped curve simulation results of PMUs network based on IEEE 802.11g with 50 $(samples/second)$.

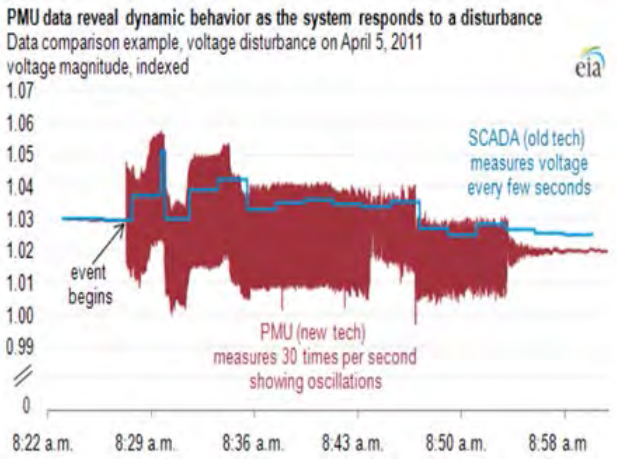

Figure 4.21: The comparison between monitoring used SCADA and PMUs systems.

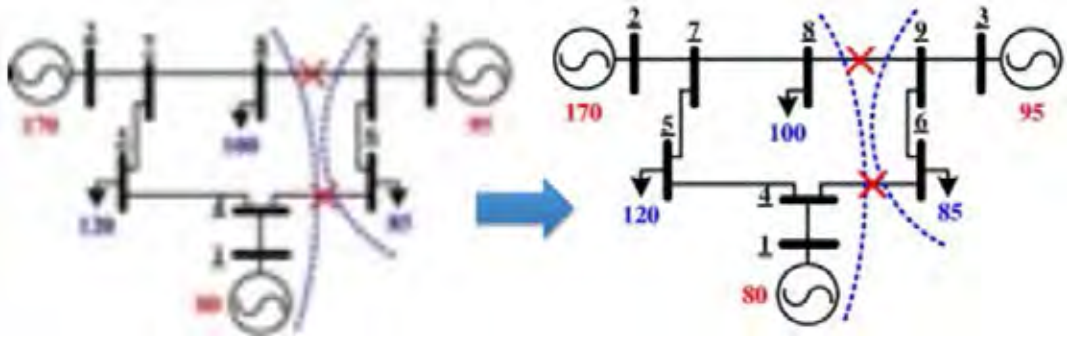

Figure 4.22: The comparison between monitoring used SCADA and PMUs systems. If we image the power grid picture provided SCADA as X-ray scan (left), then the picture from PMUs as MRI scan (right).

CHAPTER V

OPPORTUNISTIC HYBRID NETWORK CODING METHOD FOR SMART GRID DATA GATHERING

5.1 Introduction

Our research findings using S-shaped curve have shown that existing SG WNAN approaches fail to support the required QoS of Smart Grid applications. In this chapter, we relevance the benefit of Network Coding in Smart Grid context by proposing the method for data gathering, termed as Opportunistic Hybrid Network Coding (OHNC), to provide a reliable SG WNAN. The wireless channel is naturally fixed for network coding solution because it gains from the broadcasting characteristic of wireless node.

This chapter is organized as follows. Section 5.2 represents the existing applications of Network Coding in Smart Grid communication context. Their result findings have opened the innovate technique based on Network Coding to fulfill Smart Grid QoS requirements. In section 5.3, we propose our method Opportunistic Hybrid Network Coding (OHNC) for data gathering in SG WNAN. We also use the Absorbing Markov model to analyze and compare the data collection time of OHNC scheme and Non-OHNC scheme in section 5.4. In section 5.5, we investigate our OHNC in three network topologies in SG WNAN based on Matlab simulation. The result packet loss rate at receivers have shown the advantage of Network Coding method. Finally, we conclude our findings in section 5.6.

5.2 Related work

The idea of applying Network Coding for NAN smart grid was firstly proposed by Y.Phulpin et al. [49]. They suggest the potential method to leverage the benefit of Network Coding in broadcast nature of AMI based on Power Line Communication (PLC) or wireless communication. Their preliminary survey study on IEEE 123 node test feeder shows that the number of random links per node is appropriate for Network Coding approach to improve the throughput and reliability of NAN.

From that initial starting point, they later proposed a Network Coding protocol for AMI network on distribution grid [18]. This protocol is named Tunable Sparse Network Coding as they

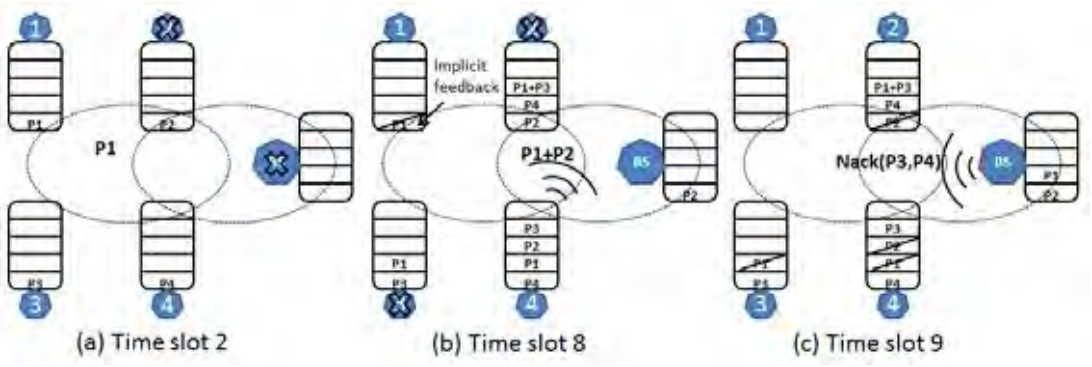

Figure 5.1: Small example of network coding protocol using Tunable Sparse Codes for 4 nodes (Adapted from the reference [18]).

use the sparse coefficient at the beginning state of coding to reduce the complexity in encoding and decoding processes. As shown in Figure 5.1, the proposed method includes two phases. In phase one, all nodes broadcast their packets alternately, as described in Table 5.1, from time slot 2 to time slot 5. When one node broadcasts packet, its neighbor nodes try to overhead and capture its packet. In phase two, each node broadcasts the XORing packets from other nodes which are over headed in phase one, as described in from time slot 6 to 8. The information flow is such as a wave forward from nodes to the sink.

The authors also proposed two feedback methods in their work: implicit and explicit feedbacks. The former is created by downstream nodes, which are closed to sink, when they broadcast their encoding packets, in order to let node deletes its packet from the queue (eg. node 1 in Figure 5.1(b)). The later is created by the sink when the number of loss packets is larger than threshold. The explicit feedback is flooded to all nodes to erase the received packets and retransmit the unreceived ones.

The simulation on IEEE 123 node test feeder shows that the protocol can achieve 100% reliability for AMI network and 10 times faster data collecting time than master-slave approach. However, the efficiency of proposed protocol is relied heavily on the feedback information of lost packets, which can slow down the throughput of network in practical application. In addition, the author implies the feedback message could not be lost, in which unreal in some NAN smart grid such as Distribution Automation, PMUs networks.

Other scholar from M. Karthick et al. proposes the NCMG by combination of multipaths transmission scheme and Network Coding technique [19]. As shown in Figure 5.2, the core idea of their method is the original sources data are mixed together and transmitted with the original data on different paths based on the operation of Rendezvous node R1 to R5. Those node play as the

Table 5.1: An example of Network Coding with explicit feedback using Tunable Sparse Codes for 4 nodes [18].

Time slot	**1**		**2**	**3**	**4**	**5**		**6**	**7**	**8**		**9**
Node 1	P1		P1	P1	P1	P1		P1	P1	~~P1~~[a]		-
Node 2	P2		P2	P2	P2	P2, P4		P2, P4, P1+P3[b]	P2, P4, P1+P3	P2, P4, P1+P3		~~P2~~, P4, P1+P3
Node 3	P3		P3, P1	P3, P1	P3, P1	P3, P1		P3, P1	P3, P1	P3, P1		P3, ~~P1~~
Node 4	P4		P4, P1	P4, P1, P2	P4, P1, P2	P4, P1, P2		P4, P1, P2, P3	P4, P1, P2, P3	P4, P1, P2, P3		P4, ~~P1~~, ~~P2~~, P3
BS	-		-	P2	P2	P2		P2	P2	P2, P1		P2, P1
Transmitter	-		Node 1	Node 2	Node 3	Node 4		Node 3	Node 2	Node 4		BS
Packet sent	-		P1	P2	P3	P4		P1+P3	P2+P4	P1+P2		Nack(P3,P4)
Reception	-		Nodes 3, 4	Nodes 1,4,BS	-	Nodes 1,2		Nodes 2,4	Nodes 3,4	Nodes 1, BS		Nodes 1,2,3,4
	initial state		uncoded packets	uncoded packets	uncoded packets	uncoded packets		coded packets	coded packets	coded packets		explicit feedback

[a] Packet is deleted in buffer.
[b] EXORing packet

coordinator between the Subscriber S1 and many Publishers (P1 to P4). When Rendezvous nodes receive the data request from S1, they track the publishers in their databases and establish disjoint paths between Publishers to Subscriber. The number of links are depended on the threshold delay parameter. However, not all Rendezvous nodes can perform Network Coding function, in Figure 5.2, only R1 and R4 can XORing packets, other nodes perform store and forward packets to destination.

The advantage of their work is that the protocol does not include feedback signal, while the simulation showed that bandwidth requirement is increased from 65% to 82% and nearly 100% reliability compared to multi-path transmission only. However, the unclear questions of the proposed method are: *(i)* The process of choosing and placing the Rendezvous nodes with or without Network Coding function; *(ii)* The number of Rendezvous nodes requirement for each service area; *(iii)* Encoding packets from more than two Publishers; and *(iv)* The results can be applied for the wireless channel.

As many above efforts, any applications of Network Coding for Smart Grid communication also due with two difficulties. The first is how to carry the random coefficients of packets. The coefficients are usually integrated in header, so it will affect the data part of the packets. The second issue is how to reduce the complexity of decoding procedure. It means that the time for recovery original packets should be minimum in order to satisfy the latency requirement. We should consider carefully those issues in other to get a trade-off solution.

5.3 Proposed Opportunistic Hybrid Network Coding scheme

5.3.1 Assumptions

In Smart Grid data gathering process, the collection of all data from all source at a particular time instant is called a *snapshot*. For example in AMI application, the power consumption of all houses at time t is a *snapshot data*. In order to formulate our OHNC scheme easily, we assume

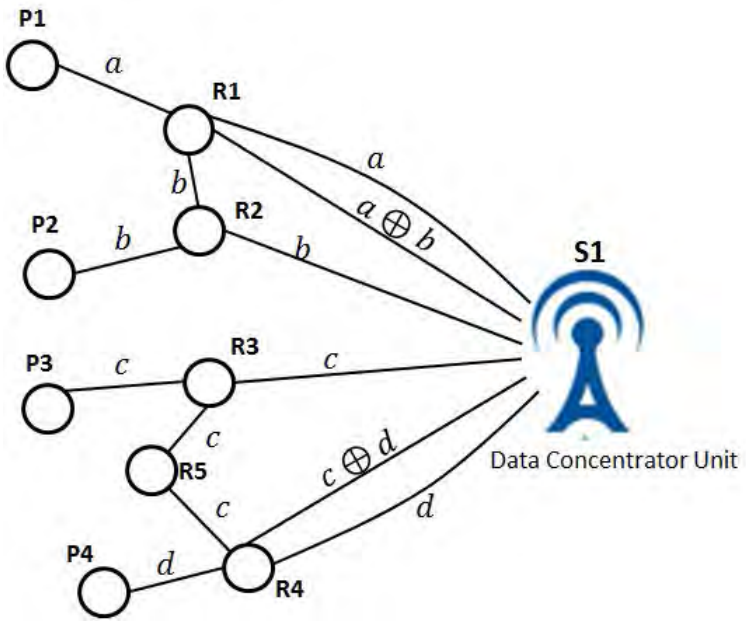

Figure 5.2: Network Coding for Monitoring Grid NCMG method (Adapted from the reference [19]).

the followings:

- All source nodes have the same data reporting rate and use random access scheme;
- All nodes use a shared wireless channel with the packet loss probability β;
- A source node can overhear and catch packets from its neighbors with the overheard packet loss probability γ;
- The stored overheard packet in a node is limited to 1, and the total number of coded packets generated from a node is limited to 1;
- Receiver sends the acknowledgment to all source nodes after the deadline for a *snapshot data* has passed.

5.3.2 Description of OHNC data gathering scheme

In this section, we represent how our proposed OHNC scheme works in the SG NAN topology described in Fig. 5.3a and Fig. 5.3b. The existing solutions for wireless SG NAN, termed Non-OHNC, are based on wireless one-hop network as in Fig. 5.3a. Each source node sends packet in one time slot with the loss probability β ($0 \leq \beta \leq 1$). The Data Concentrator Unit (DCU) is called successfully received source packets if they are stored in DCU's arrival buffer Q. While one source communicates to DCU, others are sleeping or waiting for their chances.

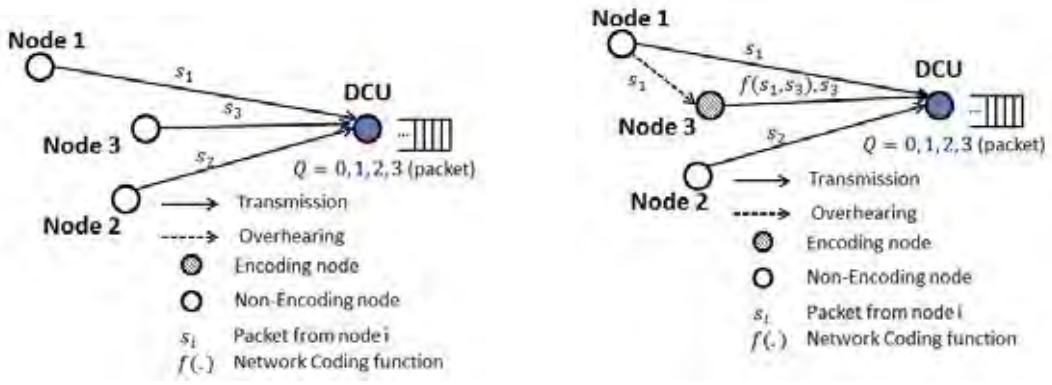

(a) Using Non-OHNC method

(b) Using OHNC method

Figure 5.3: Example of two data gathering schemes in one snapshot.

In contrast to Non-OHNC scheme, the OHNC one in Fig. 5.3b enables the ability of overhearing packet from nearby nodes when a source node sends packet to DCU. The overheard packets are stored in node's buffer for further network coding policies. Because the neighbor nodes are closed to source node than DCU, it has larger chance to collect packets. In this paper, we call γ as the loss probability of overhearing packet, which is $0 \leq \gamma \leq \beta$. The hybrid characteristic in our proposed OHNC method means that there is a mixture of nodes which have network coding capability and others which are only able to store-and-forward packets. The opportunistic feature in OHNC implies that packets are overheard randomly, not based on any routing schemes from the initial state.

5.3.3 Example of snapshot data using Non-OHNC and OHNC schemes

We provide an Non-OHNC data gathering in a snapshot in Table 5.2 and Figure 5.3a to describe how it works. Three source nodes want to send their packets s_1, s_2, s_3 to collector (Data Concentrator Unit (DCU)). The transmission channel is shown by solid lines as in Figure 5.3a, but packets can be loss with probability β. The initial buffer state is given in slot 1. From slot 2 to 6, the network starts to transmit packet. Unfortunately, node 2 consumes three time slot to send packet successfully in this example. In slot 7, DCU sends the acknowledgment message to all source nodes. Then, the next snapshot collection will start. Recall that Network Coding is not applied in this scheme.

We represent our OHNC data gathering in a snapshot in Table 5.3 and Figure 5.3b. The dashed line is the neighbor overhearing channel. This overhearing packet happens in slot 2, when node 1 has not sent packet to DCU successfully. However, node 3 has caught s_1 and stored it its overhearing buffer for encoding process later. In slot 2 and 3, node 3 and node 2 send packets

Table 5.2: Example of data gathering in a snapshot using Non-OHNC method in Figure 5.3a.

Time slot	**1**		**2**	**3**	**4**	**5**	**6**	**7**
Node 1	s_1		s_1	s_1	s_1	s_1	s_1	-
Node 2	s_2		s_2	s_2	s_2	s_2	s_2	-
Node 3	s_3		s_3	s_3	s_3	s_3	s_3	-
DCU	-		s_1	s_1	s_3, s_1	s_3, s_1	s_2, s_3, s_1	s_2, s_3, s_1
Transmitter	-		Node 1	Node 2	Node 3	Node 2	Node 2	DCU
Packet sent	-		s_1	s_2	s_3	s_2	s_2	ACK
Reception	-		DCU	DCU	DCU	DCU	DCU	Node 1, 2, 3
	initial state		uncoded packet	uncoded packet	uncoded packet	uncoded packet	uncoded packet	Feedback (ACK)

Table 5.3: Example of data gathering in a snapshot using OHNC method in Figure 5.3b.

Time slot	**1**		**2**	**3**	**4**	**5**	**6**
Node 1	s_1		s_1	s_1	s_1	s_1	-
Node 2	s_2		s_2	s_2	s_2	s_2	-
Node 3	s_3		s_3	s_3	s_3	s_3	-
DCU	-		-	s_3	s_2, s_3	s_1, s_2, s_3	s_1, s_2, s_3
Transmitter	-		Node 1	Node 3	Node 2	Node 3	DCU
Packet sent	-		s_1	s_3	s_2	$(\alpha.s_1 + \beta.s_3)$	ACK
Reception	-		Node 3	DCU	DCU	DCU	Node 1, 2, 3
	initial state		uncoded packet	uncoded packet	uncoded packet	coded packet	Feedback (ACK)

successfully. In slot 4, node 3 now encodes packet s_1 with its own packet s_3, and sends resulted coded packet $(\alpha.s_1+\beta.s_3)$ to receiver. We also call this coded packet as *redundant packet* because this process actually retransmits packets in Network Coding context.

5.4 Analytical results of OHNC scheme

5.4.1 System Model

In this section, we consider a Smart Grid NAN data gathering scheme in a snapshot using two-hop wireless network with one collector node (DCU) and three source nodes as a test case. DCU receives the periodic power consumption data from meters and also handles the critical information of other services. The data gathering activity can be modeled as an Absorbing Markov chain which is a sequence of random variables such that the next state depends only on the current state (memoryless property). For simplicity, we only investigate the packet collection in one round, called one snapshot data. Table 5.4 summaries the notations of DCU's sates used in our model [50].

Table 5.4: Table of Markov states in a snapshot.

State	Markov State Meaning
Q=0	Collector's buffer is empty. Collector has received no packet.
Q=1	One packet is in collector's buffer. Collector has received one packet from one over three sources
Q=2	Two different packets are in collector's buffer. Collector has received two packets from two over three sources
Q=3	Three different packets are in collector's buffer. Collector has received packets from three sources. The end (absorbing) state of Markov chain

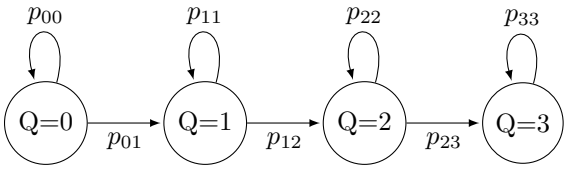

Figure 5.4: Markov model diagram of Non-OHNC scheme. Q describes the number of received packets in collector node.

5.4.2 Markov Chain Modeling of Non-Opportunistic Hybrid Network Coding (Non-OHNC) scheme

We calculate the transition probabilities values as below

$$p_{00} = \beta^3 \tag{5.1}$$

Recall that we assume the collector only sends feedback to source nodes after the snapshot deadline has passed. Hence, we have p_{11} and p_{22} as belows:

$$p_{11} = p_{22} = p_{00} = \beta^3 \tag{5.2}$$

$$p_{01} = Pr(Q = 1|Q = 0) = (1 - \beta^3) \tag{5.3}$$

$$p_{23} = p_{12} = p_{01} = (1 - \beta^3) \tag{5.4}$$

$$p_{33} = 1 \text{ absorbing state.} \tag{5.5}$$

We call $\mathbf{P}_1$ the transition probabilities matrix of data gathering method without applying

Opportunistic Hybrid Network Coding (Non-OHNC). We have

$$\begin{aligned}\mathbf{P}_1 &= \begin{pmatrix} p_{00} & p_{01} & p_{02} & p_{03} \\ p_{10} & p_{11} & p_{12} & p_{13} \\ p_{20} & p_{21} & p_{22} & p_{23} \\ p_{30} & p_{31} & p_{32} & p_{33} \end{pmatrix} = \\ &= \begin{pmatrix} p_{00} & p_{01} & 0 & 0 \\ 0 & p_{11} & p_{12} & 0 \\ 0 & 0 & p_{22} & p_{23} \\ 0 & 0 & 0 & p_{33} \end{pmatrix} = \\ &= \begin{pmatrix} \beta^3 & (1-\beta^3) & 0 & 0 \\ 0 & \beta^3 & (1-\beta^3) & 0 \\ 0 & 0 & \beta^3 & (1-\beta^3) \\ 0 & 0 & 0 & 1 \end{pmatrix}\end{aligned} \tag{5.6}$$

The transition matrix $\mathbf{P}_1$ in the canonical form is described as below

$$\mathbf{P}_1 = \left(\begin{array}{c|c} \mathbf{Q}_1 & \mathbf{R}_1 \\ \hline \mathbf{0} & \mathbf{I}_1 \end{array}\right) \tag{5.7}$$

where $\mathbf{I}_1$ is an identity matrix, $\mathbf{0}$ is a rectangular matrix of zeros, $\mathbf{R}_1$ is the transition matrix from transient states to absorbing state, and $\mathbf{Q}_1$ is the transition matrix among all transition states.

In our case, we have only one absorbing state, $\mathbf{I}_1 = 1$. Therefore, we have

$$\mathbf{Q}_1 = \begin{pmatrix} \beta^3 & (1-\beta^3) & 0 \\ 0 & \beta^3 & (1-\beta^3) \\ 0 & 0 & \beta^3 \end{pmatrix} \tag{5.8}$$

The fundamental matrix $\mathbf{N}_1$ for the absorbing chain of NonOHNC scheme is calculated

$$\mathbf{N}_1 = \mathbf{I} + \mathbf{Q}_1 + \mathbf{Q}_1^2 + \cdots = (\mathbf{I} - \mathbf{Q}_1)^{-1} \tag{5.9}$$

$$(\mathbf{I}-\mathbf{Q}_1)=\begin{pmatrix}1&0&0\\0&1&0\\0&0&1\end{pmatrix}-\begin{pmatrix}\beta^3&(1-\beta^3)&0\\0&\beta^3&(1-\beta^3)\\0&0&\beta^3\end{pmatrix}= \\ =\begin{pmatrix}(1-\beta^3)&-(1-\beta^3)&0\\0&(1-\beta^3)&-(1-\beta^3)\\0&0&(1-\beta^3)\end{pmatrix} \tag{5.10}$$

$$det(\mathbf{I}-\mathbf{Q}_1)=(1-\beta^3)^3 \tag{5.11}$$

Then

$$\mathbf{N}_1=\frac{1}{det(\mathbf{I}-\mathbf{Q}_1)}\begin{pmatrix}A_{11}&A_{12}&A_{13}\\A_{21}&A_{22}&A_{23}\\A_{31}&A_{32}&A_{33}\end{pmatrix}^T \tag{5.12}$$

where

$$A_{11}=\begin{vmatrix}(1-\beta^3)&-(1-\beta^3)\\0&(1-\beta^3)\end{vmatrix}=(1-\beta^3)^2 \tag{5.13}$$

$$A_{12}=-\begin{vmatrix}0&-(1-\beta^3)\\0&(1-\beta^3)\end{vmatrix}=0 \tag{5.14}$$

$$A_{13}=\begin{vmatrix}0&(1-\beta^3)\\0&0\end{vmatrix}=0 \tag{5.15}$$

$$A_{21}=-\begin{vmatrix}-(1-\beta^3)&0\\0&(1-\beta^3)\end{vmatrix}=(1-\beta^3)^2 \tag{5.16}$$

$$A_{22}=\begin{vmatrix}(1-\beta^3)&0\\0&(1-\beta^3)\end{vmatrix}=(1-\beta^3)^2 \tag{5.17}$$

$$A_{23}=-\begin{vmatrix}(1-\beta^3)&-(1-\beta^3)\\0&0\end{vmatrix}=0 \tag{5.18}$$

$$A_{31}=\begin{vmatrix}-(1-\beta^3)&0\\(1-\beta^3)&-(1-\beta^3)\end{vmatrix}=(1-\beta^3)^2 \tag{5.19}$$

$$A_{32}=-\begin{vmatrix}(1-\beta^3)&0\\0&-(1-\beta^3)\end{vmatrix}=(1-\beta^3)^2 \tag{5.20}$$

$$A_{33}=\begin{vmatrix}(1-\beta^3)&-(1-\beta^3)\\0&(1-\beta^3)\end{vmatrix}=(1-\beta^3)^2 \tag{5.21}$$

$$\mathbf{N}_1 = \frac{1}{(1-\beta^3)^3}\begin{pmatrix} (1-\beta^3)^2 & (1-\beta^3)^2 & (1-\beta^3)^2 \\ 0 & (1-\beta^3)^2 & (1-\beta^3)^2 \\ 0 & 0 & (1-\beta^3)^2 \end{pmatrix} = \\ = \begin{pmatrix} (1-\beta^3)^{-1} & (1-\beta^3)^{-1} & (1-\beta^3)^{-1} \\ 0 & (1-\beta^3)^{-1} & (1-\beta^3)^{-1} \\ 0 & 0 & (1-\beta^3)^{-1} \end{pmatrix} \tag{5.22}$$

Because we assume that each time slot corresponds to one transition state. Then, the expected number of time slots before the chain is absorbed, given that the initial state $Q = 0$, is calculated as belows [50]

$$E_1[t] = \sum_k N_1(1,k) = \frac{3}{(1-\beta^3)} \tag{5.23}$$

5.4.3 Markov Chain Modeling of Opportunistic Hybrid Network Coding (OHNC) scheme

We calculate the transition probabilities values as below

$$p_{00} = \beta^3 \tag{5.24}$$

Due to the same reason as in Eq. (5.2), we have p_{11} and p_{22} as belows:

$$p_{11} = p_{22} = p_{00} = \beta^3 \tag{5.25}$$

$$\begin{aligned} p_{02} = &Pr(one\ node\ sends\ packet\ loss)AND \\ &Pr(neighbour\ node\ overhears\ success)AND \\ &Pr(neighbour\ node\ sends\ success\ two\ packets) = \\ &= 3[2\beta(1-\gamma)(1-\beta)^2] \end{aligned} \tag{5.26}$$

$$p_{13} = p_{02} = 6[\beta(1-\gamma)(1-\beta)^2] \tag{5.27}$$

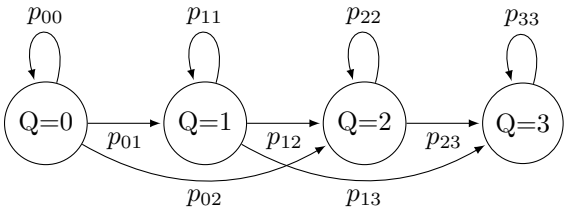

Figure 5.5: Markov model diagram of OHNC scheme.

$$
\begin{aligned}
p_{01} &= 1 - (p_{00} + p_{02}) = \\
&= 1 - [\beta^3 + 6[\beta(1-\gamma)(1-\beta)^2]] = \\
&= 1 - \beta^3 - 6[\beta(1-\gamma)(1-\beta)^2]
\end{aligned} \tag{5.28}
$$

$$
p_{23} = p_{12} = p_{01} \tag{5.29}
$$

$$
p_{33} = 1, \text{ absorbing state.} \tag{5.30}
$$

We call $\mathbf{P}_2$ the transition probabilities matrix of OHNC data gathering method. We have

$$
\begin{aligned}
\mathbf{P}_2 &= \begin{pmatrix} p_{00} & p_{01} & p_{02} & p_{03} \\ p_{10} & p_{11} & p_{12} & p_{13} \\ p_{20} & p_{21} & p_{22} & p_{23} \\ p_{30} & p_{31} & p_{32} & p_{33} \end{pmatrix} = \\
&= \begin{pmatrix} p_{00} & p_{01} & p_{02} & 0 \\ 0 & p_{11} & p_{12} & p_{13} \\ 0 & 0 & p_{22} & p_{23} \\ 0 & 0 & 0 & p_{33} \end{pmatrix} = \\
&= \begin{pmatrix} \beta^3 & 1-\beta^3-6[\beta(1-\gamma)(1-\beta)^2] & 6\beta(1-\gamma)(1-\beta)^2 & 0 \\ 0 & \beta^3 & 1-\beta^3-6[\beta(1-\gamma)(1-\beta)^2] & 6\beta(1-\gamma)(1-\beta)^2 \\ 0 & 0 & \beta^3 & (1-\beta^3) \\ 0 & 0 & 0 & 1 \end{pmatrix}
\end{aligned} \tag{5.31}
$$

The transition matrix in the canonical form is described as below

$$
\mathbf{P}_2 = \left(\begin{array}{c|c} \mathbf{Q}_2 & \mathbf{R}_2 \\ \hline \mathbf{0} & \mathbf{I}_2 \end{array}\right) \tag{5.32}
$$

In our case, we have only one absorbing state, $\mathbf{I}_2 = 1$. Therefore, we have

$$
\mathbf{Q}_2 = \begin{pmatrix} \beta^3 & 1-\beta^3-6[\beta(1-\gamma)(1-\beta)^2] & 6\beta(1-\gamma)(1-\beta)^2 \\ 0 & \beta^3 & 1-\beta^3-6[\beta(1-\gamma)(1-\beta)^2] \\ 0 & 0 & \beta^3 \end{pmatrix} \tag{5.33}
$$

The fundamental matrix $\mathbf{N}_2$ for the absorbing chain using OHNC technique is calculated

$$
\mathbf{N}_2 = \mathbf{I} + \mathbf{Q}_2 + \mathbf{Q}_2^2 + \cdots = (\mathbf{I} - \mathbf{Q}_2)^{-1} \tag{5.34}
$$

$$(\mathbf{I}-\mathbf{Q}_2)=\begin{pmatrix}1&0&0\\0&1&0\\0&0&1\end{pmatrix}-\begin{pmatrix}\beta^3&1-\beta^3-6[\beta(1-\gamma)(1-\beta)^2]&6\beta(1-\gamma)(1-\beta)^2\\0&\beta^3&1-\beta^3-6[\beta(1-\gamma)(1-\beta)^2]\\0&0&\beta^3\end{pmatrix}=$$
$$=\begin{pmatrix}(1-\beta^3)&-1+\beta^3+6[\beta(1-\gamma)(1-\beta)^2]&-6\beta(1-\gamma)(1-\beta)^2\\0&(1-\beta^3)&-1+\beta^3+6[\beta(1-\gamma)(1-\beta)^2]\\0&0&(1-\beta^3)\end{pmatrix} \tag{5.35}$$

$$det(\mathbf{I}-\mathbf{Q}_2)=(1-\beta^3)^3 \tag{5.36}$$

Then

$$\mathbf{N}_2=\frac{1}{det(\mathbf{I}-\mathbf{Q}_2)}\begin{pmatrix}A_{11}&A_{12}&A_{13}\\A_{21}&A_{22}&A_{23}\\A_{31}&A_{32}&A_{33}\end{pmatrix}^T \tag{5.37}$$

where

$$A_{11}=\begin{vmatrix}(1-\beta^3)&-(1-\beta^3)\\0&(1-\beta^3)\end{vmatrix}=(1-\beta^3)^2 \tag{5.38}$$

$$A_{12}=-\begin{vmatrix}0&-6\beta(1-\beta^2)(1-\gamma)\\0&(1-\beta^3)\end{vmatrix}=0 \tag{5.39}$$

$$A_{13}=\begin{vmatrix}0&(1-\beta^3)\\0&0\end{vmatrix}=0 \tag{5.40}$$

$$A_{21}=-\begin{vmatrix}-1+\beta^3+6[\beta(1-\gamma)(1-\beta)^2]&-6\beta(1-\beta^2)(1-\gamma)\\0&(1-\beta^3)\end{vmatrix}= \tag{5.41}$$
$$=(1-\beta^3)(1-\beta^3-6\beta(1-\gamma)(1-\beta)^2)$$

$$A_{22}=\begin{vmatrix}(1-\beta^3)&-6\beta(1-\gamma)(1-\beta)^2\\0&(1-\beta^3)\end{vmatrix}=(1-\beta^3)^2 \tag{5.42}$$

$$A_{23}=-\begin{vmatrix}(1-\beta^3)&-1+\beta^3+6\beta(1-\gamma)(1-\beta)^2\\0&0\end{vmatrix}=0 \tag{5.43}$$

$$A_{31}=\begin{vmatrix}-1+\beta^3+6\beta(1-\gamma)(1-\beta)^2&-6\beta(1-\beta^2)(1-\gamma)\\(1-\beta^3)&-1+\beta^3+6\beta(1-\gamma)(1-\beta)^2\end{vmatrix}= \tag{5.44}$$
$$=[-1+\beta^3+6\beta(1-\gamma)(1-\beta)^2]^2+6\beta(1-\beta^2)(1-\beta^3)(1-\gamma)$$

$$A_{32} = -\begin{vmatrix} (1-\beta^3) & -6\beta(1-\beta^2)(1-\gamma) \\ 0 & -1+\beta^3+6\beta(1-\gamma)(1-\beta)^2 \end{vmatrix} = \tag{5.45}$$
$$= (1-\beta^3)(1-\beta^3-6\beta(1-\gamma)(1-\beta)^2)$$

$$A_{33} = \begin{vmatrix} (1-\beta^3) & -(1-\beta^3) \\ 0 & (1-\beta^3) \end{vmatrix} = (1-\beta^3)^2 \tag{5.46}$$

Hence, the final version of $\mathbf{N}_2$ is as below

$$\mathbf{N}_2 = \frac{1}{(1-\beta^3)^3}\begin{pmatrix} A_{11} & A_{21} & A_{31} \\ A_{12} & A_{22} & A_{32} \\ A_{13} & A_{23} & A_{33} \end{pmatrix} \tag{5.47}$$

The expected number of time slots for gathering data in one snapshot using OHNC case is calculated in the same way as in Eq. (5.23), given that the initial state $Q = 0$.

$$E_2[t] = \sum_k A_1(k,1) = \tag{5.48}$$
$$= \frac{1}{(1-\beta^3)^3}[1+(1-\beta^3)(1-\beta^3-6\beta(1-\beta)^2(1-\gamma)+$$
$$+(\beta^3+6\beta(1-\beta)^2(1-\gamma)-1)^2+6\beta(1-\beta^2)(1-\beta^3)(1-\gamma)]$$

5.4.4 Analytical results

In this section, we calculate Eq. (5.23) and Eq. (5.48) in Matlab to analyze the theoretical expected time in a snapshot Smart Grid data of Non-OHNC and OHNC schemes with varying packet loss probability β and overhearing packet loss probability γ.

Figure 5.6 shows the performance of both Non-OHNC and OHNC schemes with the assumption that the packet loss probability equals to the overhearing packet loss probability ($\gamma = \beta$). Figure 5.7 presents the performance results when we set the value of overhearing packet loss $\gamma = 0.1$ and $\gamma = 0.3$. From both results, we can conclude that the average time slots needed for gathering one snapshot data of OHNC scheme is always less than those of Non-OHNC one.

Another interesting result is that when the packet loss probability goes up, the number of time slots of OHNC scheme does not change so much. This implies the reliability enhancement of network coding technique in our proposed method.

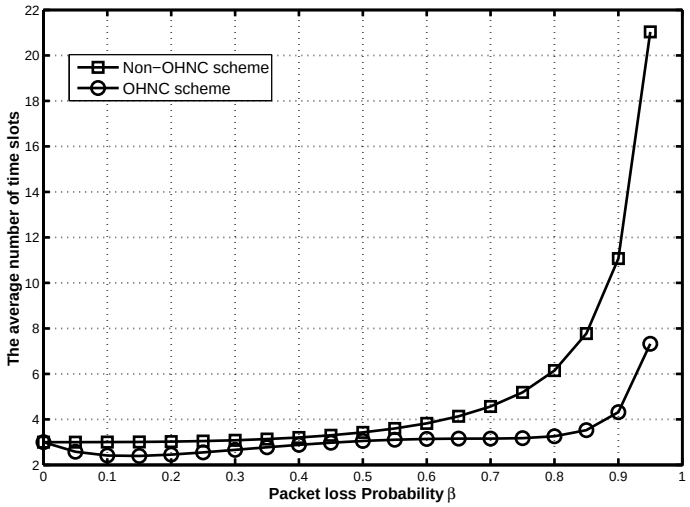

Figure 5.6: Expected data collection time slots in one snapshot with $\beta = \gamma$.

5.5 OHNC Simulations in Matlab

In this section, we simulate proposed OHNC method to show the advantage in reliability. The network topology scenarios are point-to-point, disjoint paths, and butterfly in a lossy wireless network. These chosen topologies are commonly used to simulate and compare the performance of many Network Coding approaches.

During the simulation, the packet loss patterns in wireless links are generated using the Gilbert Elliot model since this model can capture the intermittent characteristic of wireless channel. The encoding and decoding procedures in Matlab are based on the Network Coding libraries by Chamitha de Alwis [51]. We vary the following parameters in simulations

- *Number of redundant packets*: This is the number of coded packets combinations generated per generation;
- *field size*: This represents the Galois field size. Galois field $GF(2)$ corresponds to Binary Network Coding, or XORing Network Coding;
- *generation size*: This is the total number of packet combinations in linear equation per generation. In PMUs network, this is the total number of phasor messages per second per PMU. Hence, we choose $generation\ size = 30\ (packets)$ in all simulations;
- *link loss probability*: This is the packet loss probability per wireless link in the network. We have used the Gilbert Elliot model to create the loss pattern with loss probabilities $\{0.01, 0.02, 0.03, 0.04, 0.05\}$;

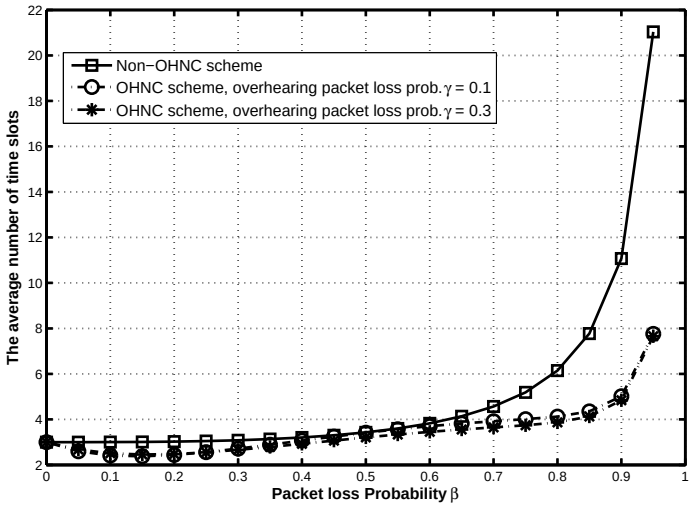

Figure 5.7: Expected data collection time slots in one snapshot with different γ.

- *packets*: The total number of packets is used in every simulation.

At the end of every simulation, we calculate the $Packet\ Loss\ Rate$ at receiver nodes as in Eq. (5.49) below

$$Packet\ Loss\ Rate = \frac{Total\ number\ of\ decoded\ packets}{Total\ number\ of\ received\ encoded\ packets} \tag{5.49}$$

We note that when we choose the Galois field $GF(2^1)$ and $Number\ of\ redundant\ packets = 0$, the data collection corresponds to Non-OHNC scheme. All the simulation Matlab codes can be found at *https://github.com/ngocthienle/Opportunistic-Hybrid-Network-Coding*.

5.5.1 Point-to-Point scenario

Figure 5.8 illustrates the point-to-point scenario in simulation. We assume that the link uses wireless channel. This scenario corresponds to the one-hop SG WNAN methods such as LTE or WiMAX. The data transmission procedure is described as below:

1. After establishing the link, source node S sends all uncoded packets in a same generation to the wireless link;
2. Source node S then combines linear combination of all uncoded packets (30 $(packets)$) in a same generation to generate coded packets ($\sum_{i=1}^{30} \alpha_i p_i$). We call this as *redundant packets*;
3. Receiver D starts to decode packets when it checks the matrix rank of coded packets begins

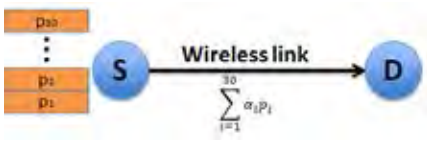

Figure 5.8: OHNC simulation in wireless point-to-point scenario.

equals or larger than packet generation size.

In the first simulation, we choose the common used Galois field $GF(2^8)$ to perform encoding and decoding packets and vary the number of redundant packets. The link loss probabilities are chosen in the set $\{0.01, 0.02, 0.03, 0.04, 0.05\}$. We plot the result packet loss rate in Figure 5.9. The obtained finding shows the effect of number of redundant packets to reliability enhancement. The higher number of redundant packets, the smaller packet loss rate at receiver. In this scheme, we observe that when redundant packets equals to 10 $(packets)$, the receiver packet loss rate reduces to nearly 0 in all cases.

Figure 5.10 shows the effects of Galois field size to packet loss rate. In smallest Galois field $GF(2^1)$, packet is represented as 0 and 1. Hence, this field corresponds to XORing packets in NCMG method [19]. The link loss probability is 0.05. From the simulation result, we conclude that when the Galois field increases, the effect on improving network reliability is also increased. The reason is that, in the high Galois field case, linear independent equations of packets are generated with very high probability.

In the last simulation of point-to-point scheme, we set up number of redundant packet equals to 10 $(coded\ packets)$, link loss 0.05 and investigate the performance of $GF(2^1)$ and $GF(2^8)$. The result box plots in Figure 5.11a and Figure 5.11b have shown the advantage of Galois field $GF(2^8)$ used in OHNC over Galois field $GF(2^1)$ used NCMG method [19].

5.5.2 Disjoint paths scenario

Figure 5.12 illustrates the disjoint paths scenario in simulation. We assume that the link uses wireless channel. This scenario corresponds to the one-hop SG WNAN approaches which enables neighborhood nodes can overhear packets surrounding and then recodes overheard packets. The data transmission procedure is described as below:

1. After establishing link to receiver, source node S sends all uncoded packets in same generation to this link;

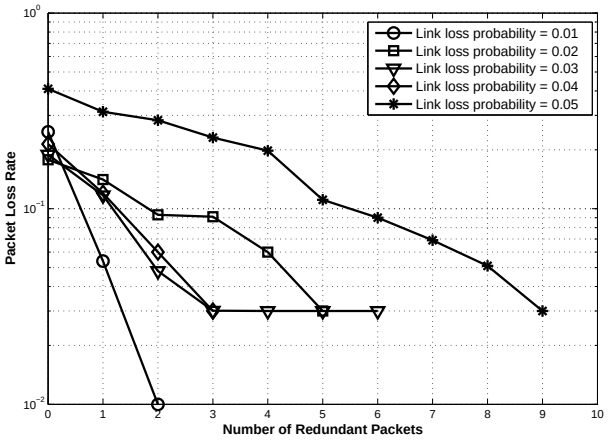

Figure 5.9: Packet loss rate at destination node in simulation using OHNC method with varying the number of redundant packets. Network Coding calculation is in Galois field (2^8).

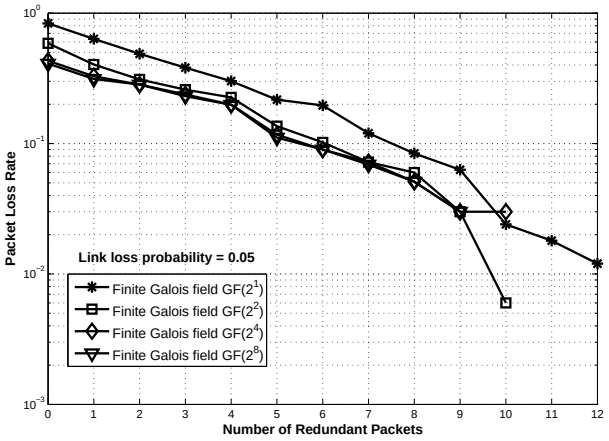

Figure 5.10: Packet loss rate comparison with different finite Galois fields. $GF(2^1)$ corresponds to XORing Netwok Coding in NCMG method [19]. The packet loss probability setting in simulation is 0.05.

2. Source node S then performs encoding process by calculating linear independent equations of all 30 $(packets)$ in same generation ($\sum_{i=1}^{30} \alpha_i p_i$). Then it sends to the receiver;

3. Relay node 2 has caught some coded packets from source node S during data transmission. Then, relay node recodes these coded packets. Finally, relay node sends these recoded packets to receiver;

4. Receiver D starts to decode packets when it checks the matrix rank of coded packets begins equals or larger than packet generation size.

We also choose Galois field $GF(2^8)$ for Network Coding in disjoint paths scheme and vary the number of redundant packets. We select the link loss probability $\{0.01, 0.03, 0.04, 0.05\}$ to use in

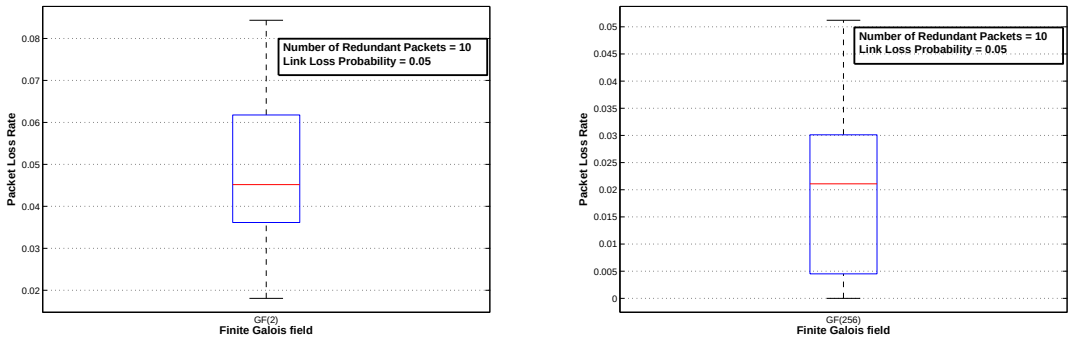

(a) Using $GF(2^1)$.

(b) Using $GF(2^8)$.

Figure 5.11: Comparison packet loss rate at sink using different finite Galois field in point-to-point scenario. The $GF(2)$ corresponds to NCMG method [19], and $GF(256)$ corresponds to Random Linear Network Coding used in our OHNC method.

Figure 5.12: OHNC simulation in wireless disjoint paths scenario.

simulation. We show the result packet loss rate at receiver in Figure 5.13. The result has shown the same trend in packet loss rate as in point-to-point case.

The main point in this disjoint paths is the role of relay node in Network Coding performance. Through recoding coded packets process, it has generated linear independent equations of packets with higher probability, compares to the point-to-point scheme.

5.5.3 Butterfly scenario

Figure 5.14 illustrates the butterfly scenario in simulation. This topology is commonly used to comparing the performance of many Network Coding approaches. We assume that the link uses wireless channel. This scenario corresponds to the multi-hops SG WNAN approaches which many relay nodes have Netwok Coding functions (Node $1, 2, 3, 4$). In this scenario, we have two receivers (Node 5 and Node 6). The data transmission procedure is described as below:

1. After establishing links to receivers, source node S sends all uncoded packets in same generation to these links;

2. Source node S then performs encoding process by calculating linear independent equations

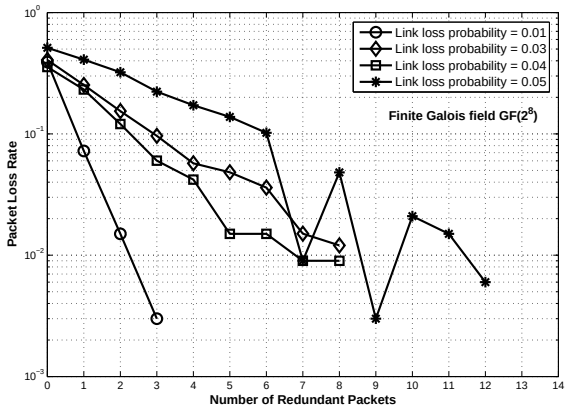

Figure 5.13: OHNC simulation results in wireless disjoint paths scenario.

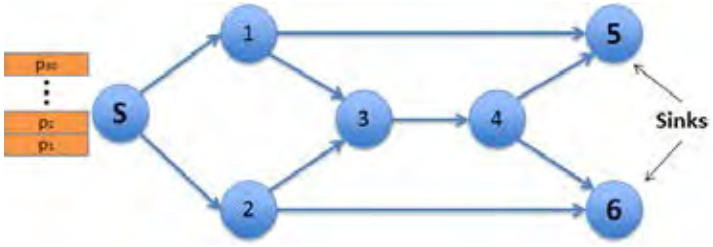

Figure 5.14: OHNC simulation in wireless butterfly scenario.

of all 30 $(packets)$ in same generation ($\sum_{i=1}^{30} \alpha_i p_i$). Then it sends to the receivers;

3. Relay nodes have caught coded packets from source node S during data transmission. Then, relay nodes recode these coded packets. Finally, relay nodes sends these recoded packets going to receiver;

4. Receivers D starts to decode packets when it checks the matrix rank of coded packets begins equals or larger than packet generation size.

In the first simulation, we compare the Network Coding performances of Galois field $GF(2^1)$ to Galois field $GF(2^8)$, with the same link loss probability 0.01. The simulation result is shown in Figure 5.15. Surprisingly that in butterfly scenario, the packet loss rate at receiver goes down quickly to 0 when we increase the number of redundant packet up to 4 $(coded\ packets)$ in $GF(2^8)$. However, this phenomenon does not happen in NCMG method [19] with Galois field $GF(2^1)$.

Figure 5.16 shows the effect of Network Coding in butterfly scheme when the loss probability increases. We have also obtained the benefit in reduced packet loss rate in the simulation results.

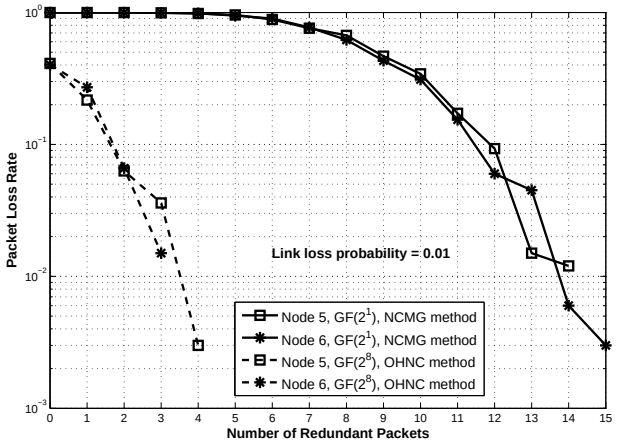

Figure 5.15: Comparison Packet Loss Rate performance between NCMG method [19] and Random Linear Network Coding in OHNC method in butterfly scenario.

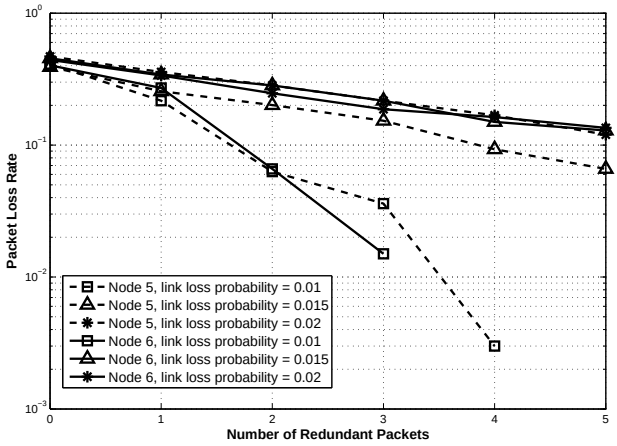

Figure 5.16: Packet loss rate at node 5 and node 6 in simulation using OHNC method with varying the number of redundant packets in butterfly scenario. Network Coding calculation is in Galois field (2^8).

In order to study the effectiveness of Network Coding to different topologies, we simulate RLNC technique with the same Galois field $GF(2^8)$ and observe the change of packet loss rate to the number of redundant packets. The simulation result in Figure 5.17 shows that there is not much different in Network Coding performance between point-to-point and disjoint paths schemes. In butterfly, relays are only useful with a large number of redundant packets.

5.6 Conclusion

In this chapter, we have proposed the innovative idea of network coding to satisfy dual requirements, reliability and delay, for coexisting Smart Grid applications in WAMS, e.g. State Estimation and Transient Stability. Our analytical results based on absorbing Markov model have

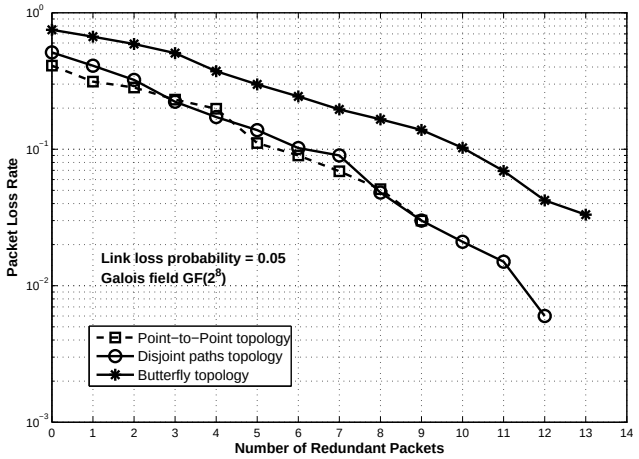

Figure 5.17: Effect of Network Coding method in many network topologies. In all case, the link loss probability is 0.05, and Galois field is $GF(2^8)$.

proven the advantage of Network Coding over other existing methods in term of the average data collection time.

In addition, through the implementation of OHNC scheme in Matlab, we have observed the effectiveness of Network Coding in three typical topologies, point-to-point, disjoint paths and butterfly scenarios. All simulation results shows that the packet loss rate of receiver nodes really decrease as the number of redundant packets increases. Network Coding also enhances network security as the coded packets received at sinks can only decode by solving independent linear equations with diverse coding coefficient vectors using a specific Galois field for every data flows.

In future work, we will implement our OHNC method using OMNeT++ [23] or other network simulators to investigate the achievable average data receiving rate and the data collection time with the larger number of source nodes.

CHAPTER VI

CONCLUSION AND FUTURE WORK

6.1 Conclusion

This work is motivated by the challenge of efficiency Smart Grid data gathering in large-scale wireless Neighborhood Area Network, where source nodes (Smart Meter or PMU) gather information, and transmit through sink node under strictly reliability and delay requirements. Due to the lack of Quality of Service (QoS) model that can capture the dedicated requirements of Smart Grid applications, it is important to propose an easy-to-use QoS model in planning and designing Smart Grid Wireless Neighborhood Area Network. This thesis has also focused on the effort of a useful Opportunistic Hybrid Network Coding data collection scheme based on Network Coding technique that satisfies the Smart Grid data requirements.

The dissertation has started with the Smart Grid applications background and theory about Network Coding. We have highlighted the main features in data requirements between Smart Grid and others such as Voice, Video, or Sensor network. From the principle compute and forward packets of Network Coding, it has been proven the advantages in reliability enhancement and reducing latency. By considering the network reliability in communication and power system domains, proposed S-shaped curve model is applied to determine the guaranteed QoS that a wireless NAN can support to particular applications. The S-shaped curves demonstrations on wireless AMI networks have shown that our QoS model can be a very useful tool to overcome the limitation of the existing approaches.

Choosing an optimal deployment and message rate for PMUs is the key success of WAMS applications in Smart Grid. However, there is no suitable designing approach for PMUs network, especially in distribution power grid running State Estimation and Transient Stability applications. While the former requires high precision to estimation, the later needs fast response decisions to protection. The coexistence of these applications has raised many challenges to Smart Grid communication system. In this thesis, the S-shaped curve demonstration on IEEE 37 nodes distribution test feeder have shown a simple method to evaluate the QoS performance of wireless PMUs using IEEE 802.11g to support these concurrent applications. From the obtained simulation results, we also have proposed the decentralized PMUs architecture approach for WAMS Smart Grid services.

Network Coding technique bases on the idea of changing relay function from store and forward to compute and forward packets. Hence, it helps communication network improving both reliability and throughput. In SG WNAN context, we have proposed the Opportunistic Hybrid Network Coding for Smart Grid data gathering. We have used absorbing Markov chain model to prove the benefit in reducing transmission time of our proposed method than existing ones. Finally, the obtained simulation results in Matlab in different network topologies have shown the advantage of Network Coding in improving packet delivery ratio. In the end, our belief is that the integration of Network Coding into Smart Grid communication will enable real-time feature to current and upcoming Smart Grid applications.

6.2 Future Work

The development of Smart Grid Communication is still in early stage and many research questions remain. In the power system point of view, more research efforts should be focus on the relation between required time for exchange application messages and the efficient of application output actions. In tandem, research on communication supporting Smart Grid needs a deeper understanding about interaction between many Smart Grid information flows. Our future works consider the following problems: (i) implement Opportunistic Hybrid Network Coding protocol for SG WNAN on the hardware rather than simulation, so that we can investigate the performance of our scheme under real wireless environment; (ii) set up Smart Grid co-simulation aid by S-shaped curve to overall investigate a Smart Grid network operation. We suggest GridLAB-D [52] power grid simulator because it can integrate the Distributed Grid and Electric Vehicle into simulation in order to support Demand Response or State Estimation applications.

References

[1] "NIST framework and roadmap for smart grid interoperability standards, release 3.0," National Institute of Standards and Technology, 2014.

[2] V. Gungor, D. Sahin, T. Kocak, S. Ergut, C. Buccella, C. Cecati, and G. Hancke, "A survey on smart grid potential applications and communication requirements," Industrial Informatics, IEEE Transactions on, vol. 9, pp. 28–42, Feb 2013.

[3] D. E. Washington DC, "Communications requirements of smart grid technologies," 2010.

[4] E. Hossain, Z. Han, and H. V. Poor, eds., Smart Grid Communications and Networking. Cambridge University Press, 2012. Cambridge Books Online.

[5] W. Wang, Y. Xu, and M. Khanna, "A survey on the communication architectures in smart grid," Computer Networks, vol. 55, no. 15, pp. 3604 – 3629, 2011.

[6] N. Saputro, K. Akkaya, and S. Uludag, "A survey of routing protocols for smart grid communications," Computer Networks, vol. 56, no. 11, pp. 2742 – 2771, 2012.

[7] J. Deshpande, E. Kim, and M. Thottan, "Differentiated services QoS in smart grid communication networks," Bell Labs Technical Journal 16(3), pp. 61–82, 2011.

[8] "IEEE vision for smart grid communications: 2030 and beyond," IEEE Standards Association, May 2013.

[9] Y. Kabalci, "A survey on smart metering and smart grid communication," Renewable and Sustainable Energy Reviews, vol. 57, pp. 302–318, 2016.

[10] Z. Fan, P. Kulkarni, S. Gormus, C. Efthymiou, G. Kalogridis, M. Sooriyabandara, Z. Zhu, S. Lambotharan, and W. H. Chin, "Smart grid communications: Overview of research challenges, solutions, and standardization activities," Communications Surveys Tutorials, IEEE, vol. 15, pp. 21–38, First 2013.

[11] J. G. Deshpande, E. Kim, and M. Thottan, "Differentiated services QoS in smart grid communication networks," Bell Labs Technical Journal 16(3), pp. 61–82, 2011.

[12] D. R. Shier, ed., Network Reliability and Algebraic Structures. Clarendon Press. Oxford New York, NY, 1992.

[13] "IEEE guide for electric power distribution reliability indices - redline," IEEE Std 1366-2012 (Revision of IEEE Std 1366-2003) - Redline, pp. 1–92, May 2012.

[14] “Smart grid networks system requirements specification, release version 5 (final),” SG-Network Task Force, November 2012.

[15] “NIST priority action plan 2, guidelines for assessing wireless standards for smart grid applications,” NIST, December 2010.

[16] R. Ahlswede, N. Cai, S.-Y. Li, and R. Yeung, “Network information flow,” Information Theory, IEEE Transactions on, vol. 46, pp. 1204–1216, Jul 2000.

[17] M. Medard, F. Fitzek, M. Montpetit, and C. Rosenberg, “Network coding mythbusting: why it is not about butterflies anymore,” Communications Magazine, IEEE, vol. 52, pp. 177–183, July 2014.

[18] R. Prior, D. Lucani, Y. Phulpin, M. Nistor, and J. Barros, “Network coding protocols for smart grid communications,” Smart Grid, IEEE Transactions on, vol. 5, pp. 1523–1531, May 2014.

[19] M. Karthick and K. Sivalingam, “Network coding based reliable and efficient data transfer for smart grid monitoring,” in Advanced Networks and Telecommuncations Systems (ANTS), 2013 IEEE International Conference on, pp. 1–6, Dec 2013.

[20] S. Chachulski, M. Jennings, S. Katti, and D. Katabi, “Trading structure for randomness in wireless opportunistic routing,” SIGCOMM Comput. Commun. Rev., vol. 37, pp. 169–180, Aug. 2007.

[21] S. Katti, H. Rahul, W. Hu, D. Katabi, M. Médard, and J. Crowcroft, “Xors in the air: Practical wireless network coding,” SIGCOMM Comput. Commun. Rev., vol. 36, pp. 243–254, Aug. 2006.

[22] T. Ho, M. Medard, R. Koetter, D. Karger, M. Effros, J. Shi, and B. Leong, “A random linear network coding approach to multicast,” Information Theory, IEEE Transactions on, vol. 52, pp. 4413–4430, Oct 2006.

[23] A. Varga, “The OMNeT++ discrete event simulation system,” in Proceedings of the European Simulation Multiconference (ESM), Jun. 2001.

[24] Y. H. Jeon, “QoS requirements for the smart grid communications system,” IJCSNS International Journal of Computer Science and Network Security, vol. 11, pp. 86–94, March 2011.

[25] M. H. Yaghmaee, Z. Yousefi, M. Zabihi, and S. Alishahi, “Quality of Service guarantee in smart grid infrastructure communications using traffic classification,” in CIRED2013 22nd International Conference on Electricity Distribution Stockholm, June 2013.

[26] W. Sun, X. Yuan, J. Wang, D. Han, and C. Zhang, "Quality of Service networking for smart grid distribution monitoring," in Smart Grid Communications (SmartGridComm), 2010 First IEEE International Conference on, pp. 373–378, 2010.

[27] H. Li and W. Zhang, "QoS routing in smart grid," in Global Telecommunications Conference (GLOBECOM 2010) IEEE, pp. 1–6, 2010.

[28] X. Deng, L. He, X. Li, Q. Liu, L. Cai, and Z. Chen, "A reliable QoS-aware routing scheme for neighbor area network in smart grid," Peer-to-Peer Networking and Applications, Springer US, pp. 1–12, 2015.

[29] R. Hou, C. Wang, Q. Zhu, and J. Li, "Interference-aware QoS multicast routing for smart grid," Ad Hoc Networks, vol. 22, pp. 13–26, 2014.

[30] Y. Cao, D. Duan, X. Cheng, L. Yang, and J. Wei, "QoS-oriented wireless routing for smart meter data collection: Stochastic learning on graph," IEEE Transactions on Wireless Communications, August 2014.

[31] D. Sahin, V. C. Gungor, T. Kocak, and G. Tuna, "Quality-of-Service differentiation in single-path and multi-path routing for wireless sensor network-based smart grid applications," Ad Hoc Networks, vol. 22, pp. 43–60, 2014.

[32] A. Varga, "INET framework for the OMNeT++ discrete event simulator, 2010.," in https://inet.omnetpp.org/.

[33] R. A. Sahner, K. S. Trivedi, and A. Puliafito, Performance and Reliability Analysis of Computer Systems: An Example-based Approach Using the SHARPE Software Package. Norwell, MA, USA: Kluwer Academic Publishers, 1996.

[34] NASPI, "Methodology for Examining the Impact of Error and Weakness in PMU Data on Operational Application. [online]," https://www.naspi.org/File.aspx?fileID=1572, (accessed February 08, 2016).

[35] M. Carrillo and J. M. Gonzalez, "A new approach to modelling sigmoidal curves," Technological Forecasting and Social Change, vol. 69, pp. 233–241, 2002.

[36] P. Meyer, "Bi-logistic growth," Technological Forecasting and Social Change, vol. 47, pp. 89–102, 1994.

[37] F. J.C. and P. R. H., "A simple substitution model of technological change," Technological Forecasting and Social Change, vol. 3, pp. 75–88, 1971.

[38] R. H. Khan and J. Y. Khan, "A comprehensive review of the application characteristics and traffic requirements of a smart grid communications network," Computer Networks, vol. 57, pp. 825–845, 2013.

[39] V. C. Gungor, D. Sahin, T. Kocak, S. Ergt, C. Buccella, C. Cecati, and G. P. Hancke, "Smart grid technologies: Communication technologies and standards," IEEE TRANSACTIONS ON INDUSTRIAL INFORMATICS, vol. 7, pp. 529–539, November 2011.

[40] "WiMAX Forum." www.wimaxforum.org, (accessed November 15, 2015).

[41] "The ZigBee Alliance." www.zigbee.org, (accessed November 15, 2015).

[42] S. Chen, Y. Wang, X. Y. Li, and X. Shi, "Data collection capacity of random-deployed wireless sensor networks," in Global Telecommunications Conference, 2009. GLOBECOM 2009. IEEE, pp. 1–6, Nov 2009.

[43] A. Phadke and J. Thorp, eds., Synchronized Phasor Measurements and Their Applications. Springer, New York, 2008.

[44] "C37.118.1a-2014 - IEEE standard for synchrophasor measurements for power systems – amendment 1: Modification of selected performance requirements," IEEE STANDARD, 2014.

[45] K. Martin, "Synchrophasor characteristics terminology," Presented to ERCOT Synchrophasor Work Group, March 2014.

[46] F. C. Schweppe and J. Wildes, "power system staticstate estimationpart i, ii iii," IEEE Trans. Power App. Syst., vol. 89, pp. 120–135, Jan 1970.

[47] Y. F. Huang, S. Werner, J. Huang, N. Kashyap, and V. Gupta, "State estimation in electric power grids: Meeting new challenges presented by the requirements of the future grid," IEEE Signal Processing Magazine, vol. 29, pp. 33–43, Sept 2012.

[48] P. Kansal and A. Bose, "Bandwidth and latency requirements for smart transmission grid applications," IEEE Transactions on Smart Grid, vol. 3, pp. 1344–1352, Sept 2012.

[49] Y. Phulpin, J. Barros, and D. Lucani, "Network coding in smart grids," in Smart Grid Communications (SmartGridComm), 2011 IEEE International Conference on, pp. 49–54, Oct 2011.

[50] C. M. Grinstead and J. L. Snell, Introduction to Probability, Second Edition. American Mathematical Society. Free access, last accessed November 15, 2015.

[51] C. de Alwis, "Network coding simulator, [online]," in http://www.mathworks.com/matlabcentral/fileexchange/53750-network-coding-simulator, (accessed May 15, 2016).

[52] D. P. Chassin, K. Schneider, and C. Gerkensmeyer, "GridLAB-D: An open-source power systems modeling and simulation environment," in 2008 IEEE/PES Transmission and Distribution Conference and Exposition, pp. 1–5, April 2008.

APPENDICES

APPENDIX A

PMU IEEE C37.118.1A - 2014 STANDARD

Table A.1: Steady-state synchrophasor measurement requirements [IEEE C37.118.1a-2014].

Influence quantity	**Reference condition**	**Minimum range of influence quantity over which PMU shall be within TVE limit**			
		P class		**M class**	
		Range	**Max TVE(%)**	**Range**	**Max TVE(%)**
Signal frequency range-f_{dev} (test applied nominal + deviation:$f_0 + f_{dev}$)	$F_{nominal}$ (f_0)	$\pm$2.0 Hz	1	$\pm$2.0 Hz for $F_s < 10$ $\pm(F_s/5)$ for $10 \leq F_s < 25$ $\pm$5.0 Hz for $F \geq 25$	1
The signal frequency range tests above are to be performed over the given ranges and meet the given requirements at three temperatures: T=nominal ($\sim 23^0C$), T=0^0C, and T=50^0C					
Signal magnitude-Voltage	100% rated	80% to 120% rated	1	10% to 120% rated	1
Signal magnitude-Current	100% rated	10% to 200% rated	1	10% to 200% rated	1
Phase angle with $\mid f_{in} - f_0 \mid < 0.25Hz$ (See NOTE 1)	Constant or slowly varing angle	$\pm\pi$ radians	1	$\pm\pi$ radians	1
Harmonic distortion (single harmonic)	<0.2% (THD)	1% each harmonic up to 50th	1	10% each harmonic up to 50th	1
Out-of-band interference as in NOTE 2 and 3	$< 0.2\%$ of input signal magnitude		None	10% of input signal magnitude for $F_s \geq 10$, No requirement for $F_s < 10$	1.3
Out-of-band interference testing: The passband at each reporting rate is defined as $\|f - f_0\| < F_s/2$. An interfering signal outside the filter passband is a signal at frequency f where: $\|f - f_0\| \geq F_s/2$. For test the input test signal frequency f_m is varied between f_0 and $\pm(10\%)$ of the Nyquist frequency of the reporting rate. That is: $f_0 - 0.1(F_s/2) \leq f_m \leq f_0 + 0.1(F_s/2)$ where: F_s = phasor reporting rate f_0 = nominal system frequency f_m = fundamental frequency of the input test signal					
NOTE 1 - The phase angle test can be performed with the input frequency f_m offset from f_0 where $\|f_m - f_0\| < 0.25Hz$. This provides a slowly varying phase angle that simplifies compliance verification without causing significant other effects. **NOTE 2** - A signal whose frequency exceeds Nyquist rate for the reporting rate F_s can alias into the passband. The test signal described for the out-of-band interference test verifies the effectiveness of the PMU anti-allias filtering. The test signal shall include those frequencies outside of the bandwidth specified above that cause the greatest TVE. **NOTE 3** - Compliance with out-of-band rejection can be confirmed by using a single frequency sinusoid added to the fundamental power signal at the required magnitude level. The signal frequency is varied over a range from below the passband (at least down to $10Hz$) and from above the passband up to the second harmonic. If the positive sequence measurement is being tested, the interfering signal is a positive sequence.					

Table A.2: Steady-state frequency and ROCOF measurement requirements [From IEEE C.37.118.1a-2014].

Influence quantity	**Reference condition**	**Error requirements for compliance**			
Signal frequency	Frequency = f_0 ($f_{nominal}$) Phase angle constant	**P class**		**M class**	
		Max FE (Frequency Error)	Max RFE (Rate of change FE)	Max FE	Max RFE
		0.005 Hz	0.01 Hz/s	0.005 Hz	0.01 Hz/s
Harmonic distortion (single harmonic)	$< 0.2\%$ THD	1% each harmonic up to 50th		10% each harmonic up to 50th	
		Max FE	Max RFE	Max FE	Max RFE
	$F_s > 20$	0.005 Hz	0.01 Hz/s	0.025 Hz	6 Hz/s
	$F_s \leq 20$	0.005 Hz	0.01 Hz/s	0.005 Hz	2 Hz/s
Out-of-band interference	<0.2% of input signal magnitude	No requirements		Interfering signal 10% of signal magnitude	
				Max FE	Max RFE
		None	None	0.01 Hz	0.1 Hz/s

Biography

Ngoc Thien Le was born in Vietnam, on June, 1983. He received the B.E. degree in electrical engineering from HCMC University of Technology and Education, Vietnam, in 2006, and the M.E. degree in telecommunication from HoChiMinh City University of Technology, Vietnam, in 2008. Since 2006, he is a lecturer at Department of Urban Engineering, HoChiMinh City University of Architecture for undergraduate courses related to telecommunication infrastructure planning and designing.

Since 2013, he is a PhD student at the Department of Electrical Engineering, Chulalongkorn University, Thailand under support grant from Scholarship Program 2013 for ASEAN Countries, funded by Chulalongkorn University, Thailand. His doctorate has been under the supervision of Associate Professor Watit Benjapolakul. His research interests include wireless sensor network, Smart Grid communication and Network Coding.